[EA]New Insights into the Tectono-Stratigraphic Evolution and Hydrocarbon Systems of the Pannonian Basin: A 2D Basin Modeling Study*

Attila Bartha[1], Attila Balázs[2], and Árpád Szalay[3]

Search and Discovery Article #11349 (2021)**
Posted January 25, 2021

*Adapted from extended abstract based on oral presentation given at 2019 AAPG Europe Region Regional Conference, Paratethys Petroleum Systems Between Central Europe and the Caspian Region, Vienna, Austria, March 26-27, 2019
 DOI:10.1306/11349Bartha2020

[1]Schlumberger, Germany (abartha@slb.com)
[2]Department of Sciences, Università Degli Studi Roma Tre, Rome, Italy (balatt@gmail.com)
[3]Independent Exploration Geologist, Szolnok, Hungary (dr.szalay@hotmail.com)

Abstract

Two-dimensional basin modeling was carried out in the Pannonian basin of Central Europe to investigate the Miocene extension, post-rift evolution, subsequent basin inversion, associated sedimentation, hydrocarbon generation (Bartha et al. 2018, Figure 1), and the interplay between the biogenic and thermogenic gas systems.

In the known Hungarian reservoirs – like gas reserves discovered worldwide – more than 20% of gases are biogenic (Figure 2). To investigate the vertical distribution of gases the carbon stable isotope ratio and gas wetness trends were generated for the Hungarian part of the Pannonian Basin taking more than 300 measurements into consideration (Figure 3). In the shallowest part of the basin – down to around 1,000 m – the trends show a biogenic origin (Figure 4). Going further down to around 3,000 m the signature of these trends changes and justifies a mixed origin (Figure 5). In the deepest part of the basin/section the heavier (i.e., less negative) stable carbon isotope ratio and decreasing gas wetness values suggest a thermogenic origin (Figure 6).

In Hungary, the gas fields are related to these three intervals and belong to three gas accumulation types: thermogenic, mixed and biogenic (Figure 7). The mixed gas accumulations are most likely connected to neo-tectonic elements (acting as migration conduits) and deep depocenters (serving as kitchen areas for thermogenic hydrocarbons) meanwhile the biogenic ones to structural highs surrounded by thick Pliocene sediments generating the biogenic gases (Figure 8 and Figure 9).

The model is situated in the Pannonian Basin crossing the Mid Hungarian Fault Zone and tying two depocenters (Figure 10 and Figure 11). Three wells located close to the section were considered for calibration purposes (Figure 12).

The tectono-sedimentary evolutionary model constrained by seismic and well data represented the input for dynamic modeling. The basin and petroleum systems model was analyzed with petroleum systems modeling software to integrate the spatial and temporal variations of episodes of subsidence and uplift, sedimentation and erosion, as well as the dynamics of biogenic and thermogenic gas generation, migration, accumulation, and loss. The high-resolution approach enabled an assessment of the impact of the shelf-margin slope progradation and sequential sediment loading on mechanical compaction, pore pressure development, source rock maturation, hydrocarbon charge, interplay between the biogenic and thermogenic gas systems, and preservation of hydrocarbons (Figure 13).

The diachronous depositional setting of facies, mixed thermogenic-biogenic sourcing, mixed fault-stratigraphic trapping, and calibration of the model with known fields represented the key technical challenges. To deal with these challenges, high resolution facies modeling (calibrated to well and seismic) combined with the coupled Darcy/Invasion Percolation (IP) migration simulator were used (Figure 14 and Figure 15).

Generation and migration processes were genetically controlled by the deposition of the SSE-ward-prograding Pannonian (s.l.) shelf-margin slope sediments and repeated tectonic inversions along the Mid Hungarian Fault Zone (Figures 16-29).

The tectono-stratigraphic evolution had an impact on the heat flow history of the area as well. At the end of the syn-rift phase (around 10 Ma) the heat flow values were higher in the depocenters but as the thermal subsidence progressed the heat flow curves along the modeled section became more equilibrated. The basal heat flow values are around 85 mW/m^2 at present-day (Figure 30).

The model was calibrated to temperature, maturity and pressure data measured in the wells. Different vitrinite reflectance kinetic models were tested and the impact of different generation reaction schemes on charge were compared (Figure 31).

One of the goals of this study was to analyze the impact of shelf-margin slope progradation on hydrocarbon generation. Organic matter content was assigned to presumed biogenic and thermogenic source rocks. However, high amount and high-quality organic matter were not required to calibrate the model to known accumulations (Figure 32 and Figure 33). The biogenic generation zone was defined by a temperature distribution within 40 and 60°C, and with a mean of 50°C, while thermogenic generation was controlled by reaction kinetics assigned to Miocene source rocks (Figure 34).

Both generation zones evolved together through geologic time. The biogenic generation zone was more sensitive to the variations of paleo geometries as the shelf-margin slope prograded. The thermogenic sources generated oil first and then gas. With increasing thermal stress, a part of the oil was cracked into gas. Both types of source rocks are still generating hydrocarbons at present-day. Biogenic gas generation was associated with the deposition of almost the entire sedimentary succession in the studied Jászság and Békés sub-basins; however, the preservation of these gases was limited in time and space. Most of the thermogenic gases were sourced by the deepwater marls in the Békés sub-basin (Figures 35-48).

The development of gas hydrates was also investigated in this numerical model. Simulation results indicated the presence of gas hydrate stability zones in the deeper parts of the basin at the end of syn-rift phase when all the conditions for their formation were in place. They started to diminish as the shelf-margin slope prograded and the water depth became shallower (Figure 49).

In the migration scenarios the coupled Darcy Flow/Invasion Percolation (IP) approach was used. It enabled the best match with the model resolution and property distributions, as well as with the pressure and migration processes. The generation of gas started in the deepest part of the section. With continuous deposition the generation and migration of hydrocarbons became ubiquitous along the entire section. Most of the gases were lost as they migrated to the surface due to the absence of proper seals. However, with continuing overburden formation the seals became tighter and tighter and an increasing part of the hydrocarbons was retained. The inversion at around 5.3 Ma had a slight impact on hydrocarbon generation and retention. Since then, the deposition of sediments has continued until present-day. The faults served as conduits and/or seals in migration processes. The gas hydrate zones that developed between 10.0 and 7.0 Ma could act as a seal and play a temporal role in the retention of both thermogenic and biogenic gases. However, further investigations are needed to understand better their contribution to gas accumulations with mixed origins present at shallower depths in the Pannonian basin. (Figures 50-63 and Figures 64-78).

Processes related to dissolution and diffusion were also considered in the migration model. Dissolution resulted in higher amounts of retained gases in formation waters, which therefore could not contribute to the charge of both known and predicted accumulations. Diffusion transport did not have a major impact on the final migration model because it was restricted to a range of few hundred meters in the Pannonian (s.l.) sediments.

Based on model results the composition of the gases changes in the reservoirs. There are more biogenic gases in the fractured basement, and more thermogenic gases in the Miocene reservoirs. The Pliocene reservoirs contain exclusively biogenic gases coming from different biogenic sources (Figure 79). The ratio of the biogenic gases in the model accumulations was around 26% (in mass ratio), a value similar to the biogenic gas content of the Hungarian reservoirs (Figure 80).

If the charge is analyzed through geologic time and across the stratigraphic column, it can be noticed that the generation started with the biogenic gases, then continued with the thermogenic hydrocarbons from the bottom to the top of the section. Both biogenic and thermogenic sources are still active and generating gases at present day (Figure 81).

The predicted hydrocarbon phases and compositions are in a good agreement with the results of geochemical analyses of the gas samples from the basin (Figure 82). Even though the hydrocarbon balance shows a predominance of biogenic gases, due to the inefficient sealing most of them were lost by migration to the surface.

These results could be achieved by applying a high definition model for facies refinement and calibrating 2D petroleum systems model to known accumulations (Figure 83).

The final conclusions of the study are (Figure 84):

- Two gas generation systems are present in the Pannonian Basin, which:
  - developed in a unique tectono-stratigraphic framework,
  - coexisted and interacted in time and space, and
  - resulted in 3 types of gas accumulations.
- There is a good agreement between the simulation results and observed trends.

- Based on study results there are most likely further exploration opportunities for mixed (type II) and biogenic (type I) gas accumulations related to stratigraphic/combined traps.

References

Bartha A, Balázs A, Szalay Á (2018) - On the tectono-stratigraphic evolution and hydrocarbon systems of extensional back-arc basins: inferences from 2D basin modelling from the Pannonian basin. Acta Geodaetica et Geophysica. https://doi.org/10.1007/s40328-018-0225-0

Tectono-stratigraphic Evolution and Hydrocarbon Systems of the Pannonian Basin

Acta Geodaetica et Geophysica
https://doi.org/10.1007/s40328-018-0225-0

ORIGINAL STUDY

On the tectono-stratigraphic evolution and hydrocarbon systems of extensional back-arc basins: inferences from 2D basin modelling from the Pannonian basin

Attila Bartha[1] · Attila Balázs[2] · Árpád Szalay[3]

Received: 22 May 2018 / Accepted: 13 July 2018

Figure 1

Goal: Model Gas Generation Systems Interconnected in Time and Space Using Numerical Simulation

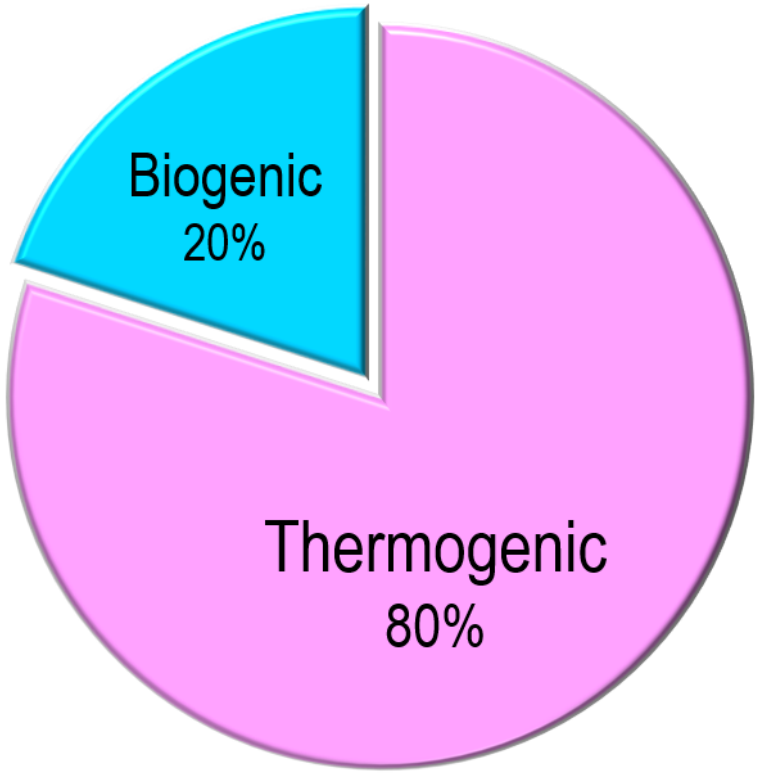

- Almost 20% of discovered gas reserves in Hungary have biogenic origin
- Biogenic gas accounts for more than 20% of the world's gas reserves*

* *(Rice and Claypool 1981; Katz 2011)*

Figure 2

Biogenic vs. Thermogenic: Three Gas Accumulation Types

Carbon Isotope Ratio ($\delta^{13}C$)

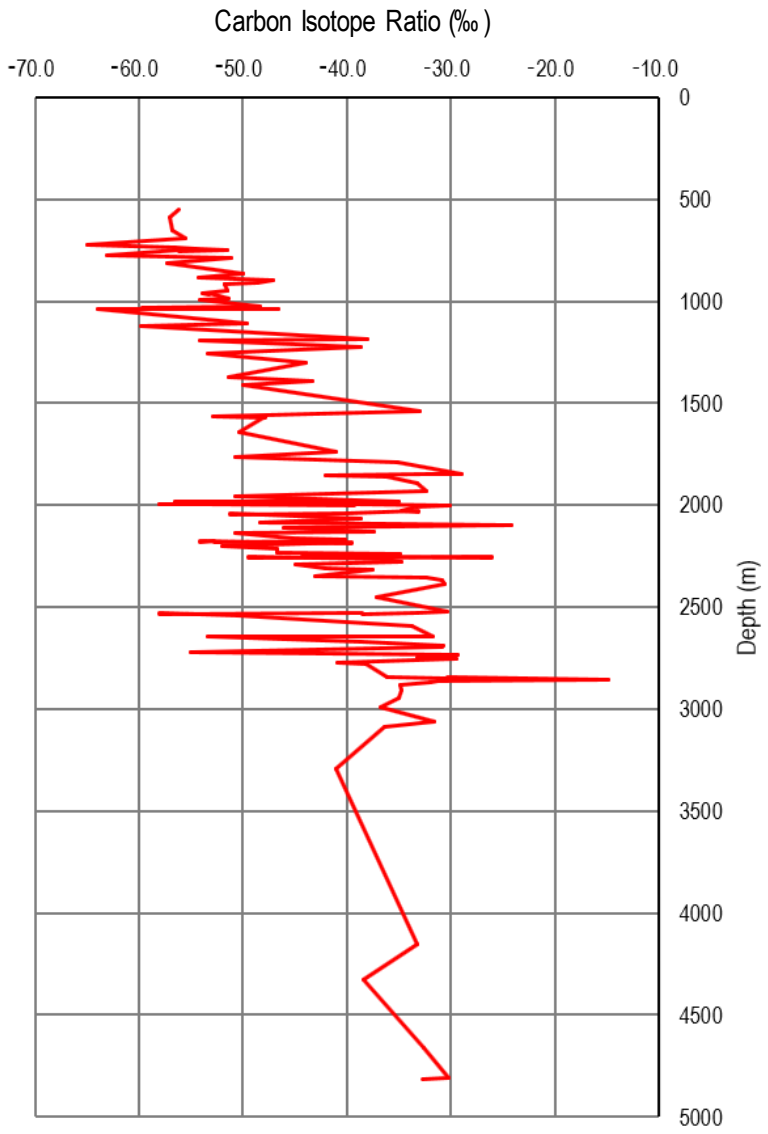

Gas Wetness [$(C_2/C_1+C_2)x100$]

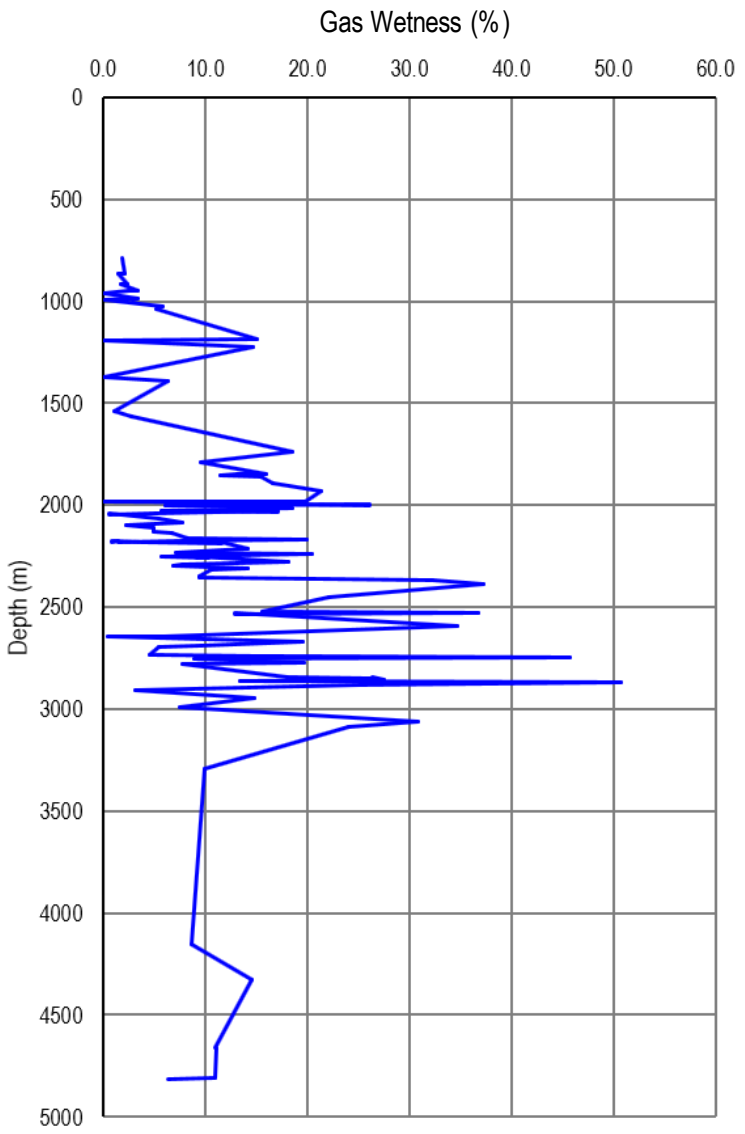

Plots based on more than **300 measurements** taken in the wells located in the Pannonian Basin.

Source: Clayton et al. 1990

Figure 3

Biogenic vs. Thermogenic: Biogenic (Type I)

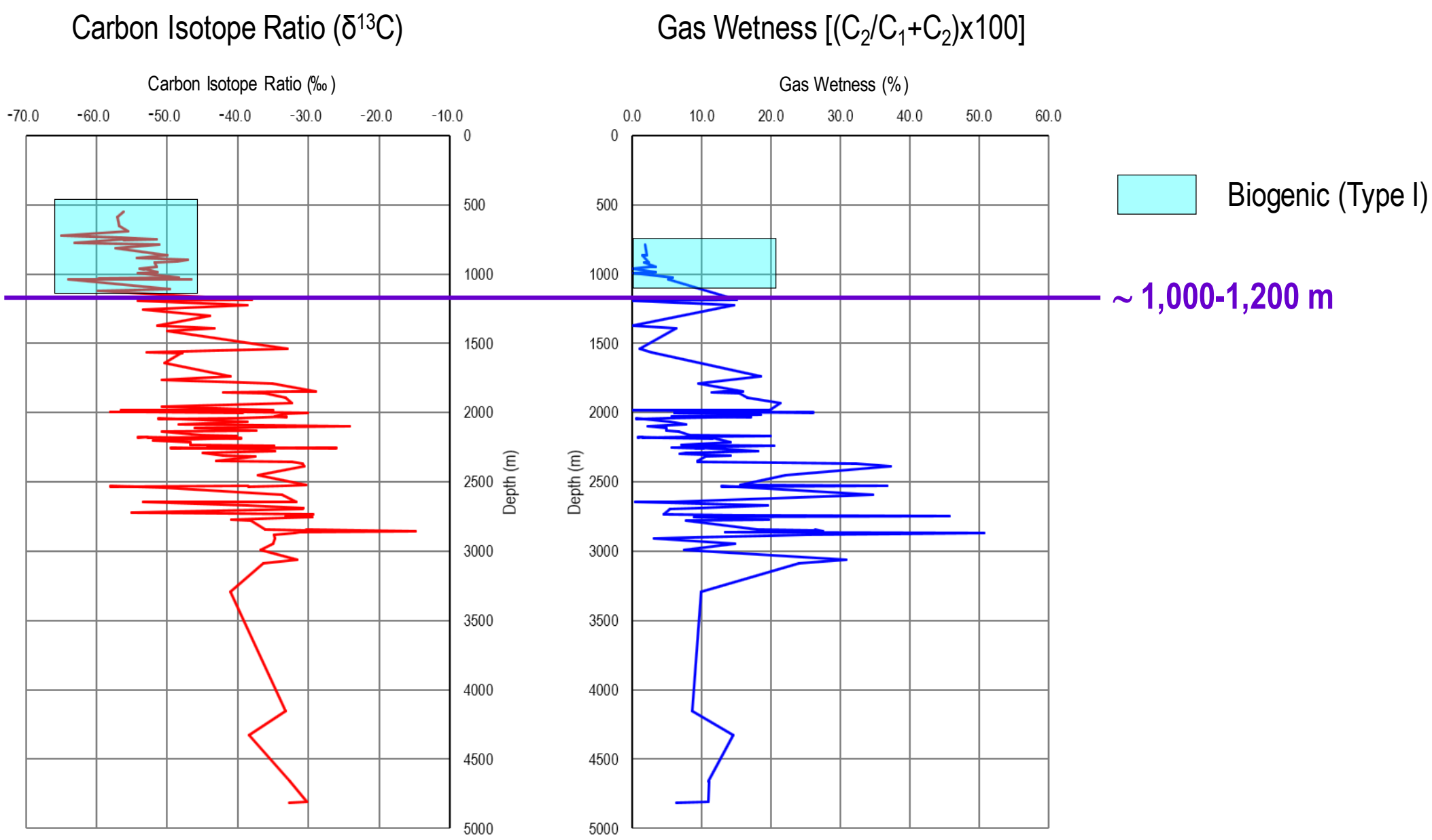

Figure 4

Biogenic vs. Thermogenic: Mixed (Type II)

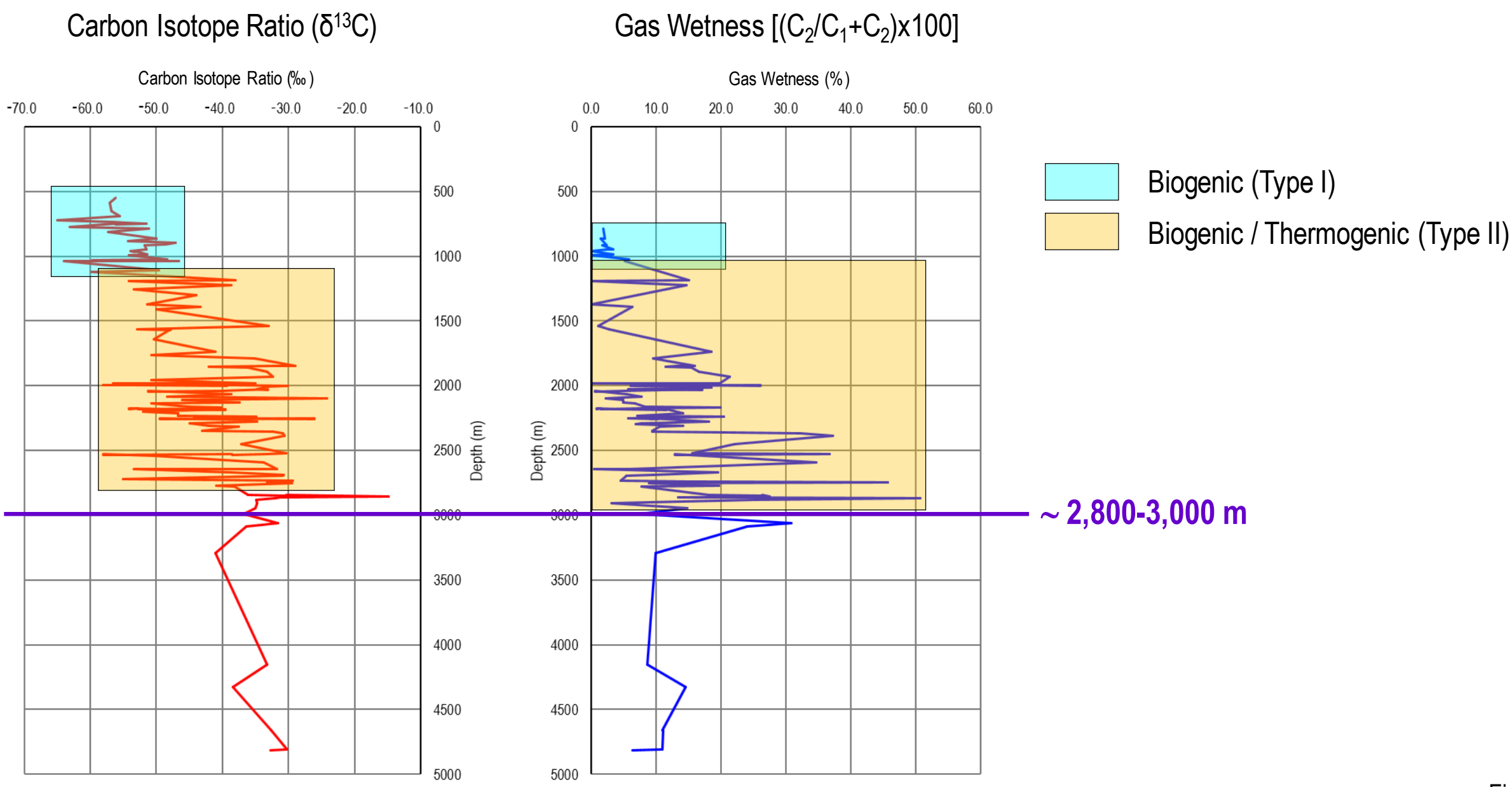

Figure 5

Biogenic vs. Thermogenic: Thermogenic (Type III)

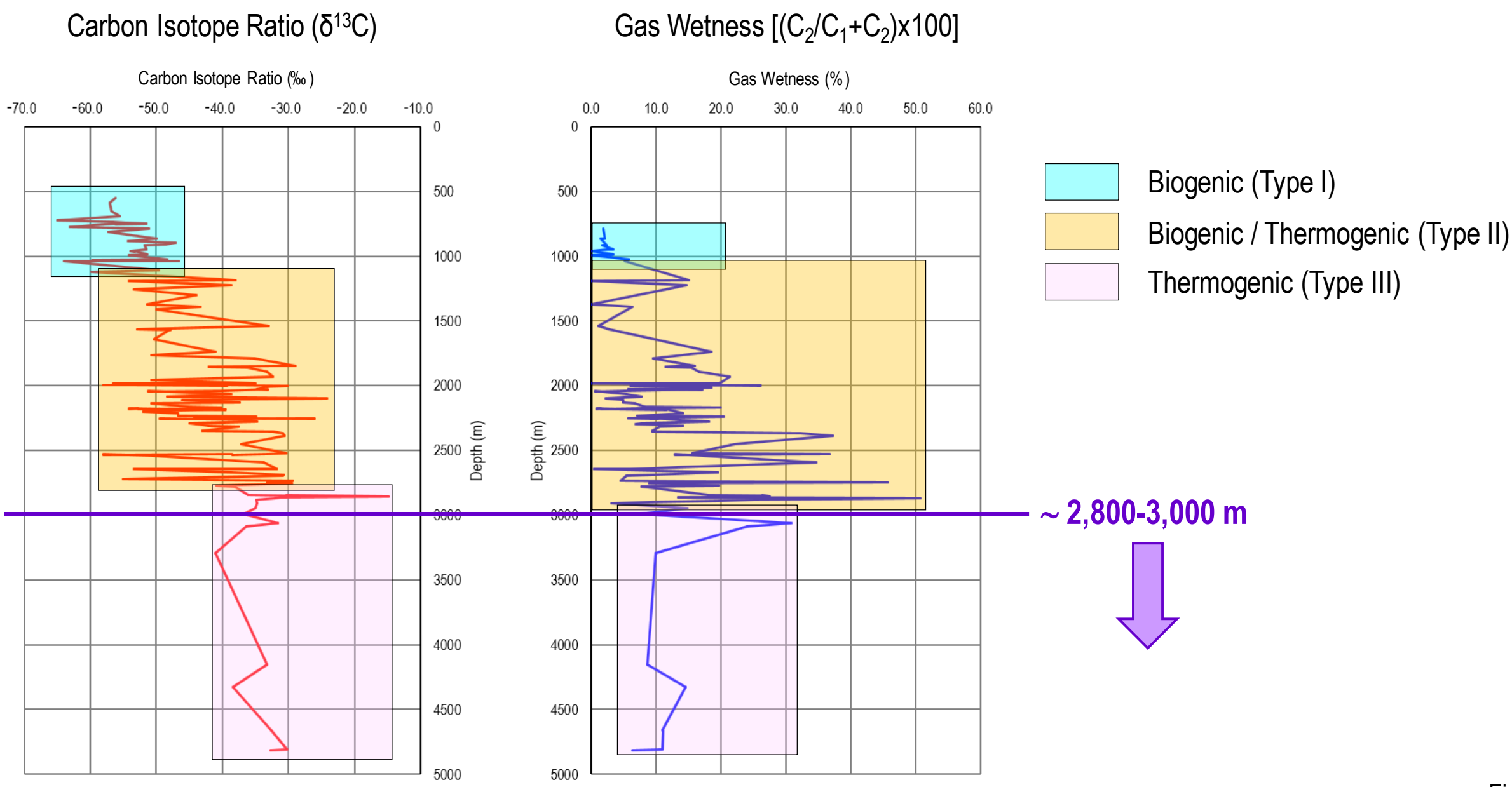

Figure 6

Hydrocarbon Accumulations: Fractured Basement, and Middle and Late Miocene Reservoirs

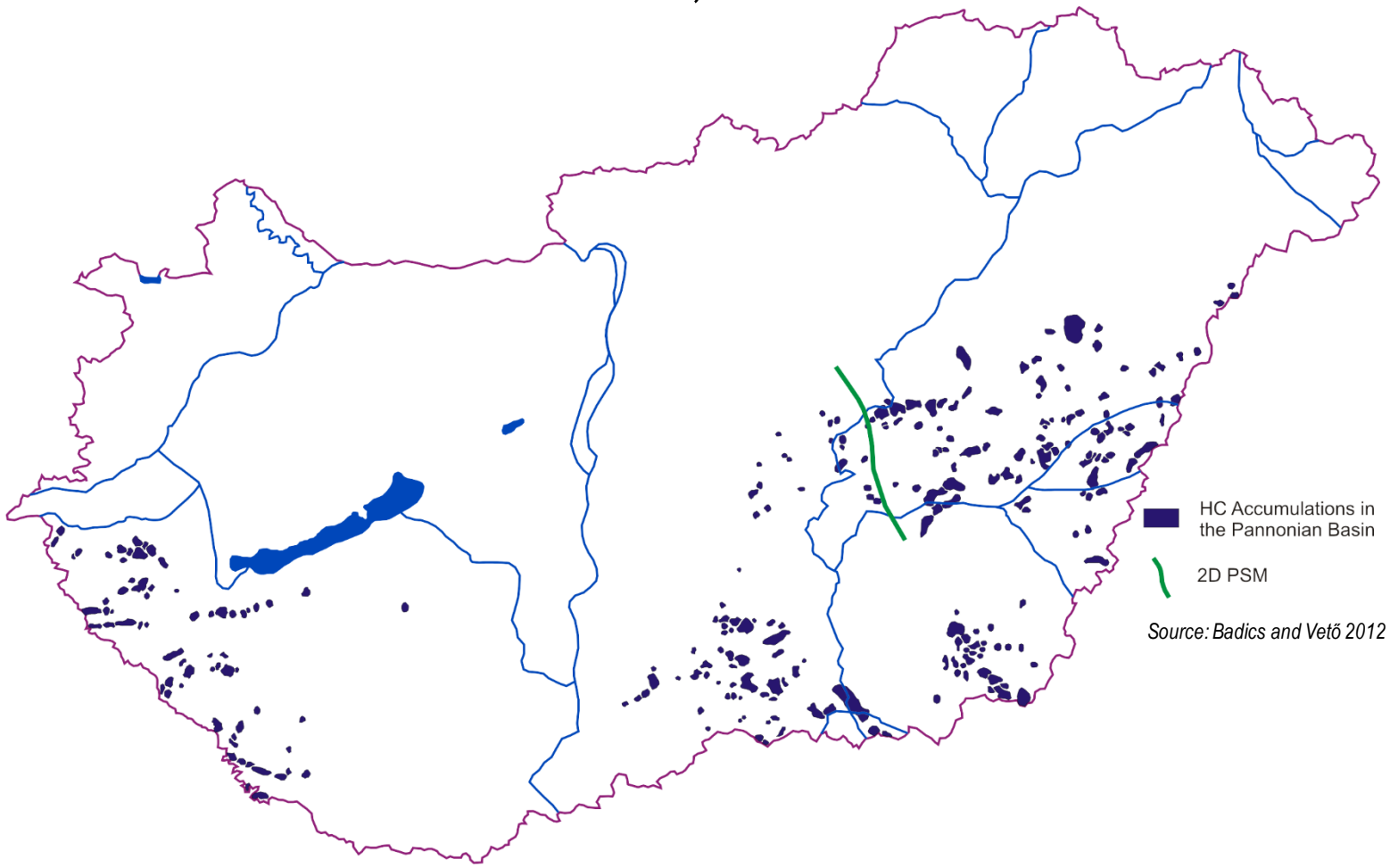

Type I	biogenic
Type II	mixed
Type III	thermogenic

Figure 7

Gas Accumulations: Mixed (Type II)

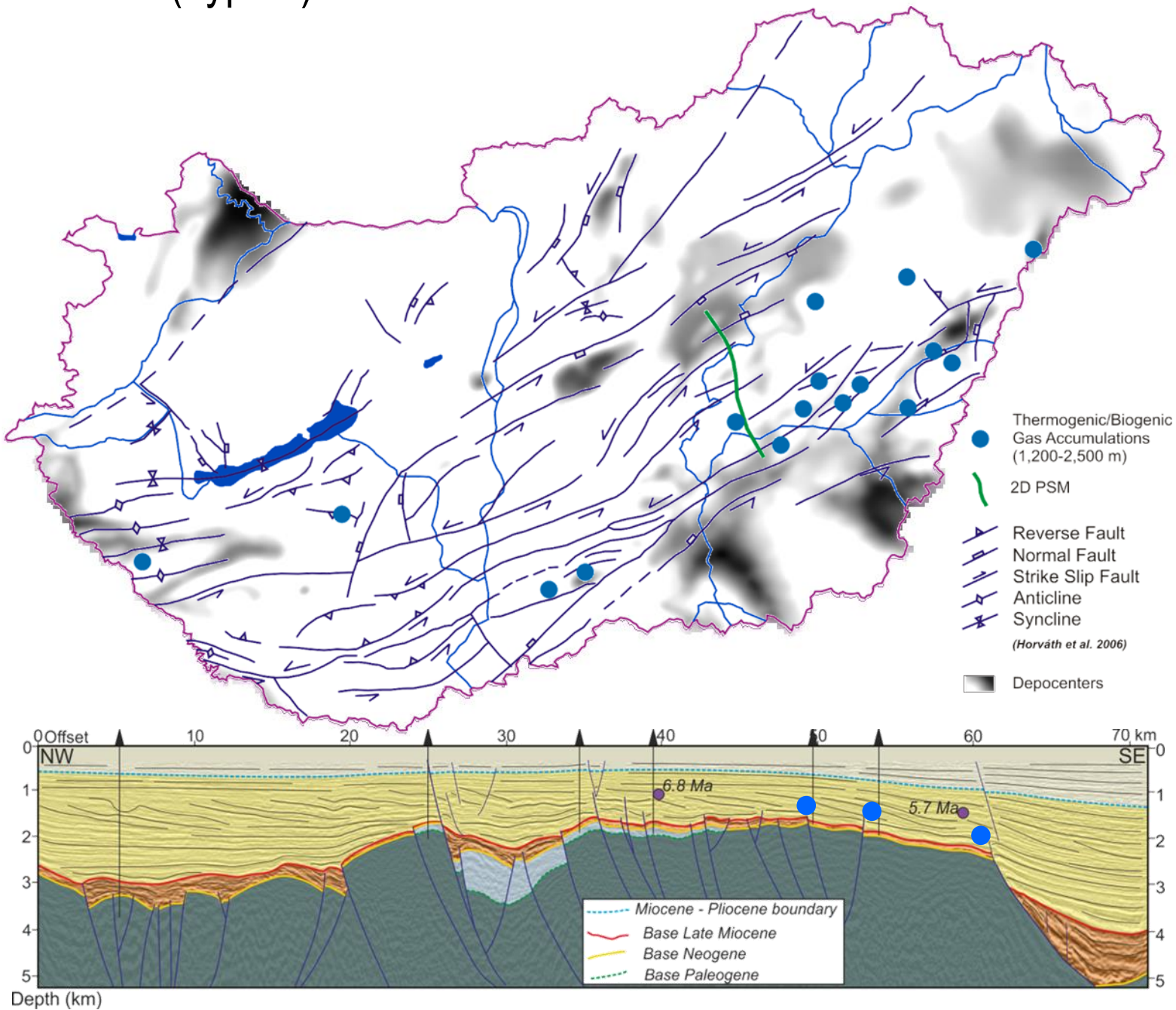

Figure 8

Gas Accumulations: Biogenic (Type I)

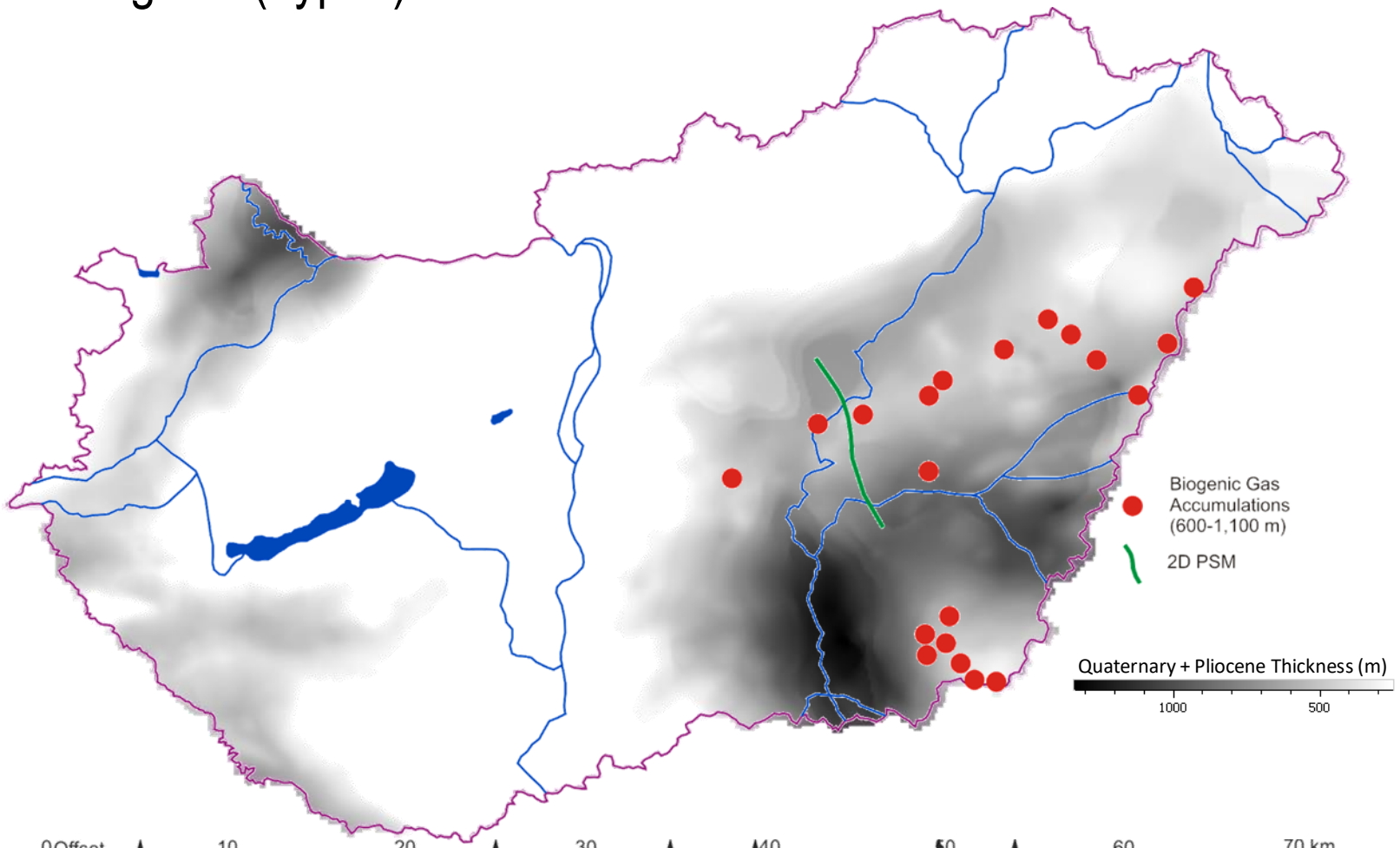

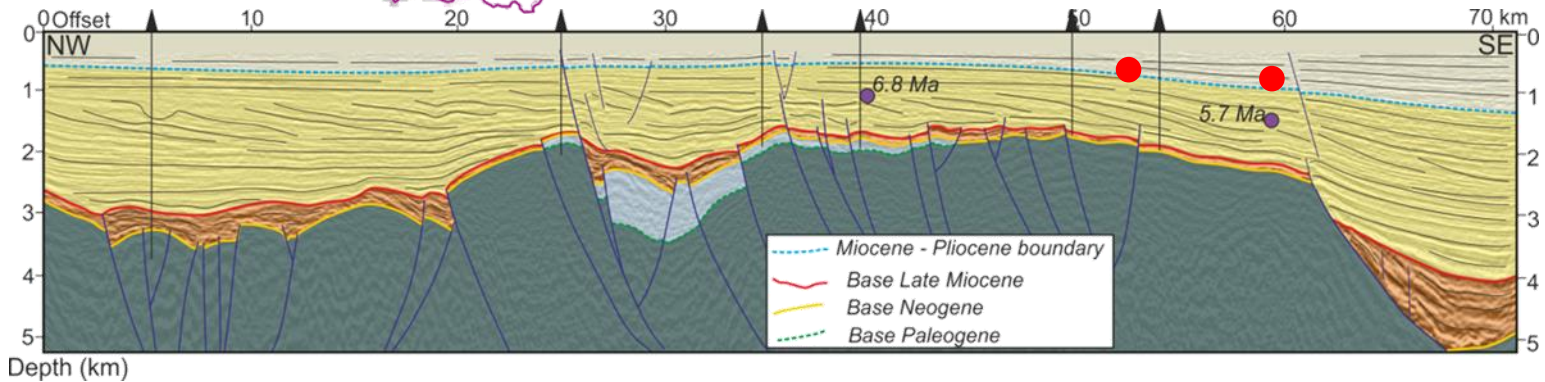

Figure 9

Model Area: Regional Setting

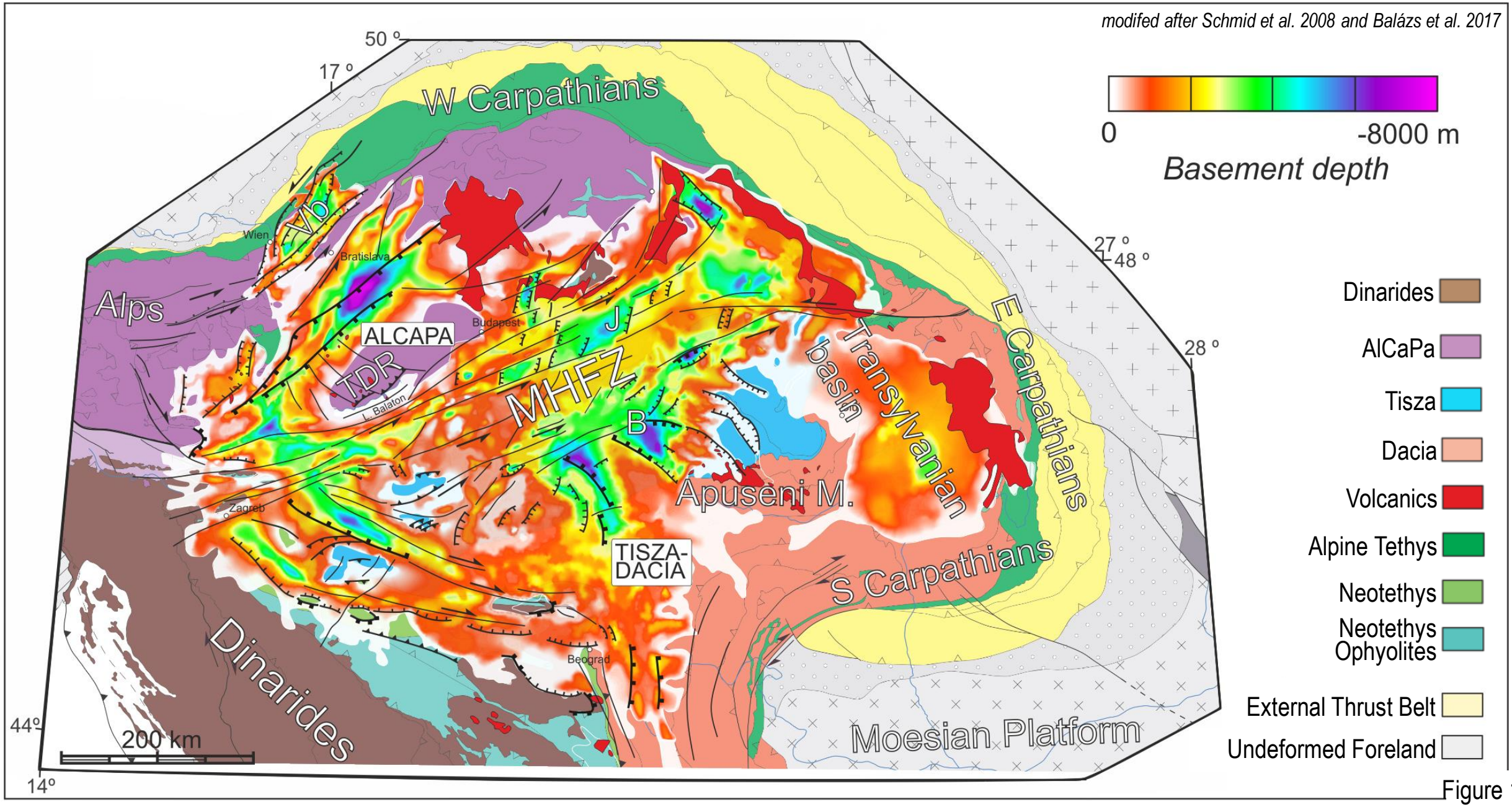

Figure 10

Model Area: Regional Setting

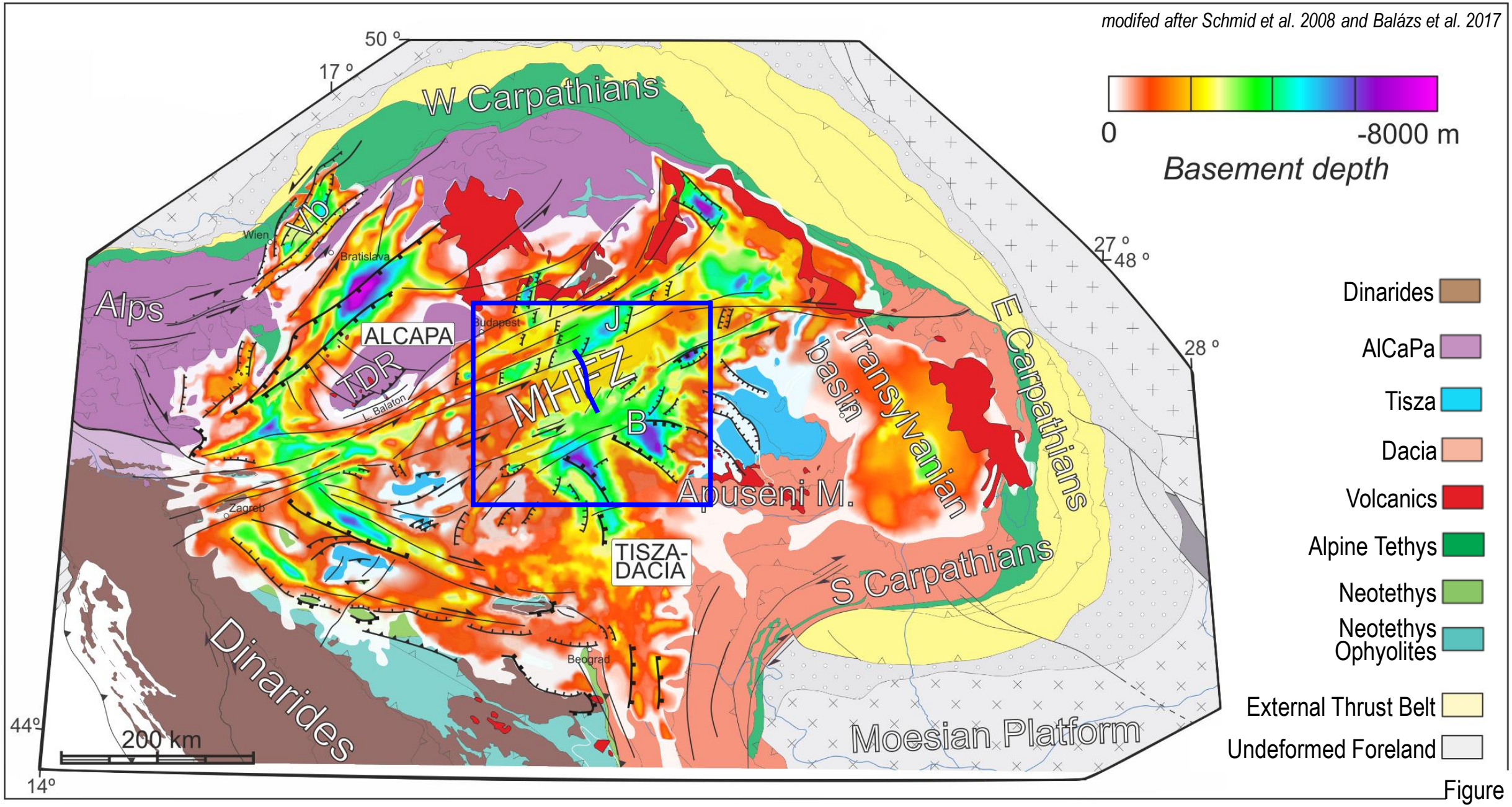

Figure 11

Model Area: 2D Model Location

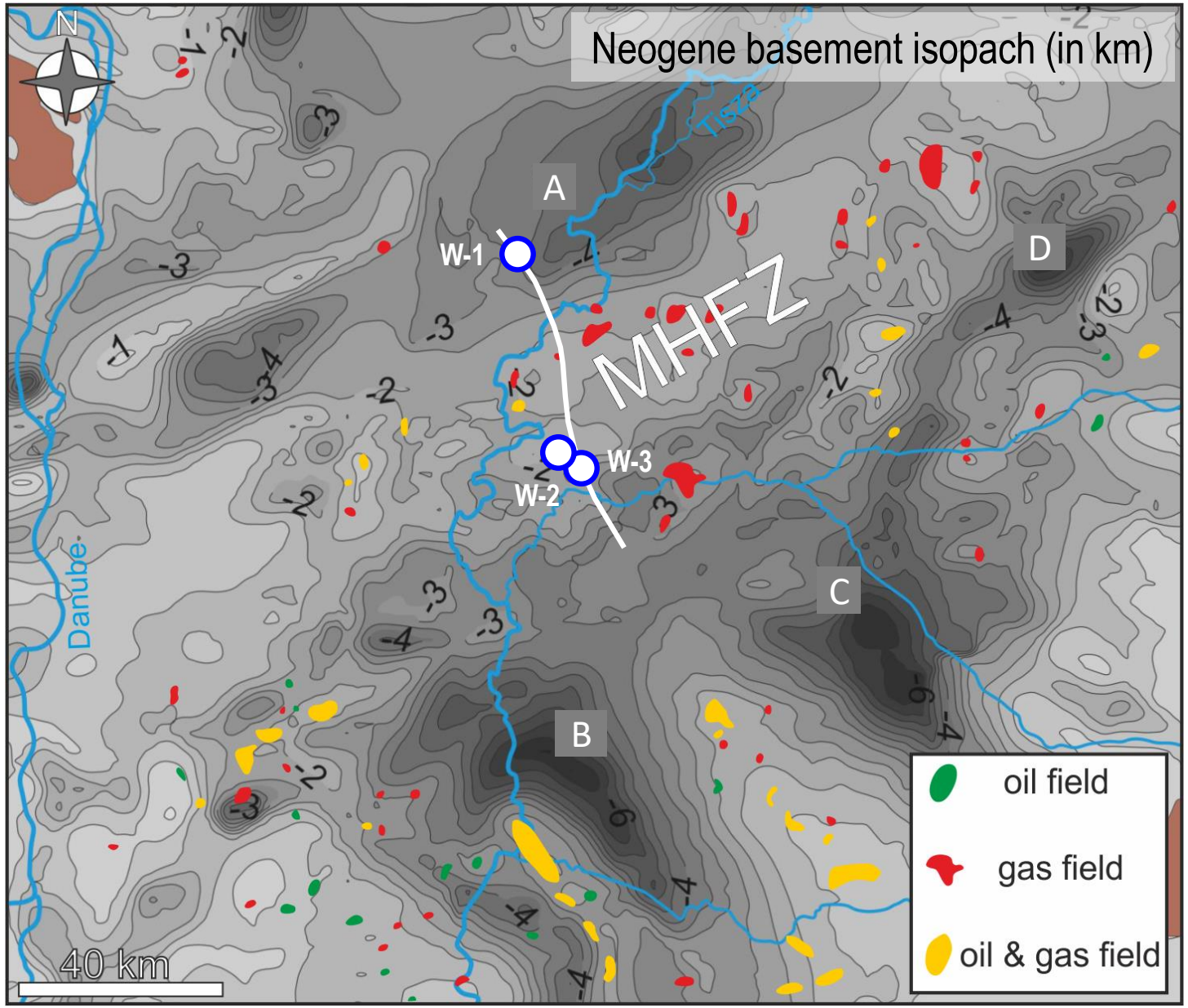

after Haas et al. 2010; Balázs et al. 2016, Tari and Horváth 2006; Badics and Vető 2012

A/B/C/D – Depocenters

MHFZ – Mid-Hungarian Fault Zone

○ – Calibration Wells

Figure 12

Petroleum Systems Model: Model Building from Published Data

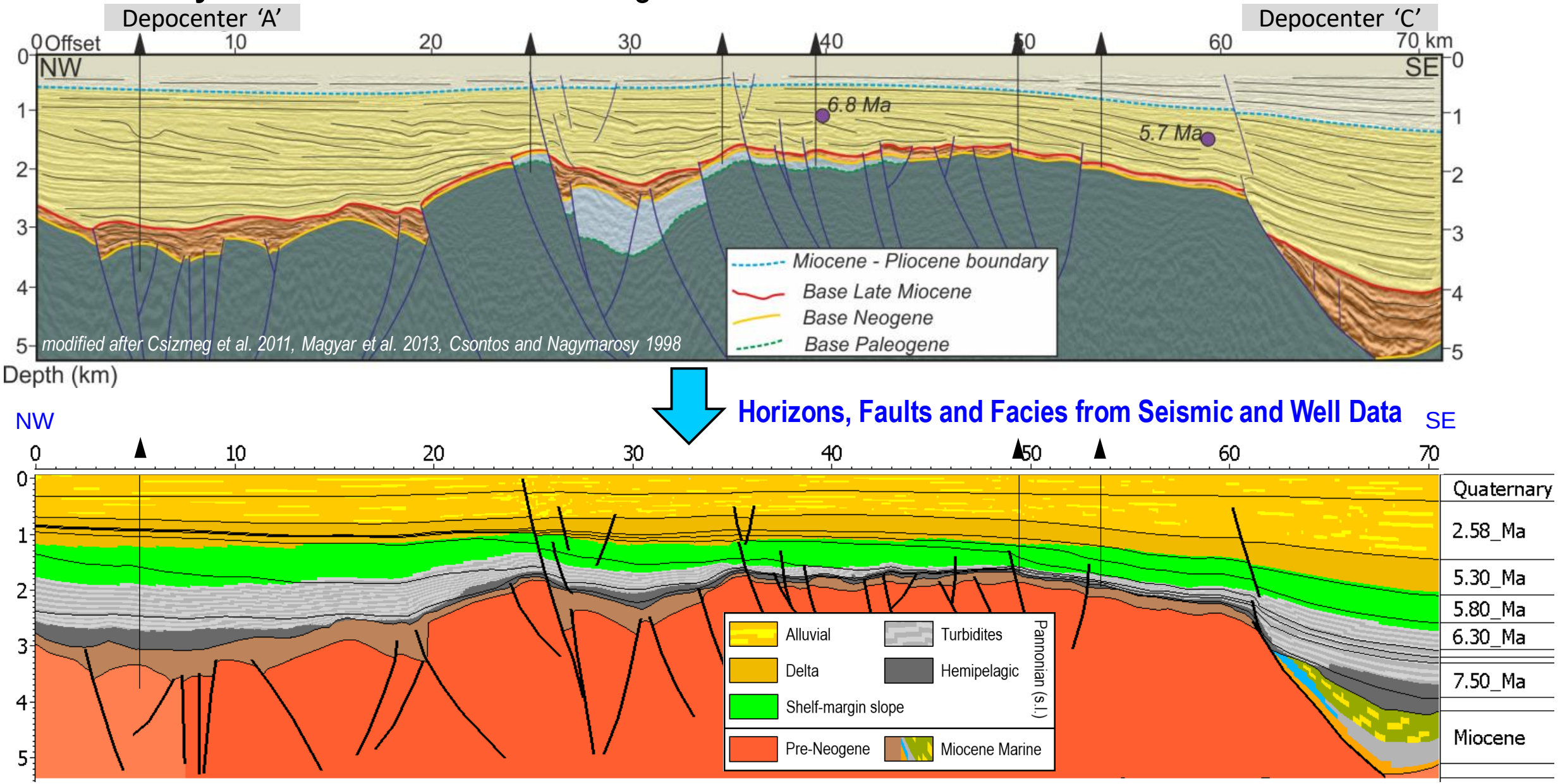

Figure 13

Petroleum Systems Model: Technical Challenges

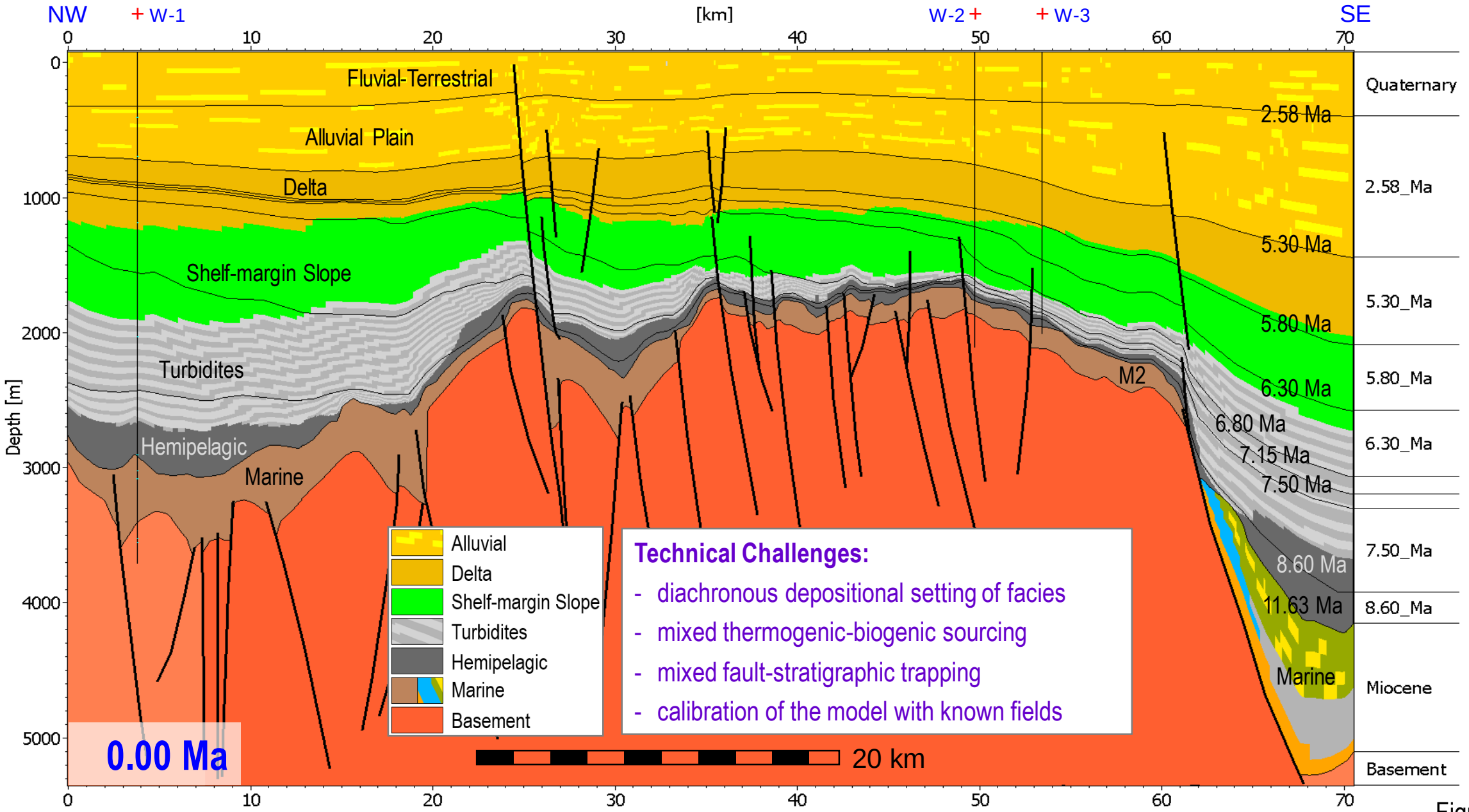

Figure 14

Petroleum Systems Model: Technical Solutions

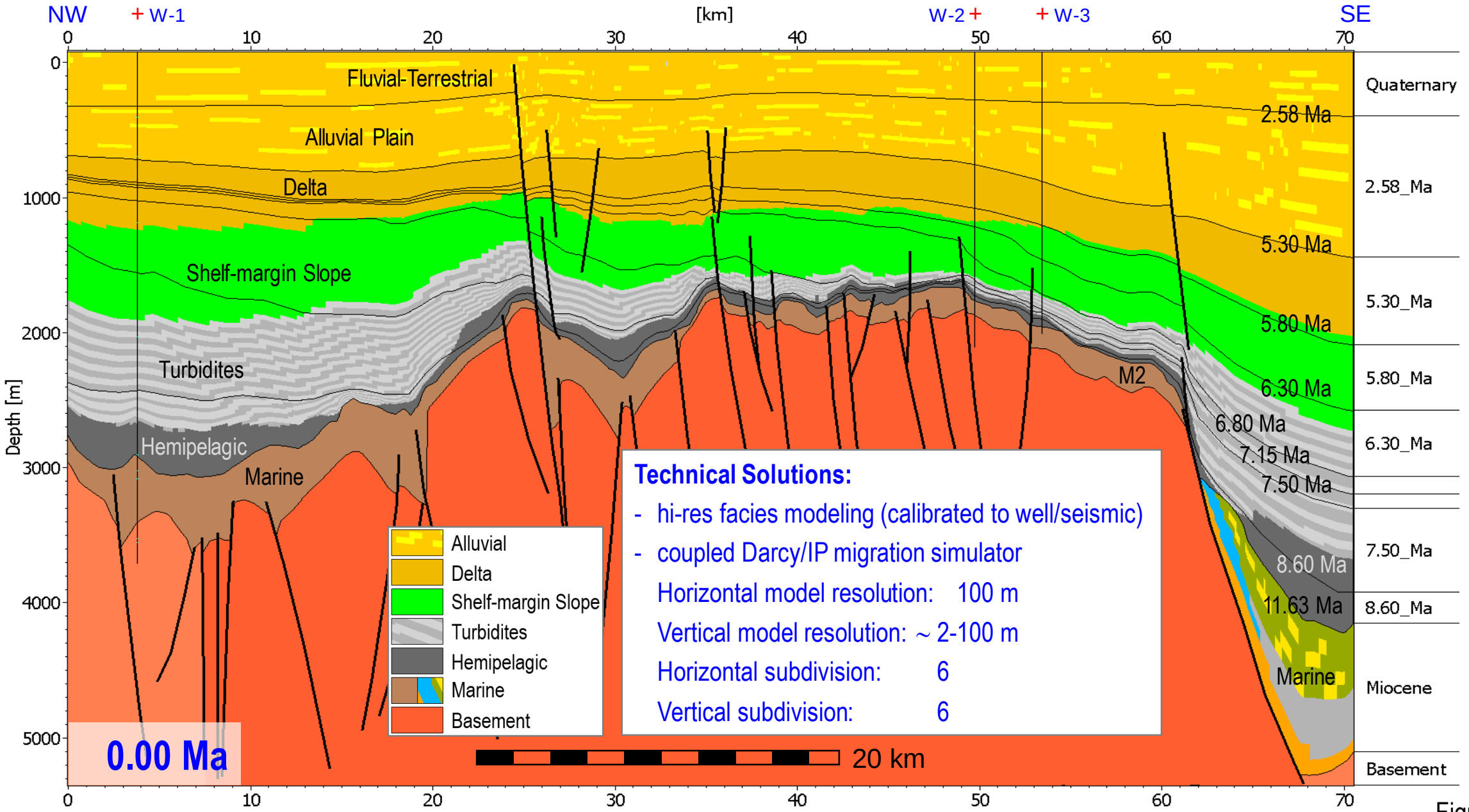

Figure 15

Structural Restoration: Combining Event-stepping with Paleo-stepping

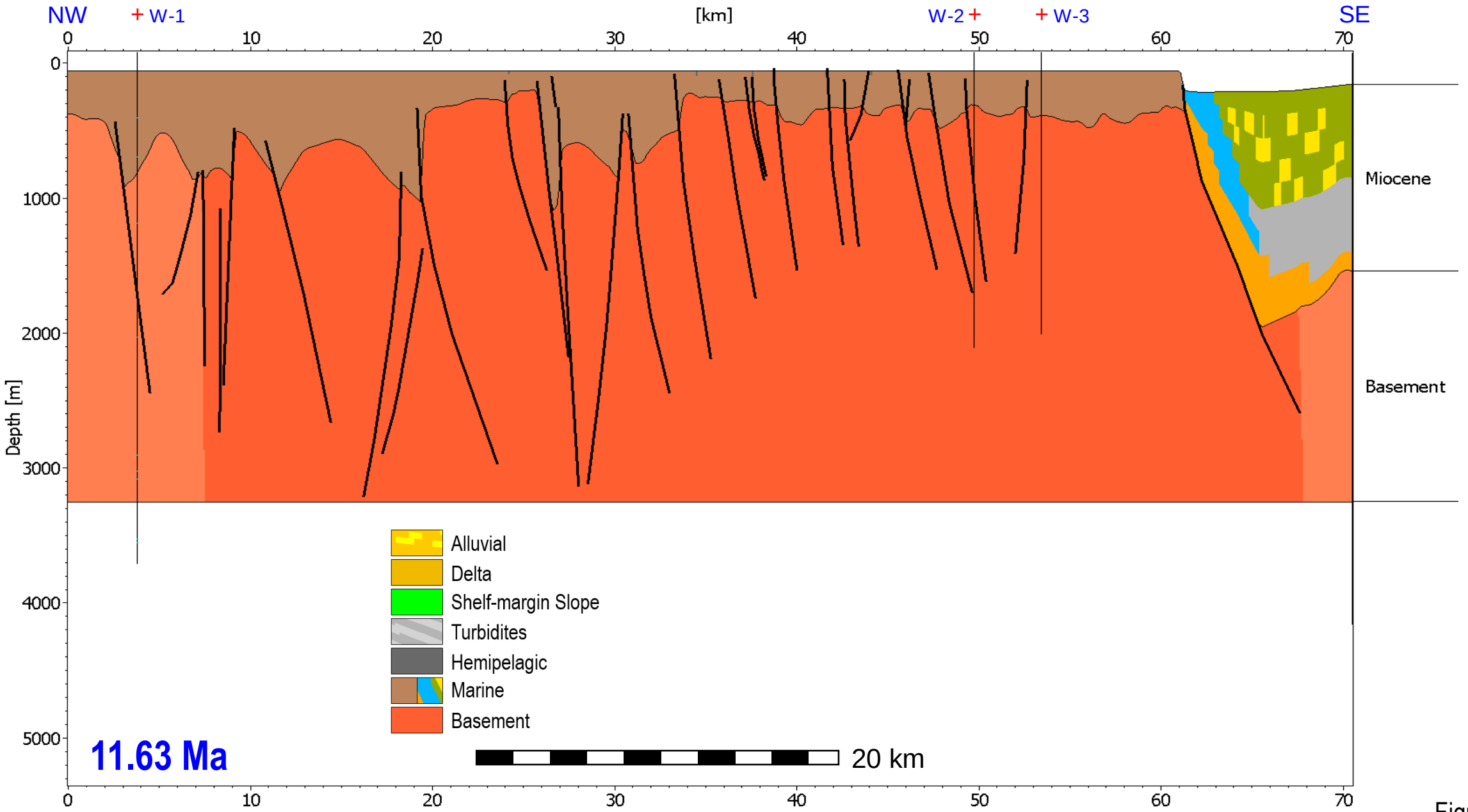

Figure 16

Structural Restoration: Combining Event-stepping with Paleo-stepping

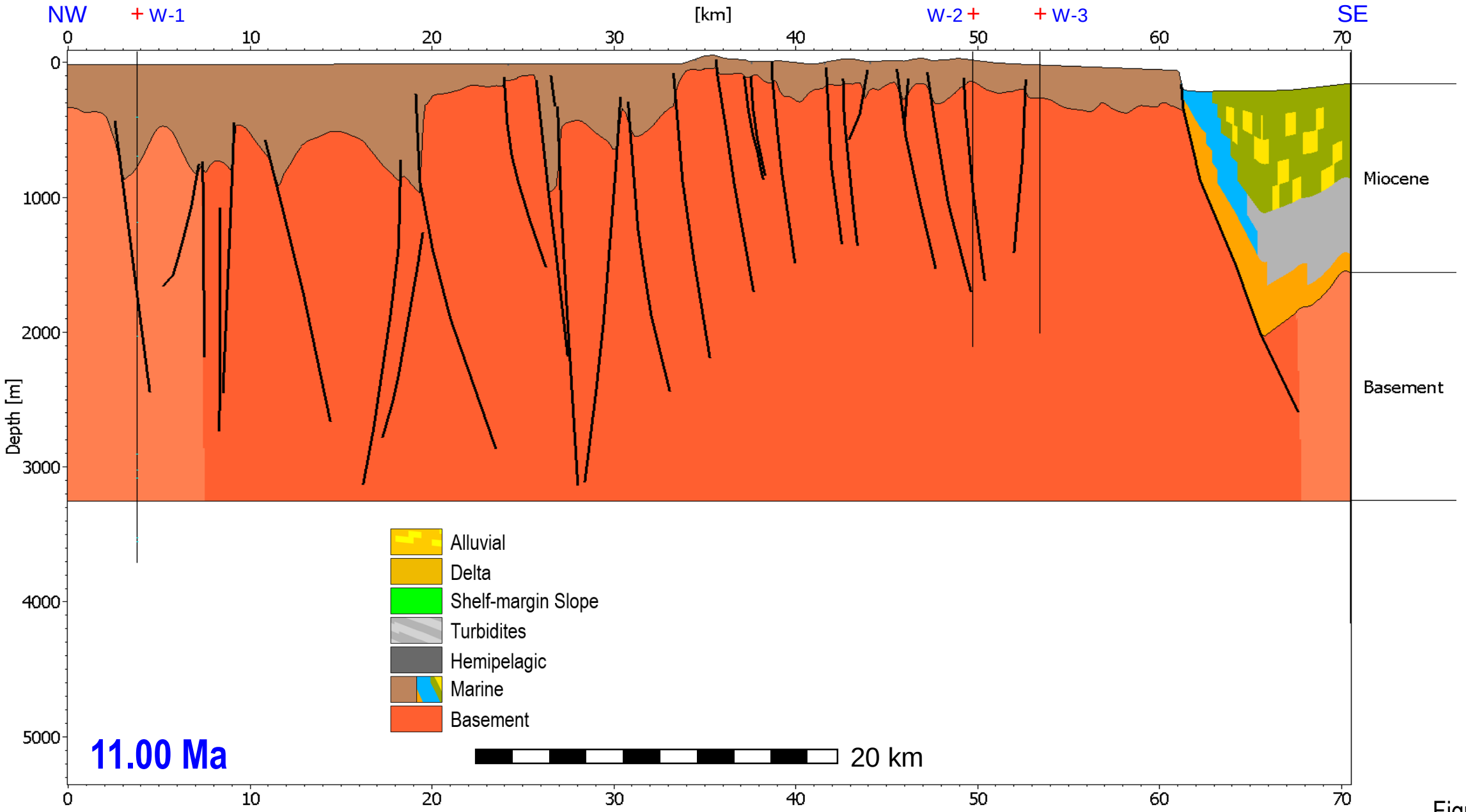

Figure 17

Structural Restoration: Combining Event-stepping with Paleo-stepping

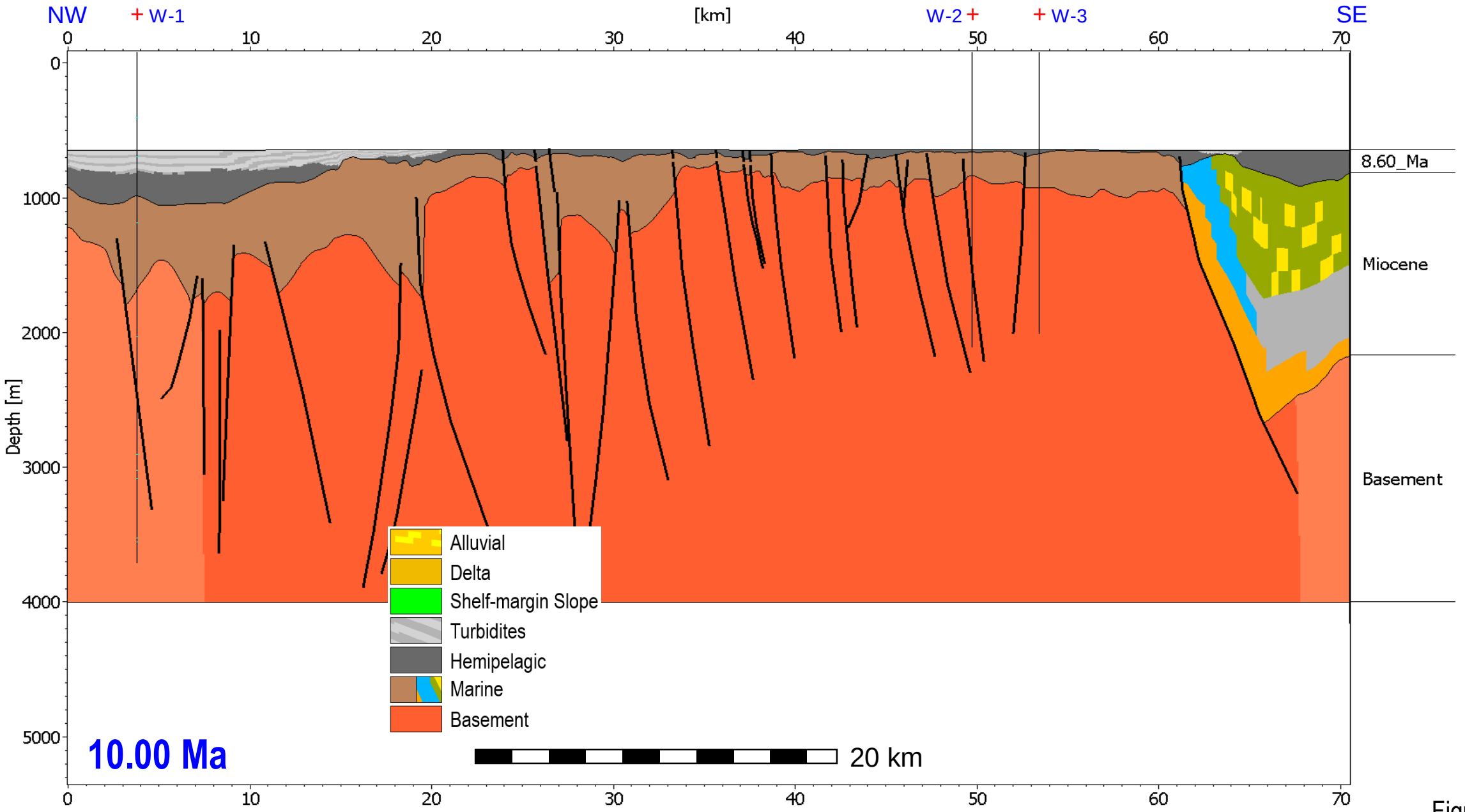

Figure 18

Structural Restoration: Combining Event-stepping with Paleo-stepping

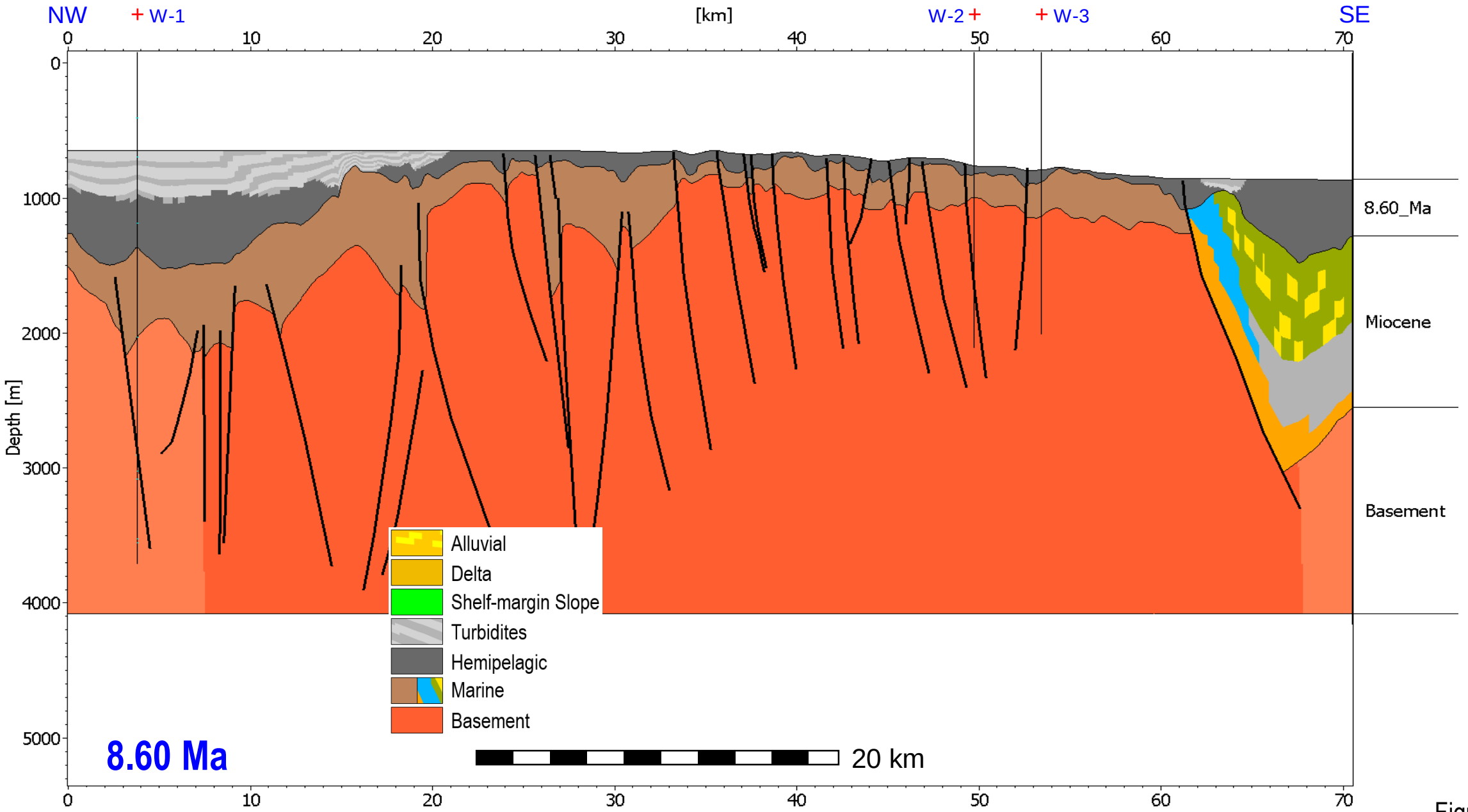

Figure 19

Structural Restoration: Combining Event-stepping with Paleo-stepping

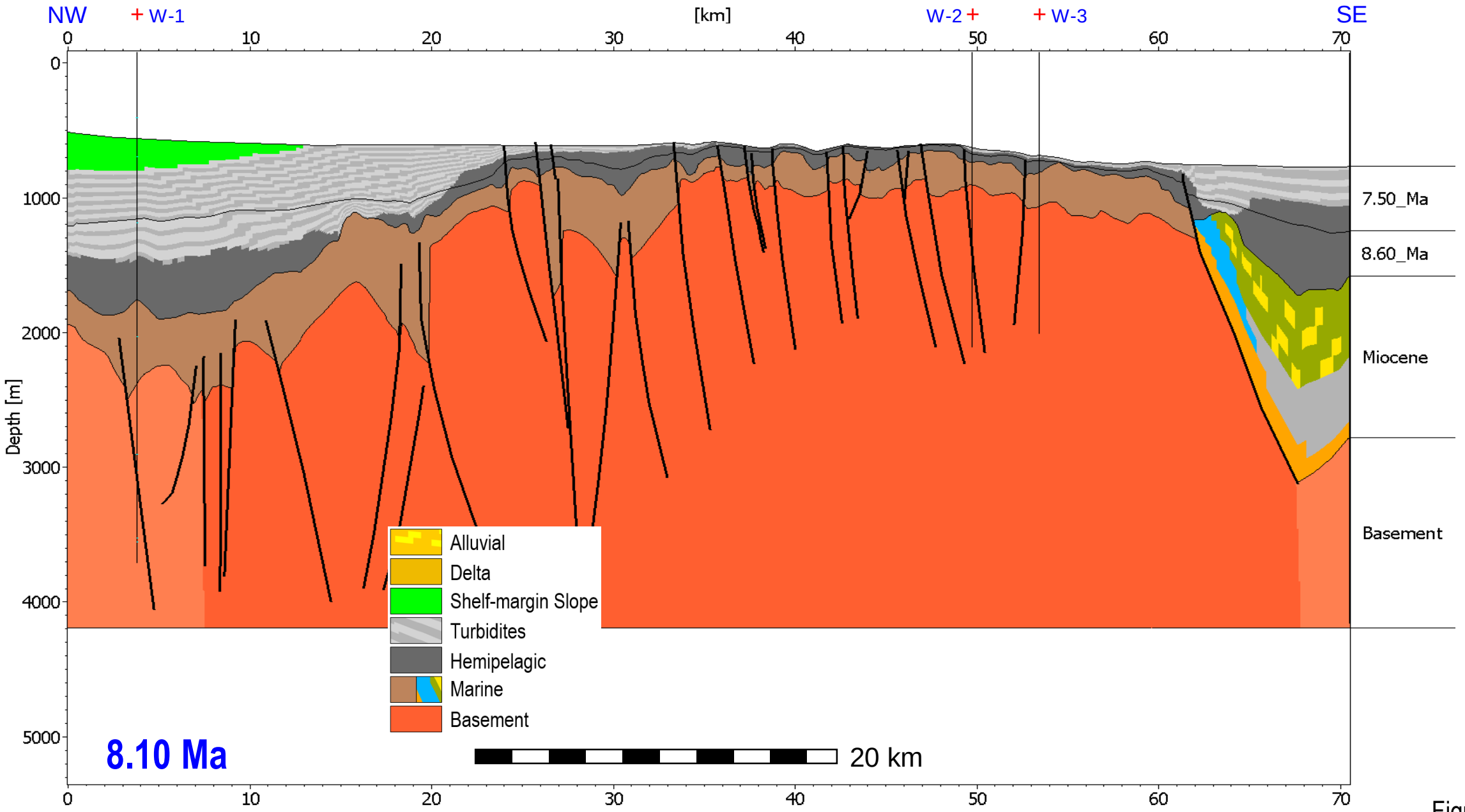

Figure 20

Structural Restoration: Combining Event-stepping with Paleo-stepping

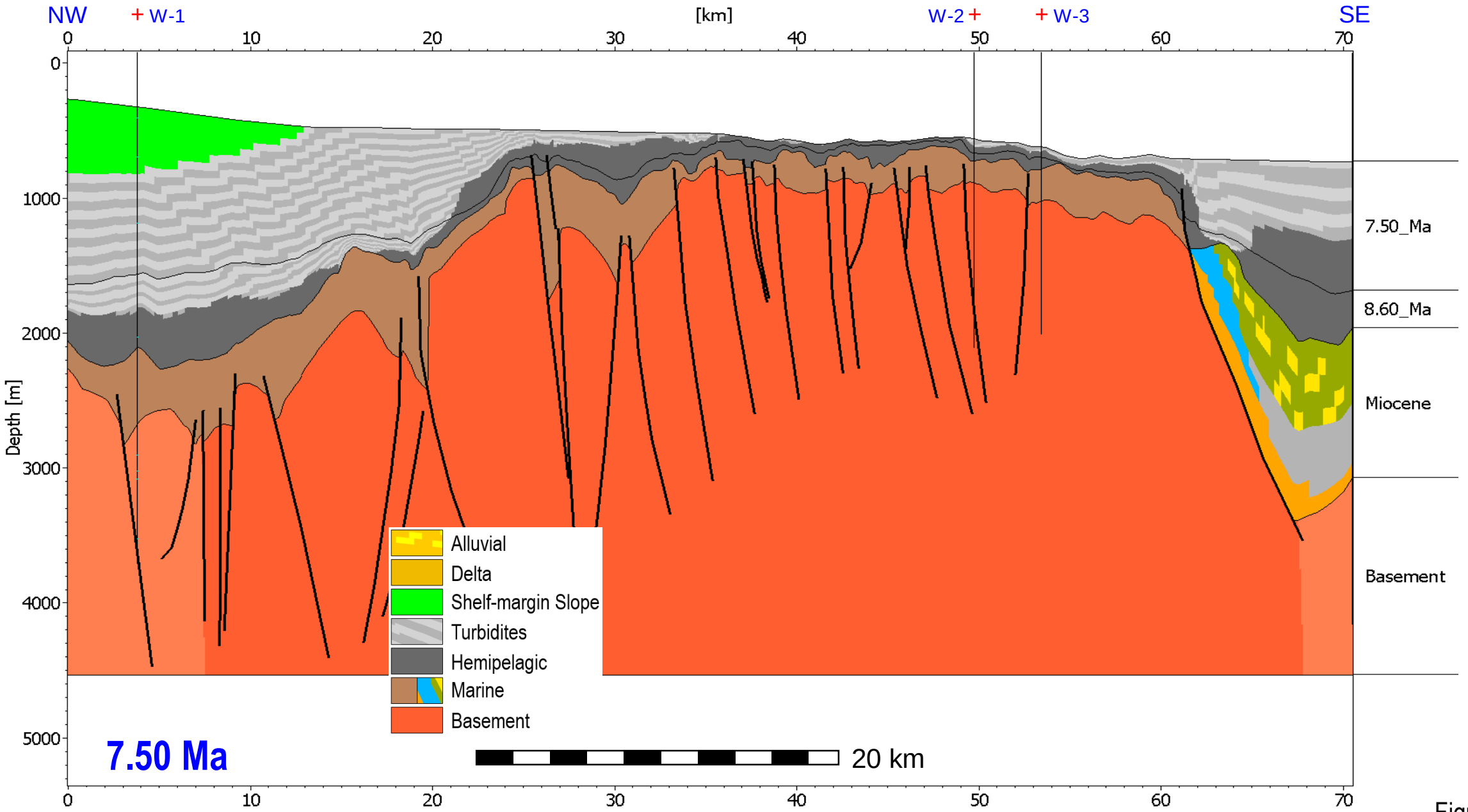

Figure 21

Structural Restoration: Combining Event-stepping with Paleo-stepping

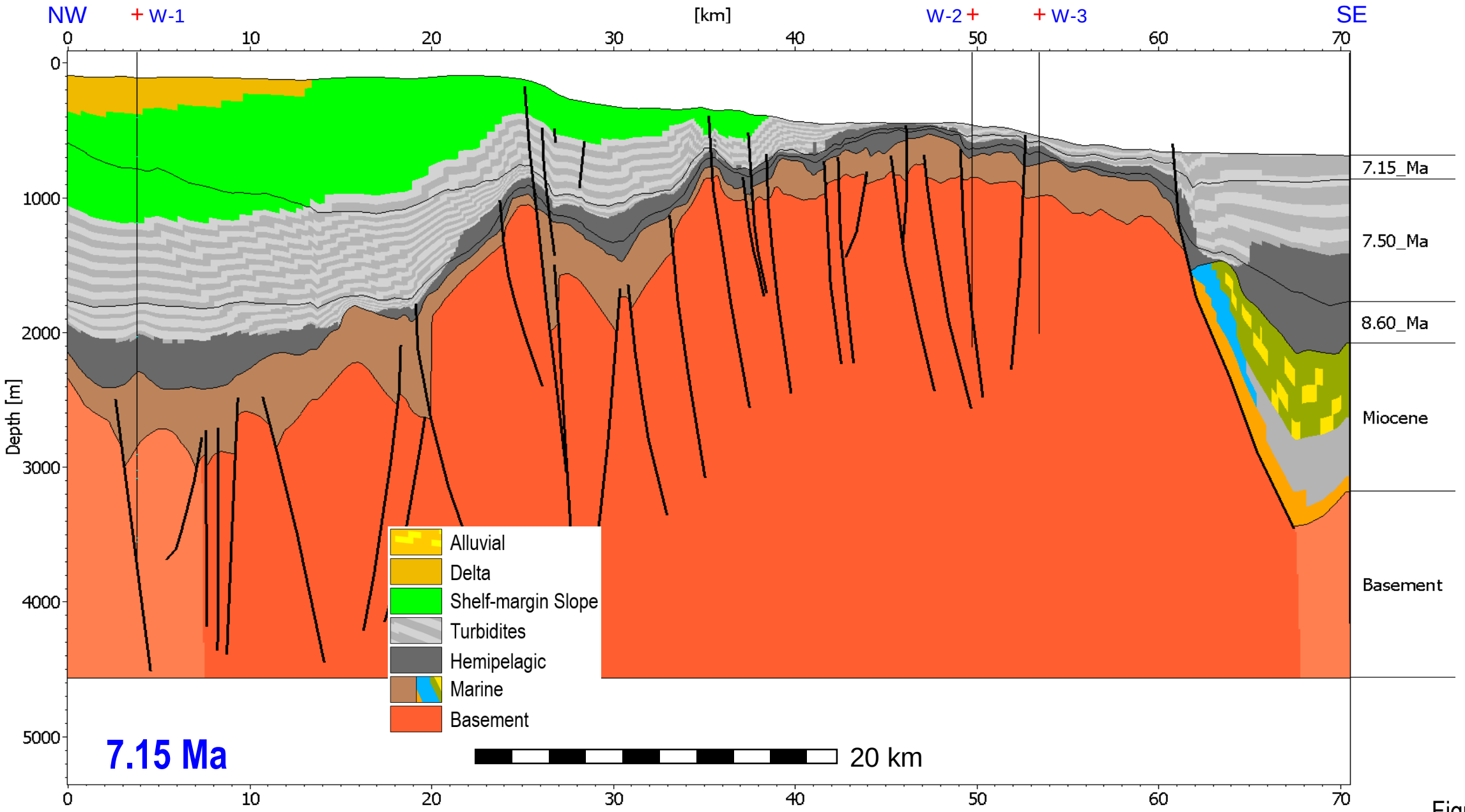

Figure 22

Structural Restoration: Combining Event-stepping with Paleo-stepping

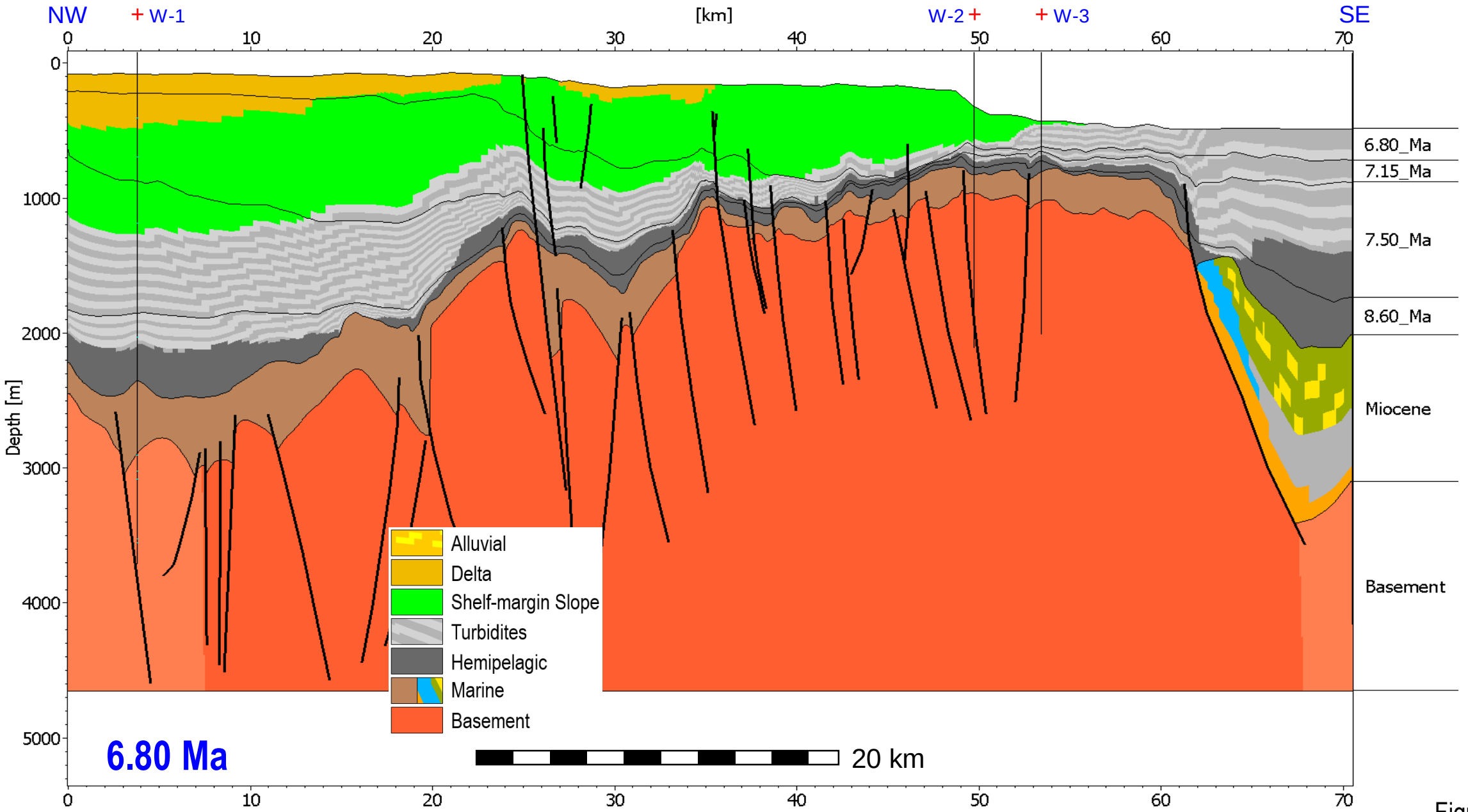

Figure 23

Structural Restoration: Combining Event-stepping with Paleo-stepping

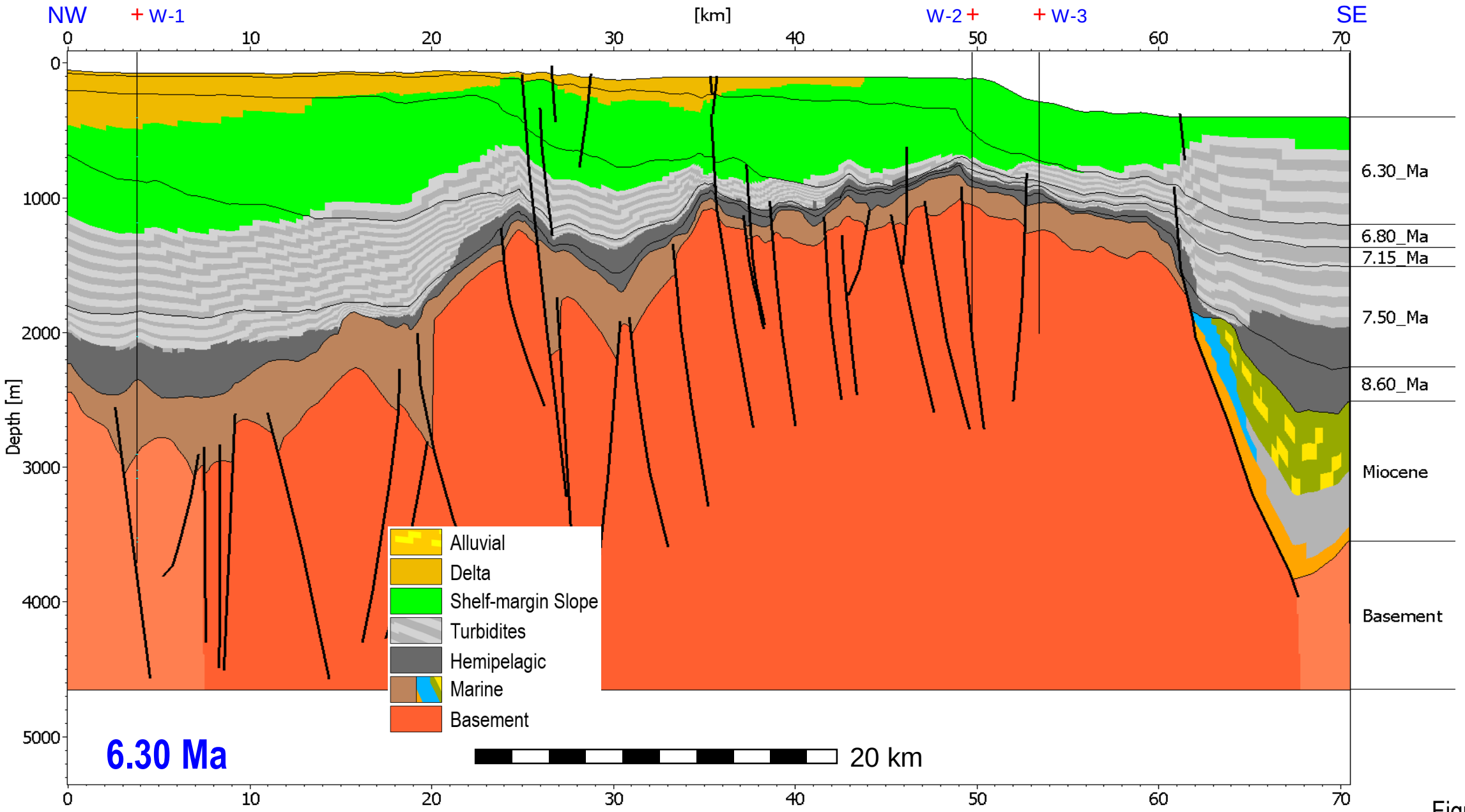

Figure 24

Structural Restoration: Combining Event-stepping with Paleo-stepping

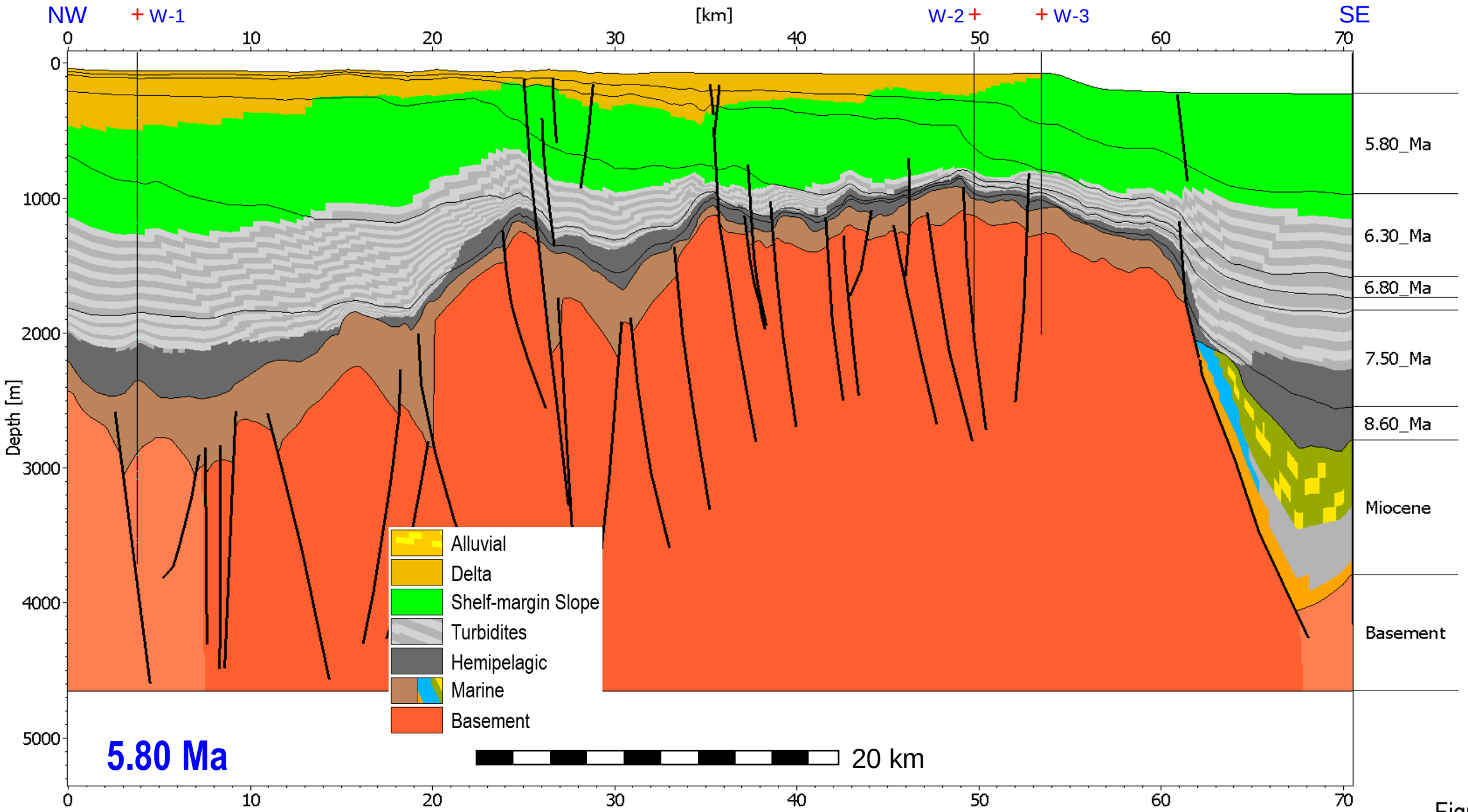

Figure 25

Structural Restoration: Combining Event-stepping with Paleo-stepping

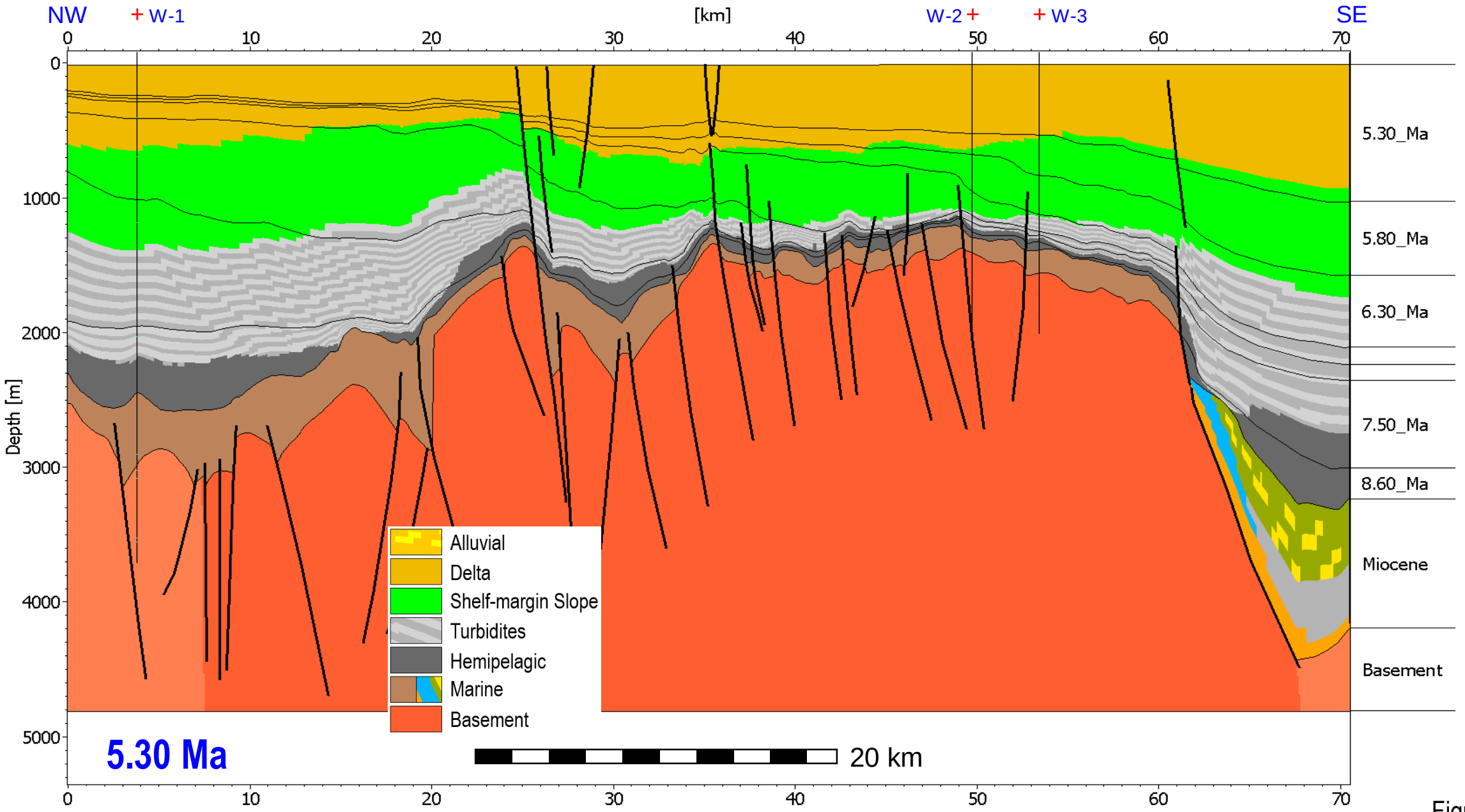

Figure 26

Structural Restoration: Combining Event-stepping with Paleo-stepping

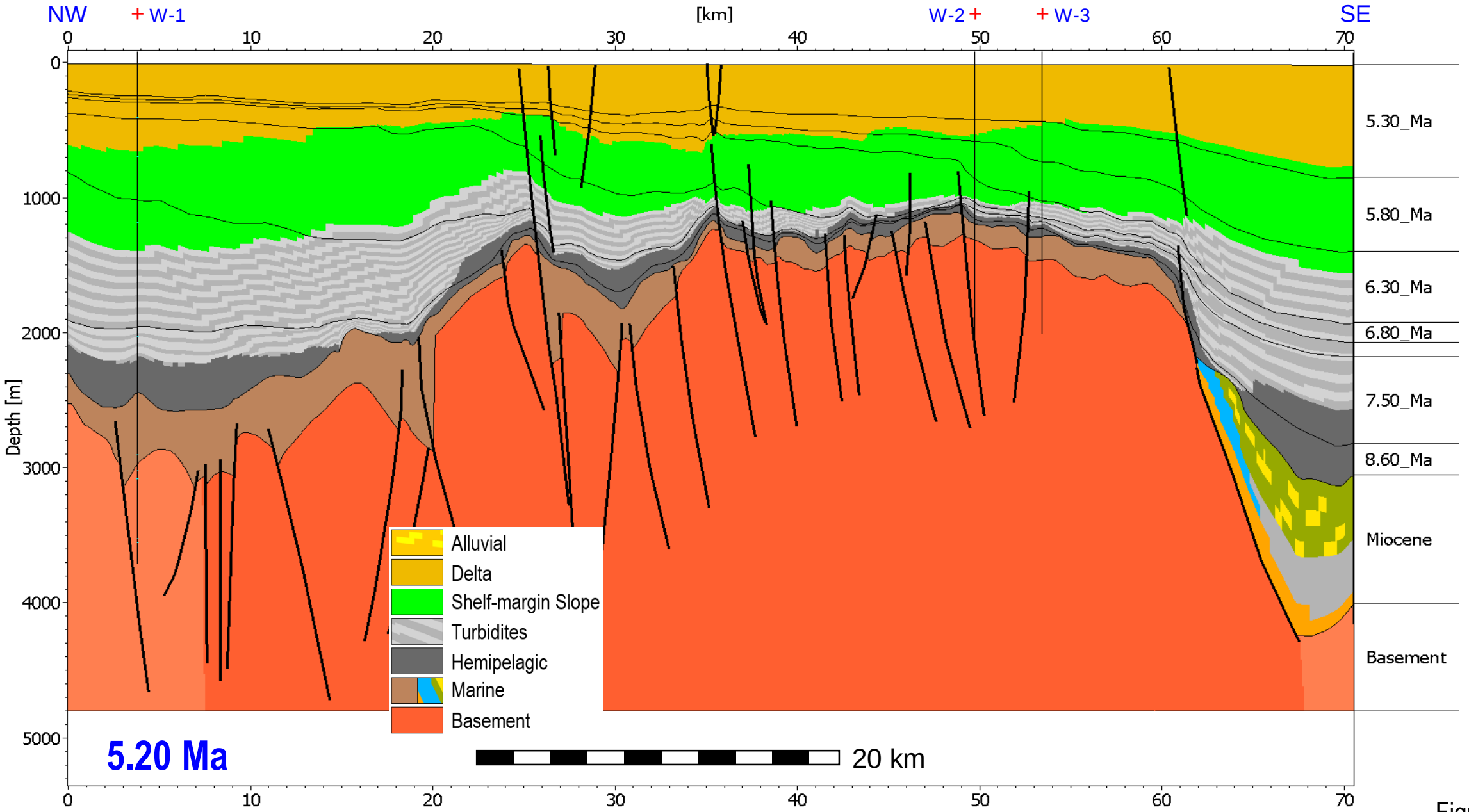

Figure 27

Structural Restoration: Combining Event-stepping with Paleo-stepping

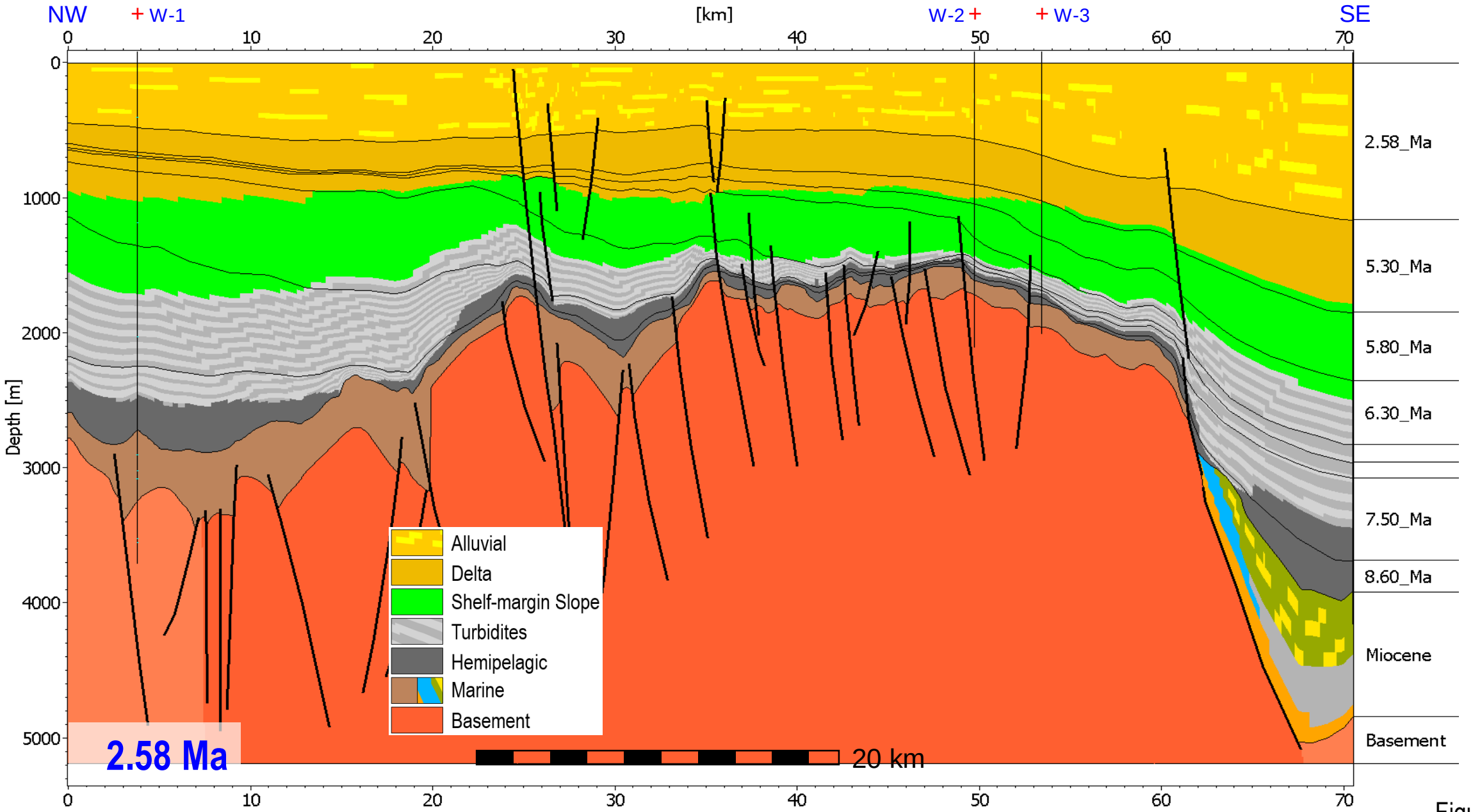

Figure 28

Structural Restoration: Combining Event-stepping with Paleo-stepping

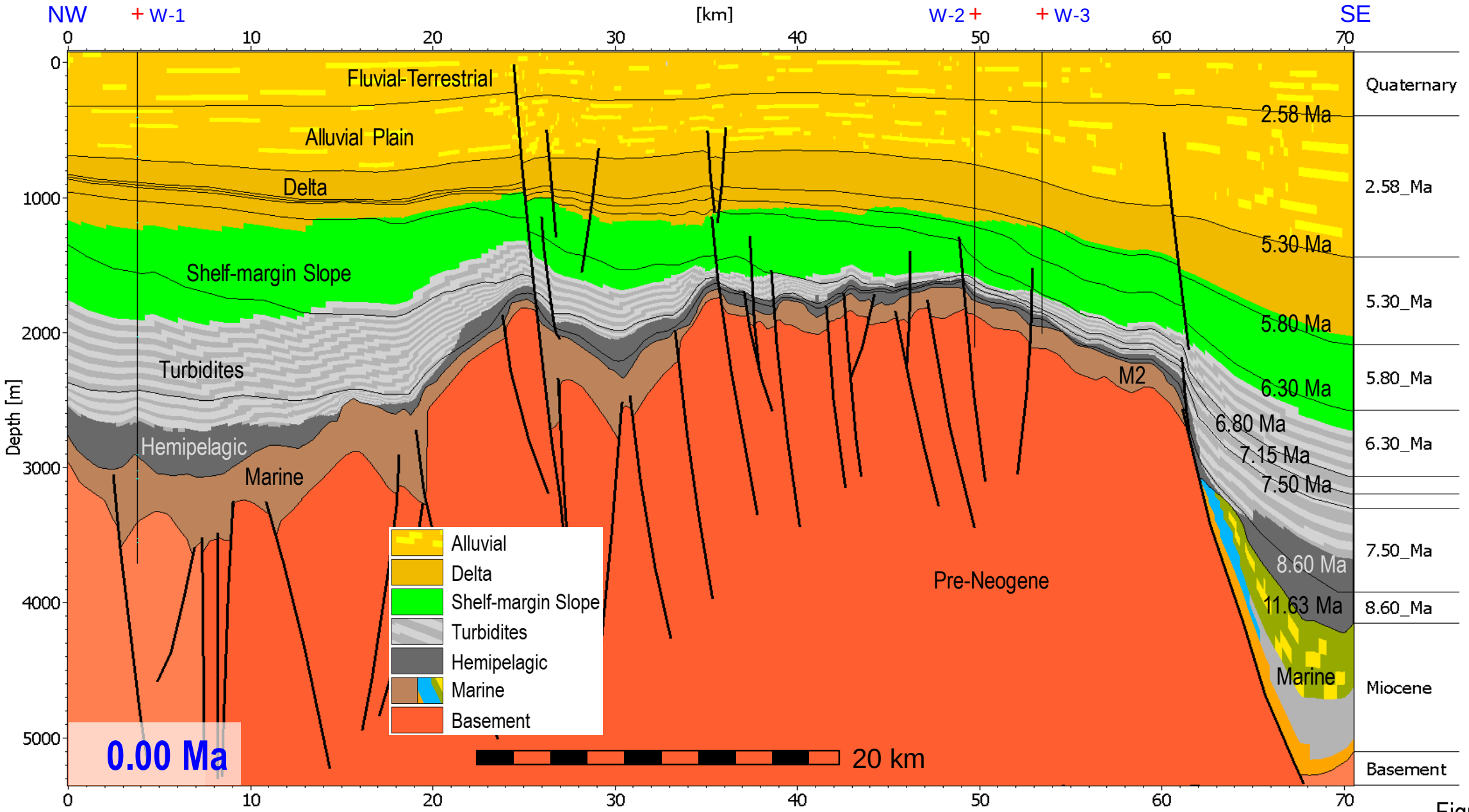

Figure 29

Petroleum Systems Model: Crustal Heat Flow Modeling

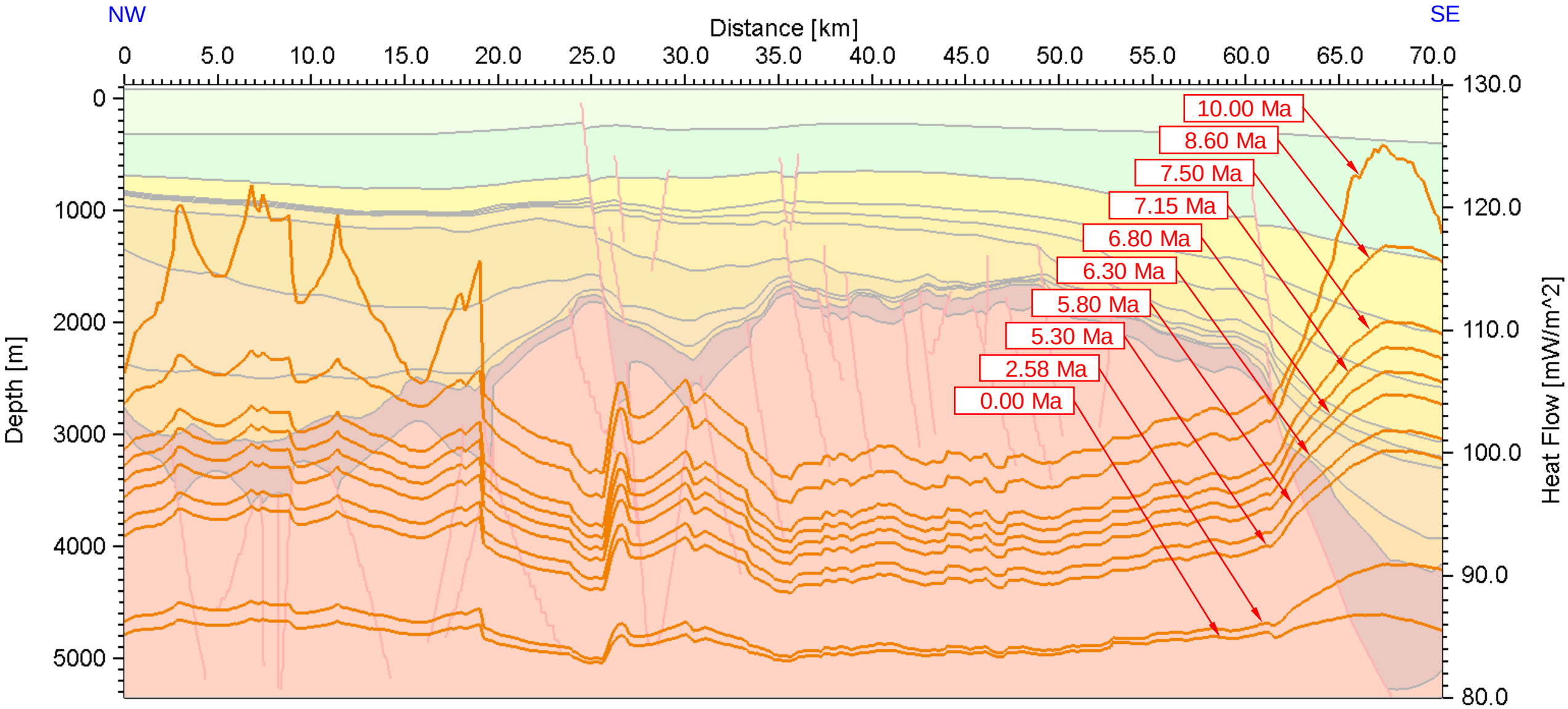

Distribution of basal heat flow values (in mW/m^2) along the modeled section at different time-steps defined in the model.

Figure 30

Petroleum Systems Model: Calculated Trends Are in Good Agreement with Measured Data (W-1)

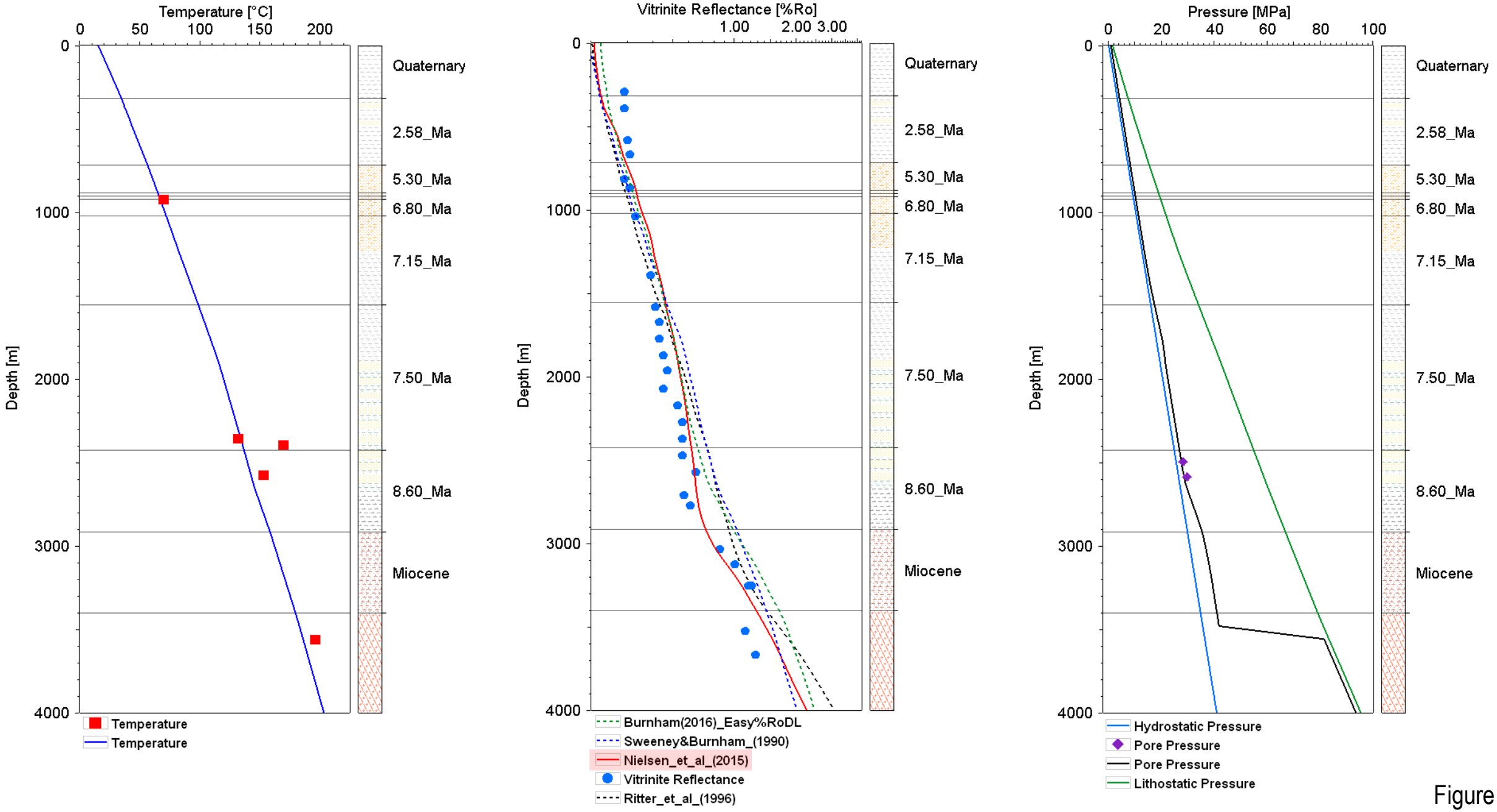

Figure 31

Controlling Factors: Sufficient Charge Does Not Require High Amounts and High Quality Organic Matter

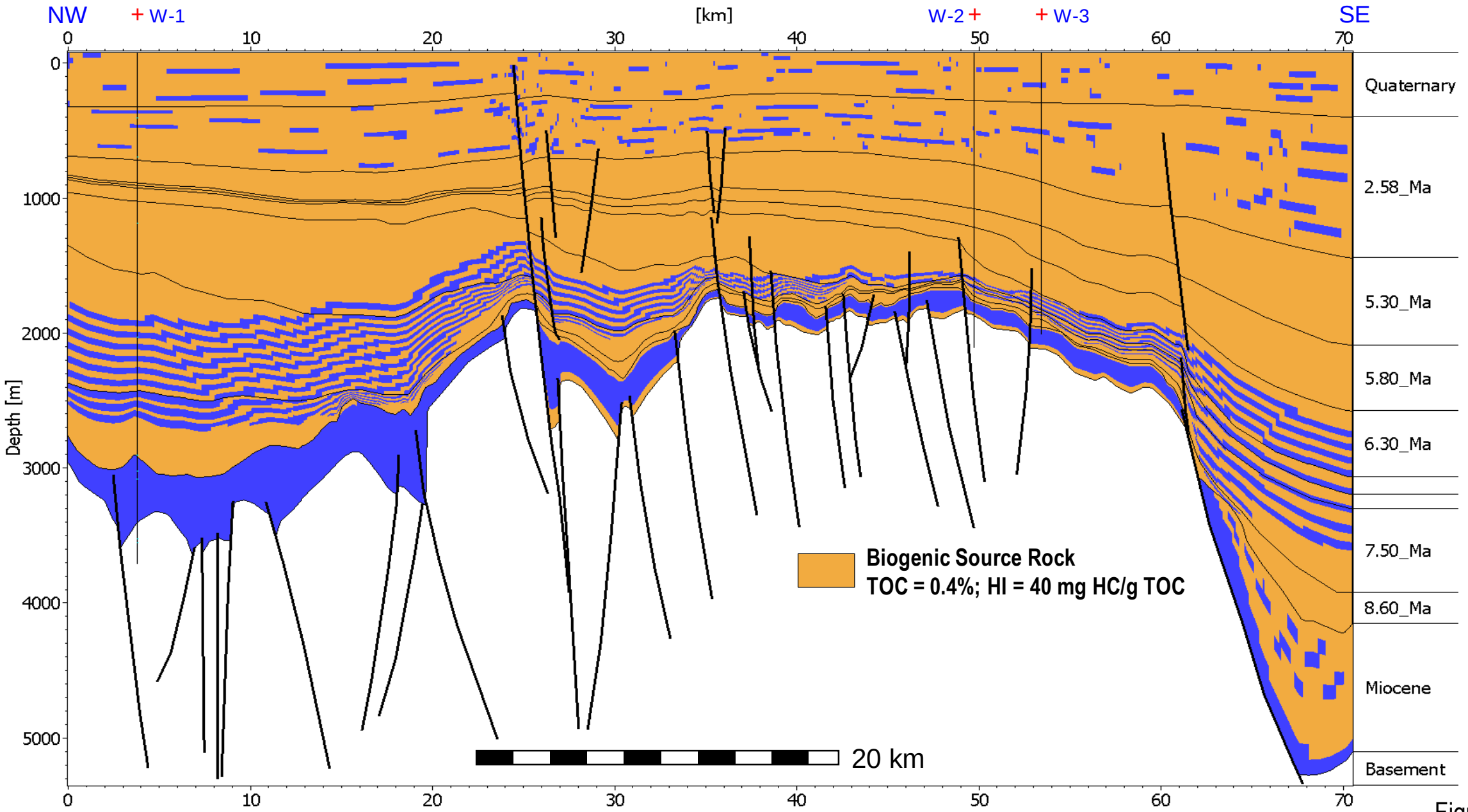

Figure 32

Controlling Factors: Sufficient Charge Does Not Require High Amounts and High Quality Organic Matter

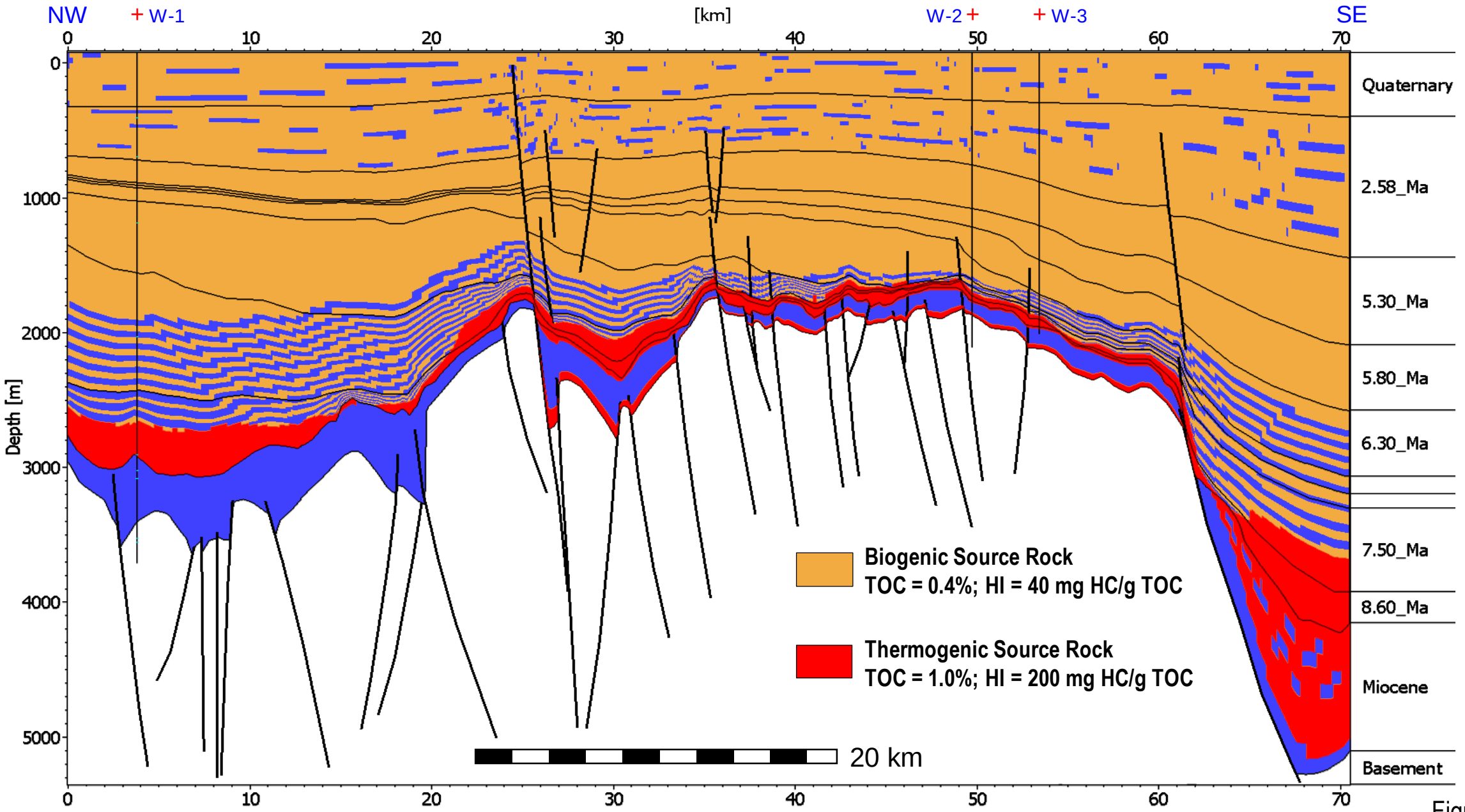

Figure 33

Controlling Factors: Hydrocarbon Generation Zones at Present Day

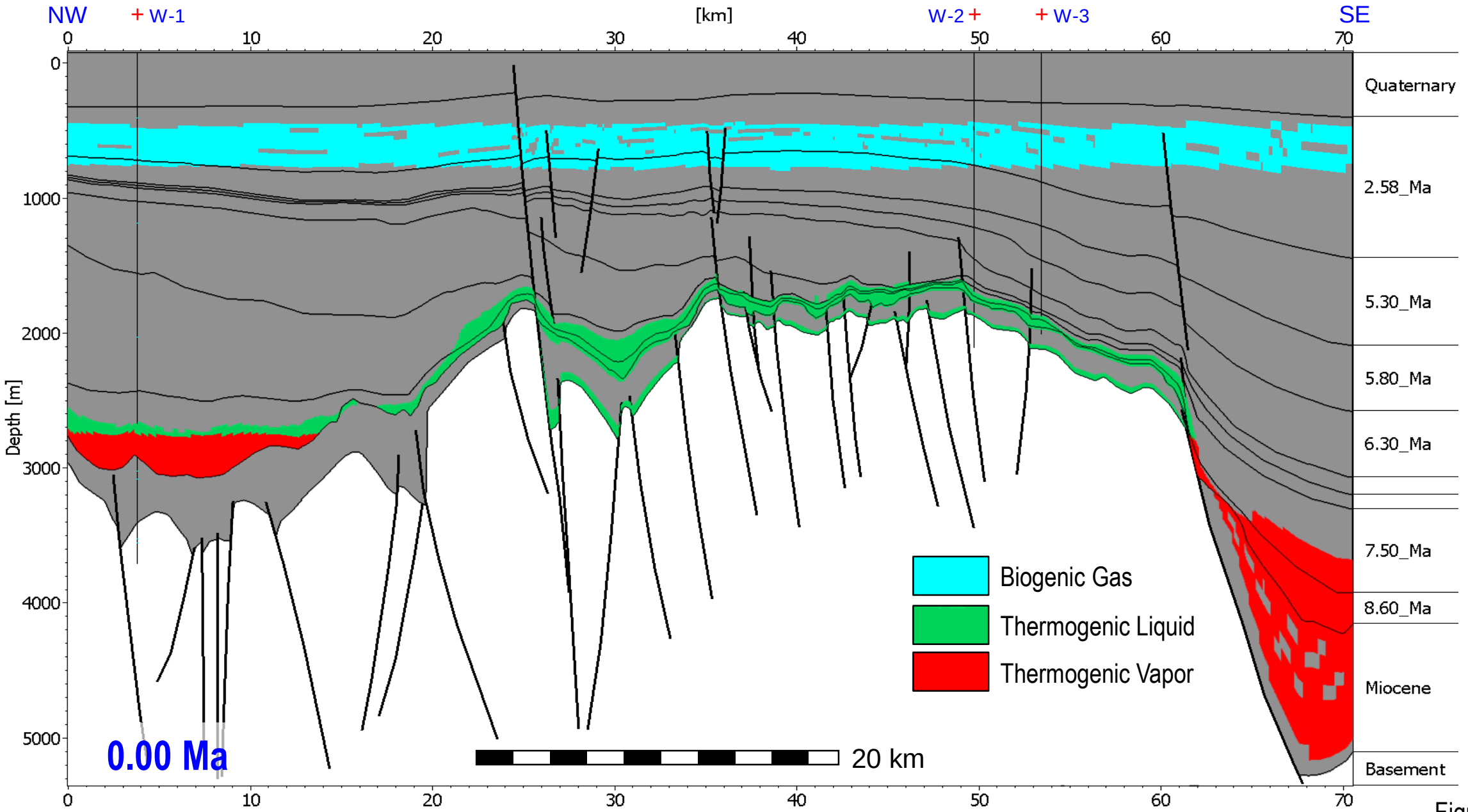

Figure 34

Controlling Factors: Interplay Between Biogenic and Thermogenic Source Rocks

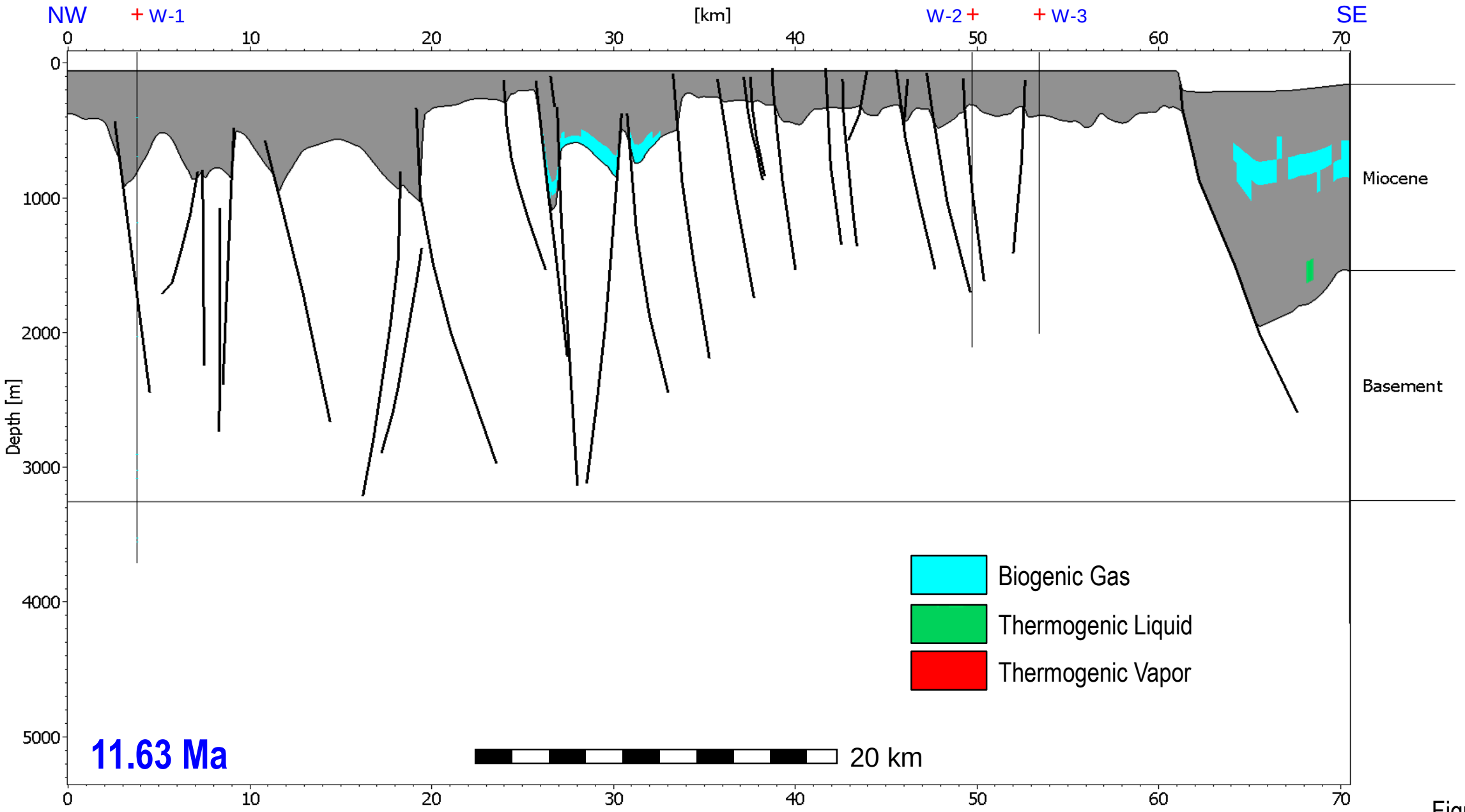

Figure 35

Controlling Factors: Interplay Between Biogenic and Thermogenic Source Rocks

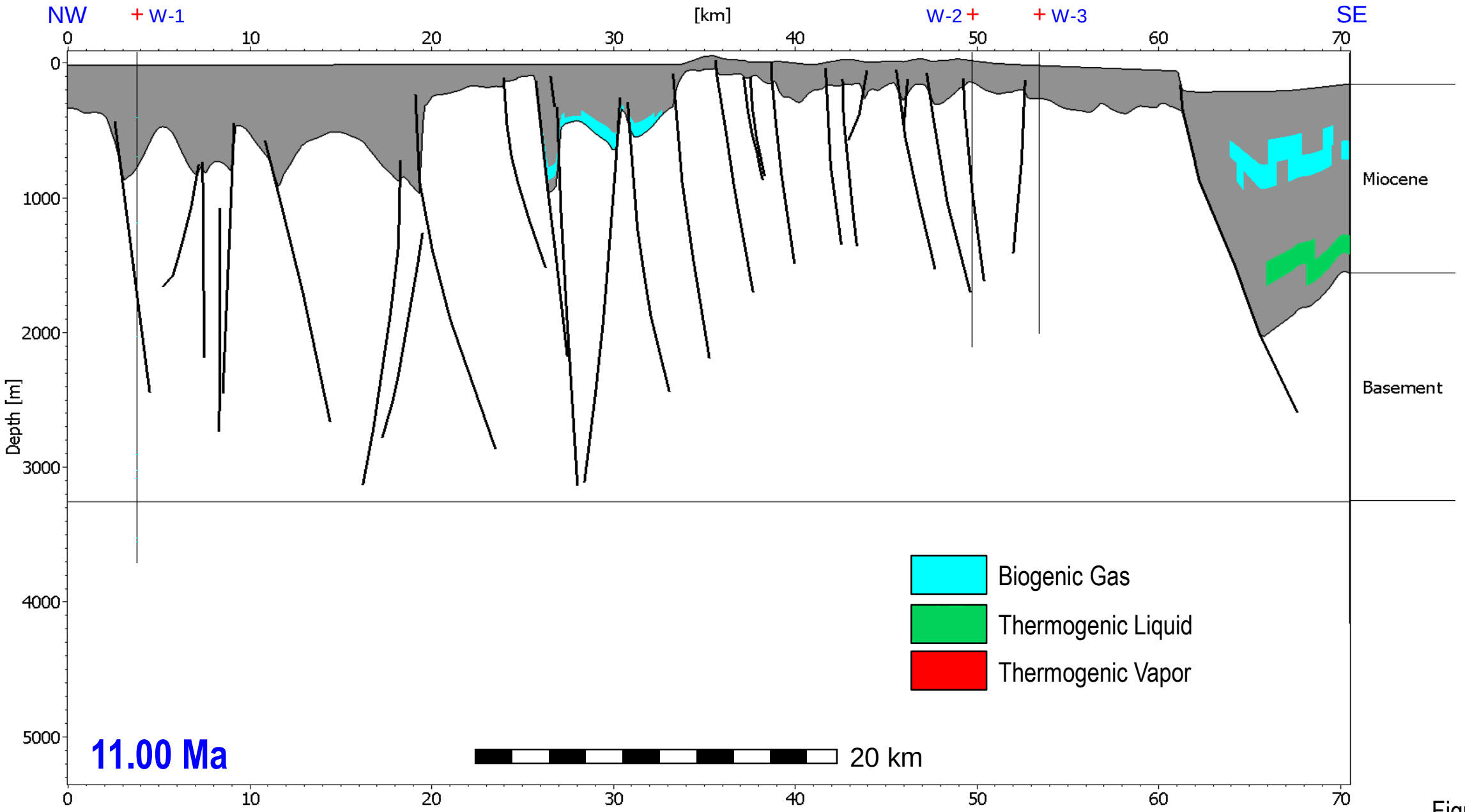

Figure 36

Controlling Factors: Interplay Between Biogenic and Thermogenic Source Rocks

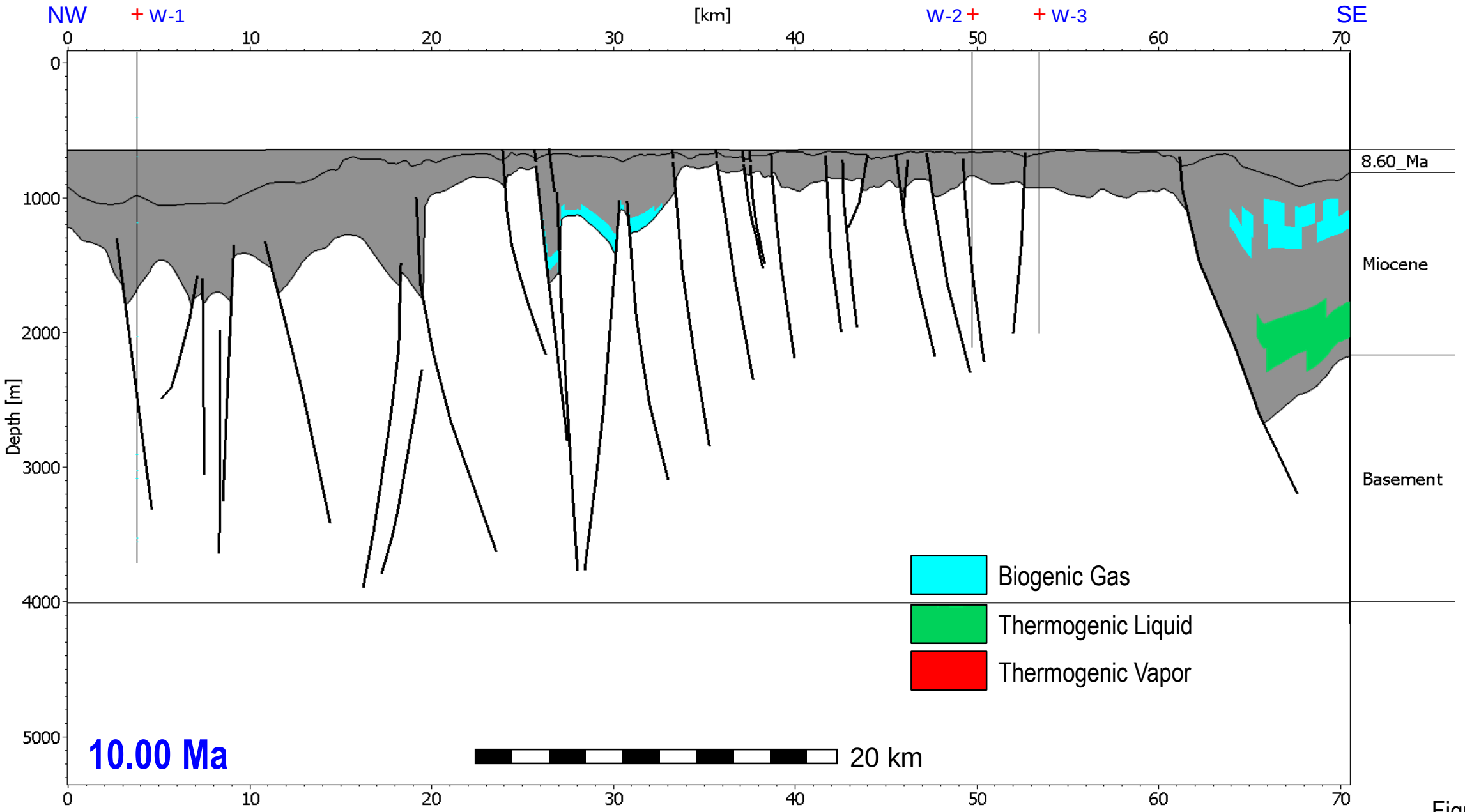

Figure 37

Controlling Factors: Interplay Between Biogenic and Thermogenic Source Rocks

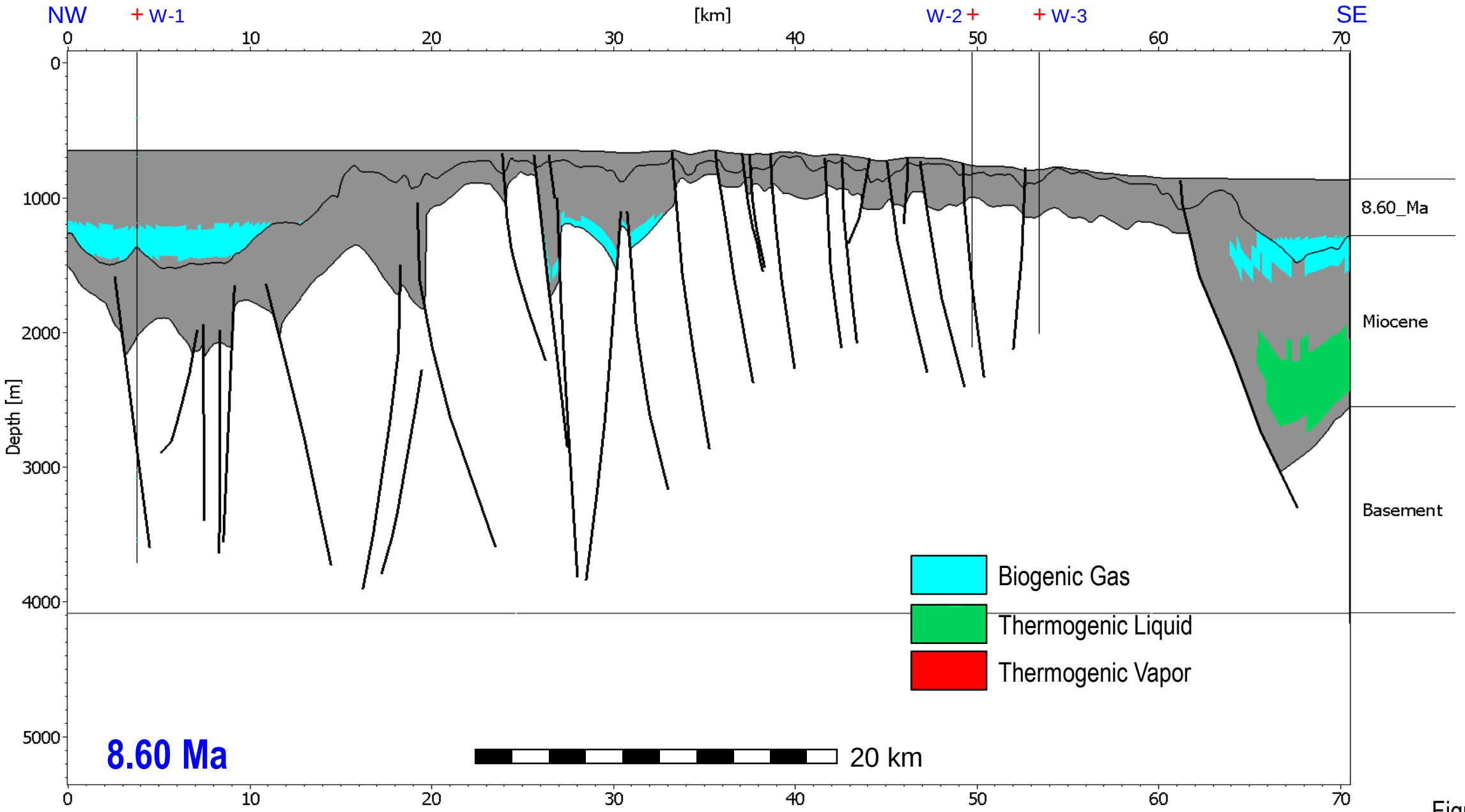

Figure 38

Controlling Factors: Interplay Between Biogenic and Thermogenic Source Rocks

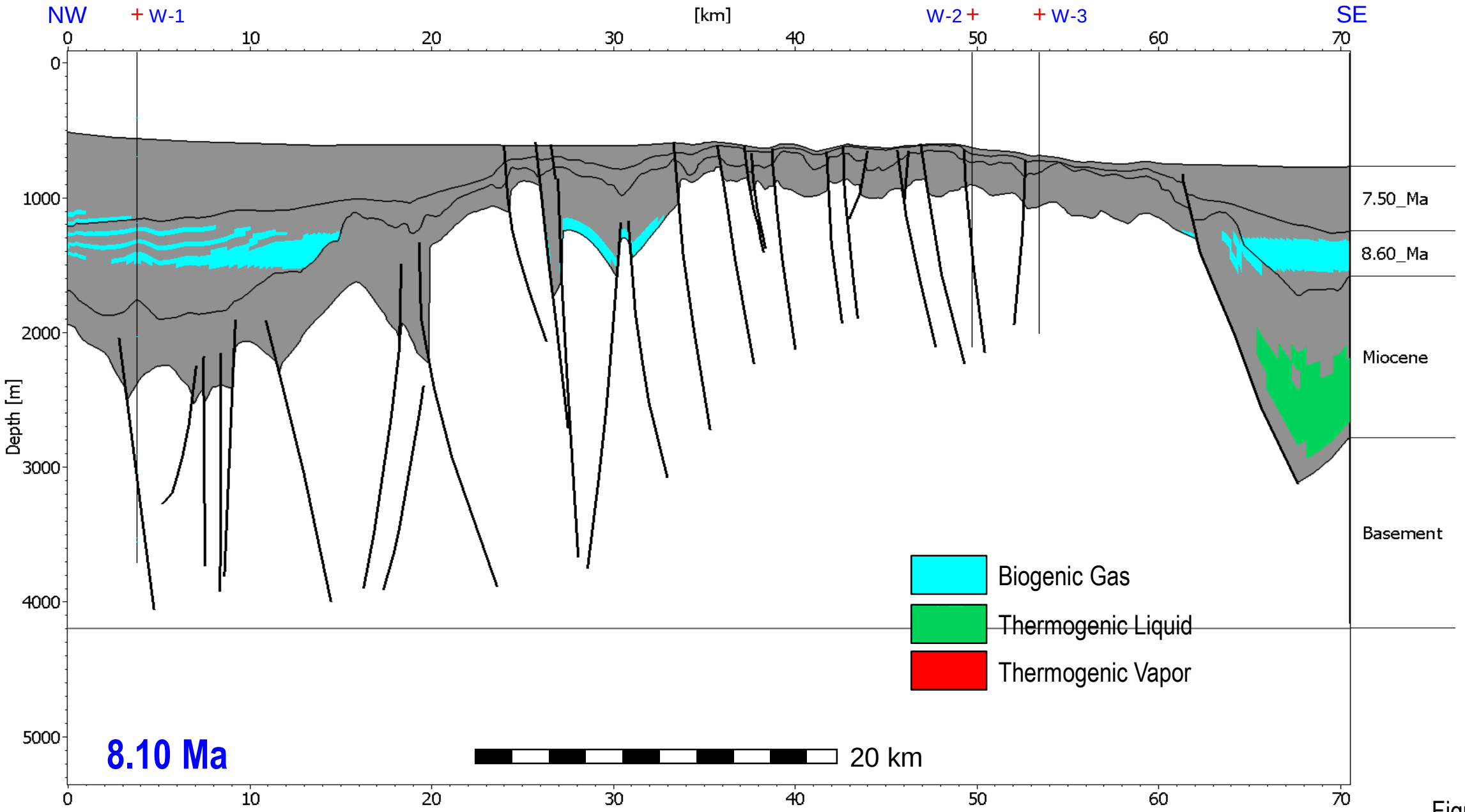

Figure 39

Controlling Factors: Interplay Between Biogenic and Thermogenic Source Rocks

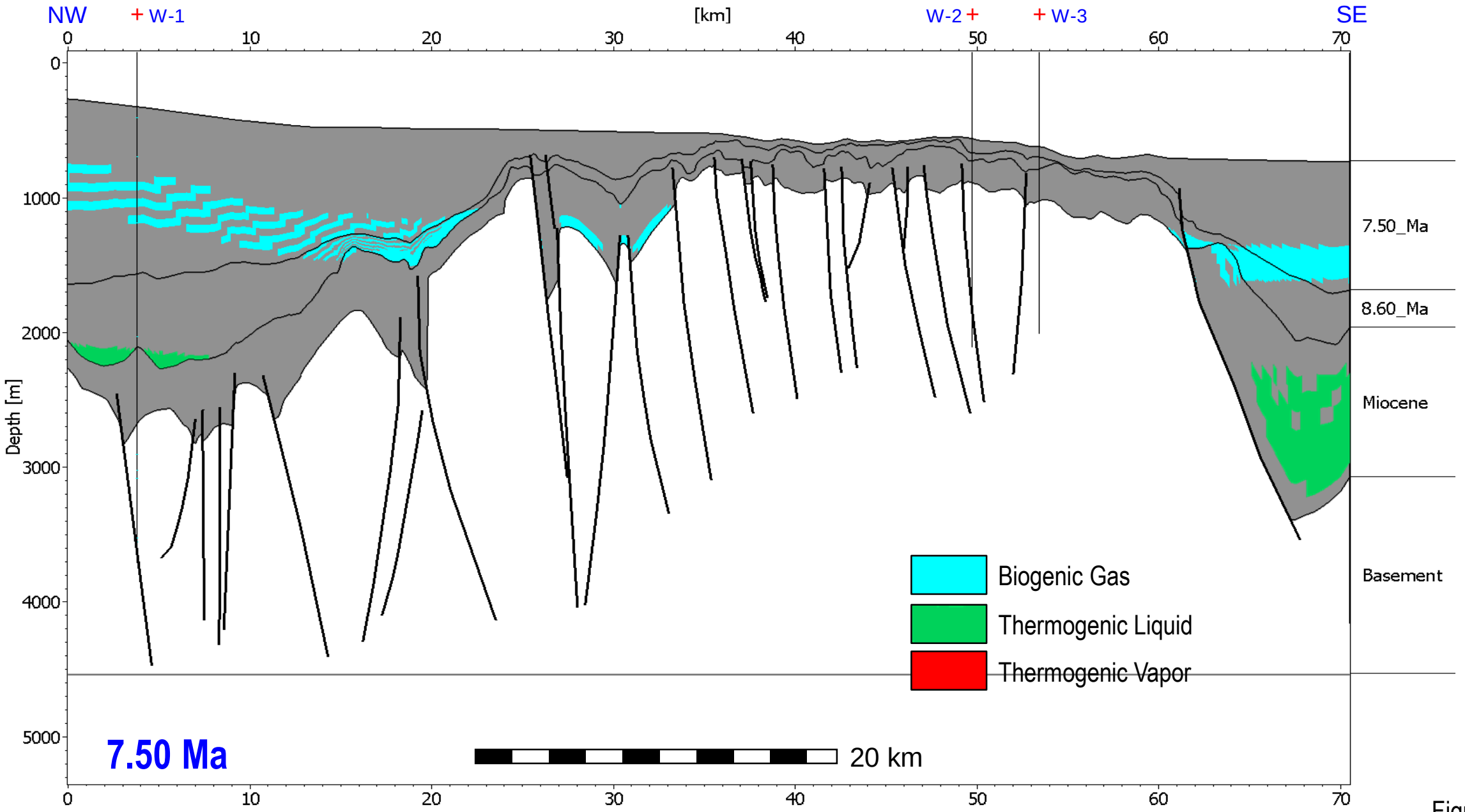

Figure 40

Controlling Factors: Interplay Between Biogenic and Thermogenic Source Rocks

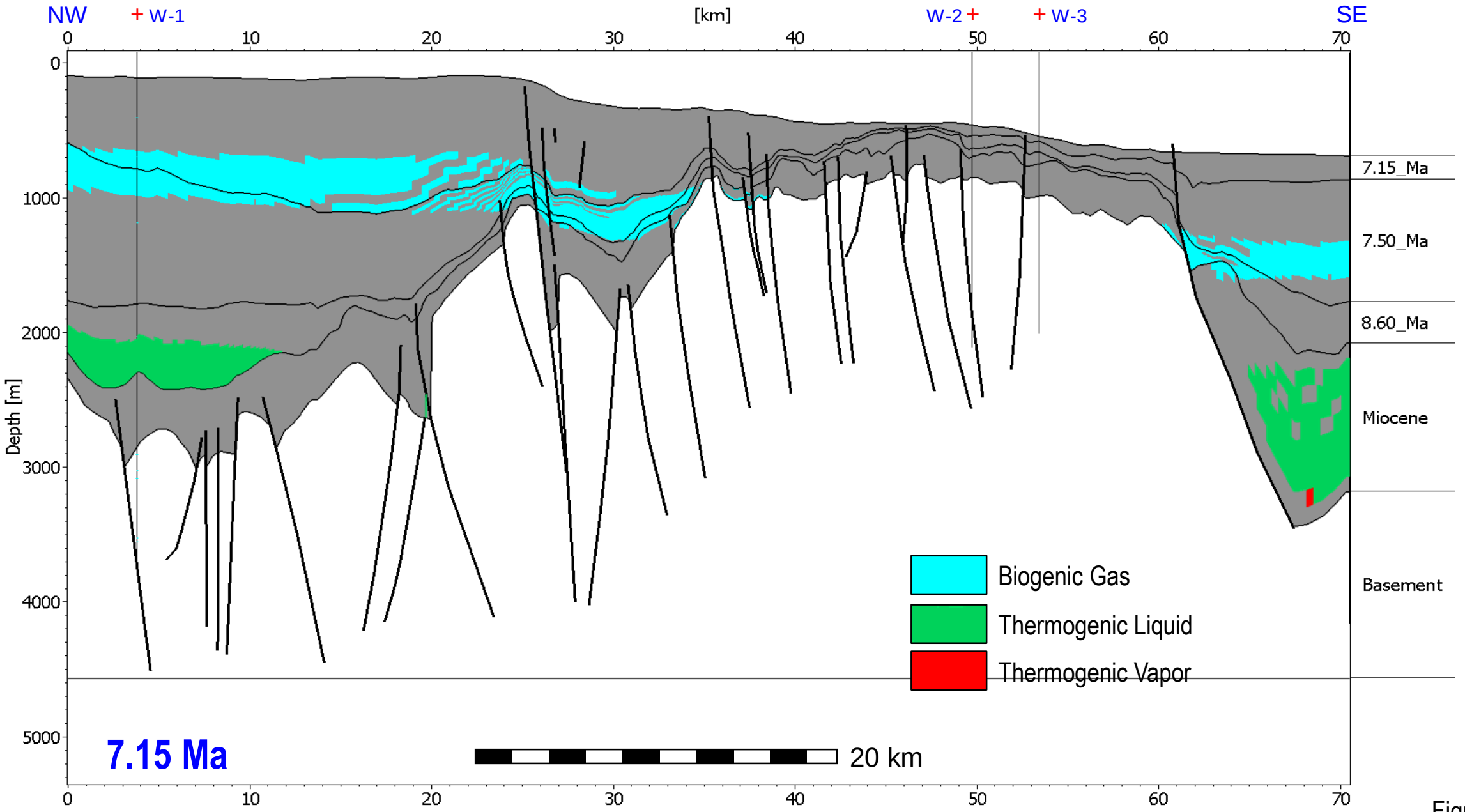

Figure 41

Controlling Factors: Interplay Between Biogenic and Thermogenic Source Rocks

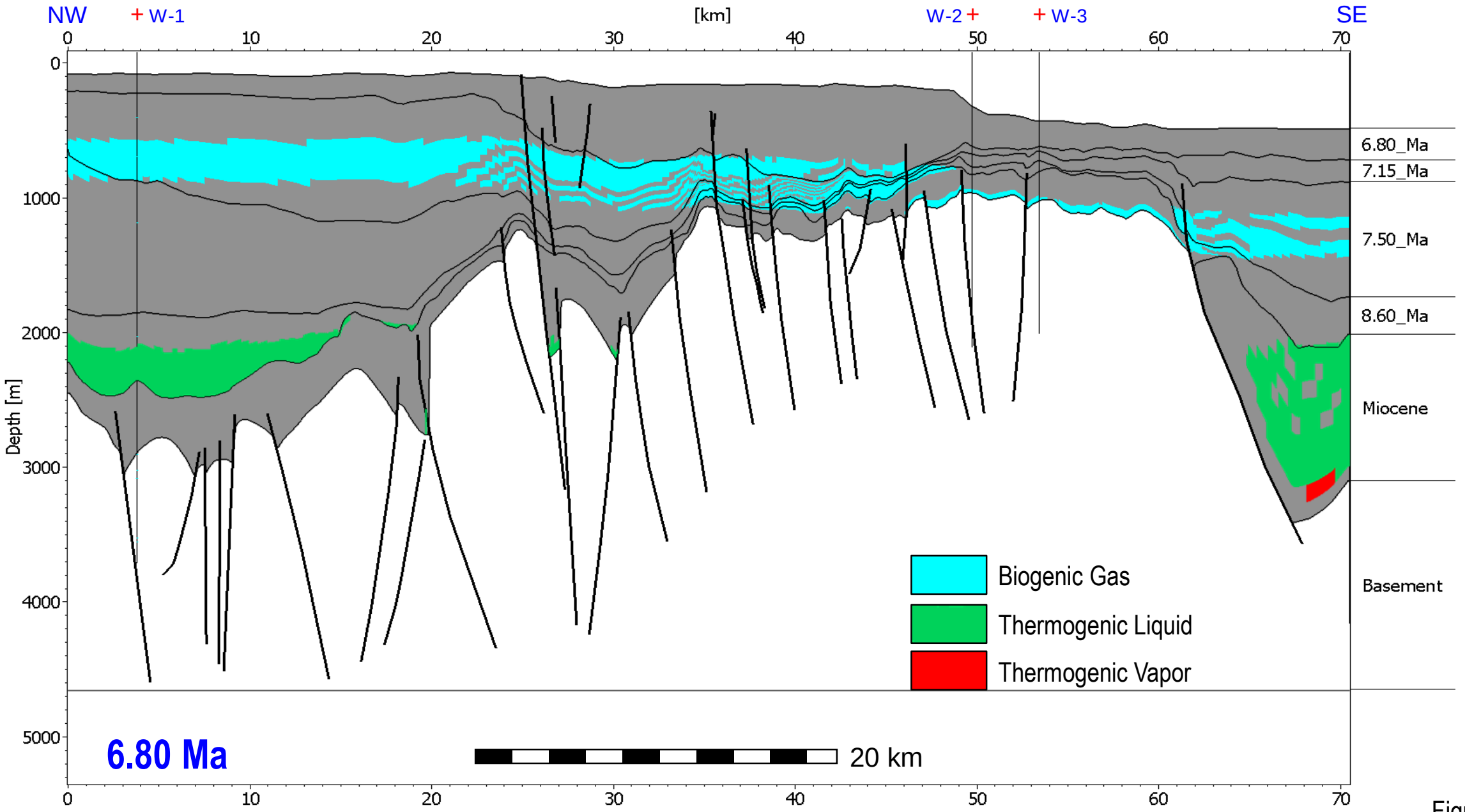

Figure 42

Controlling Factors: Interplay Between Biogenic and Thermogenic Source Rocks

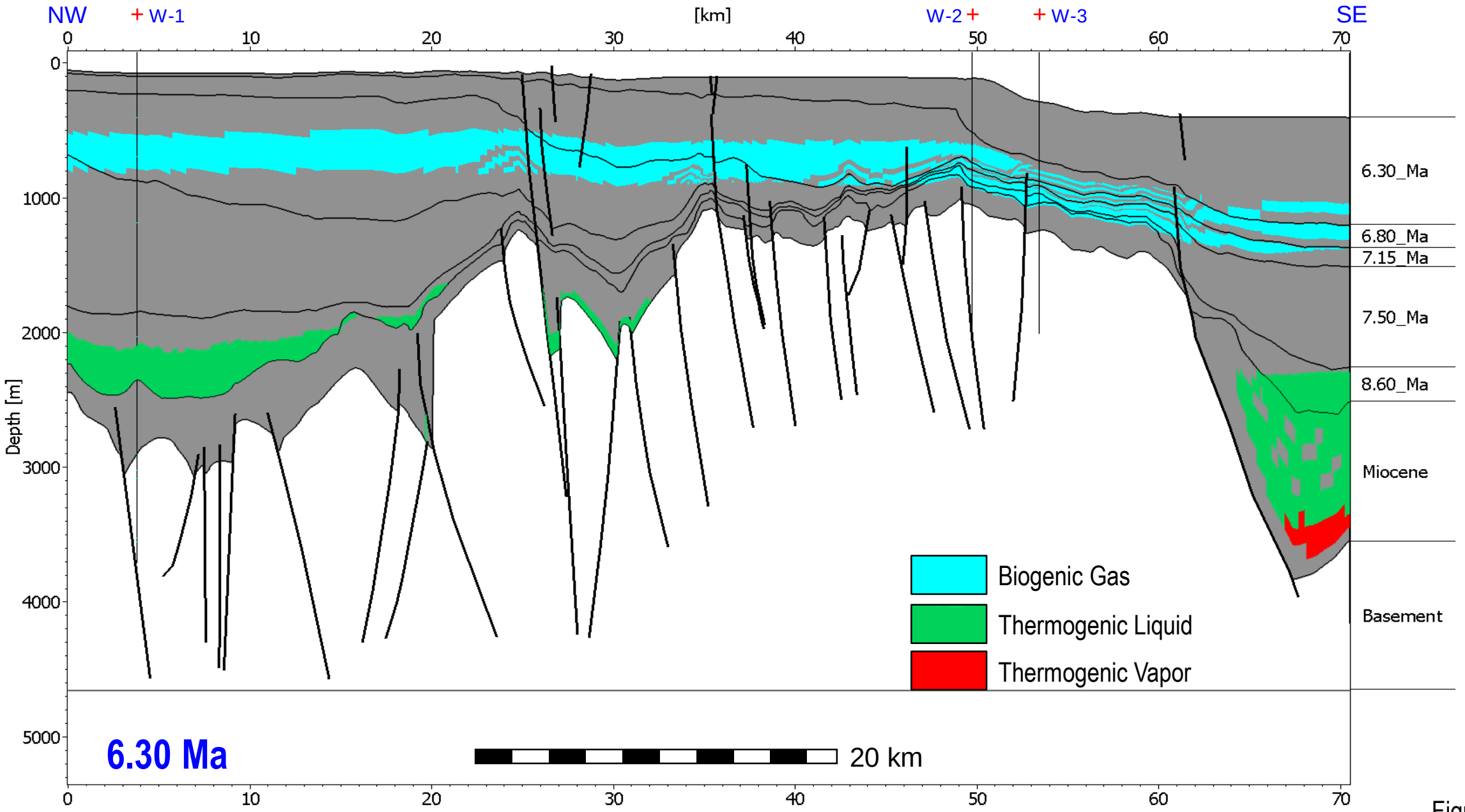

Figure 43

Controlling Factors: Interplay Between Biogenic and Thermogenic Source Rocks

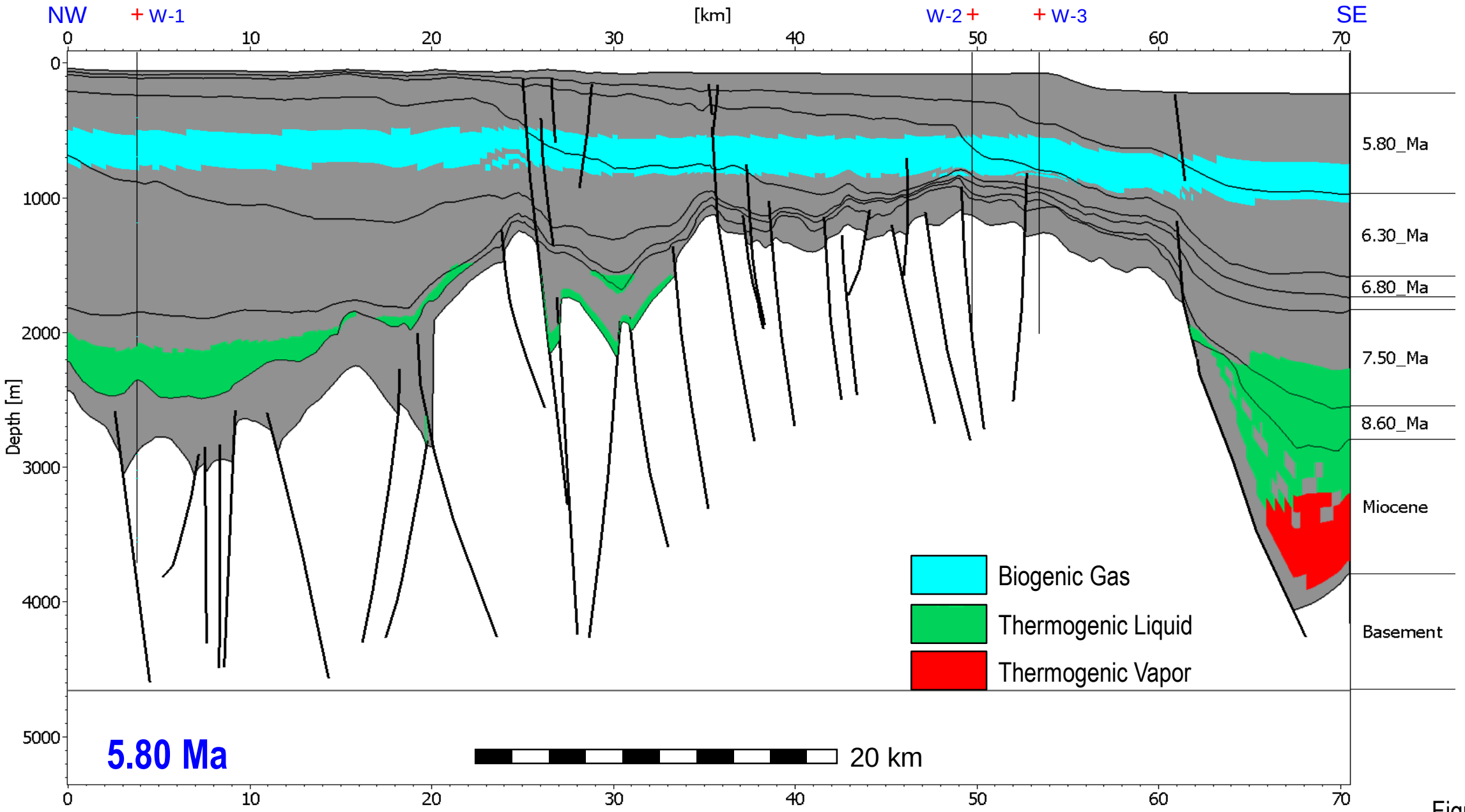

Figure 44

Controlling Factors: Interplay Between Biogenic and Thermogenic Source Rocks

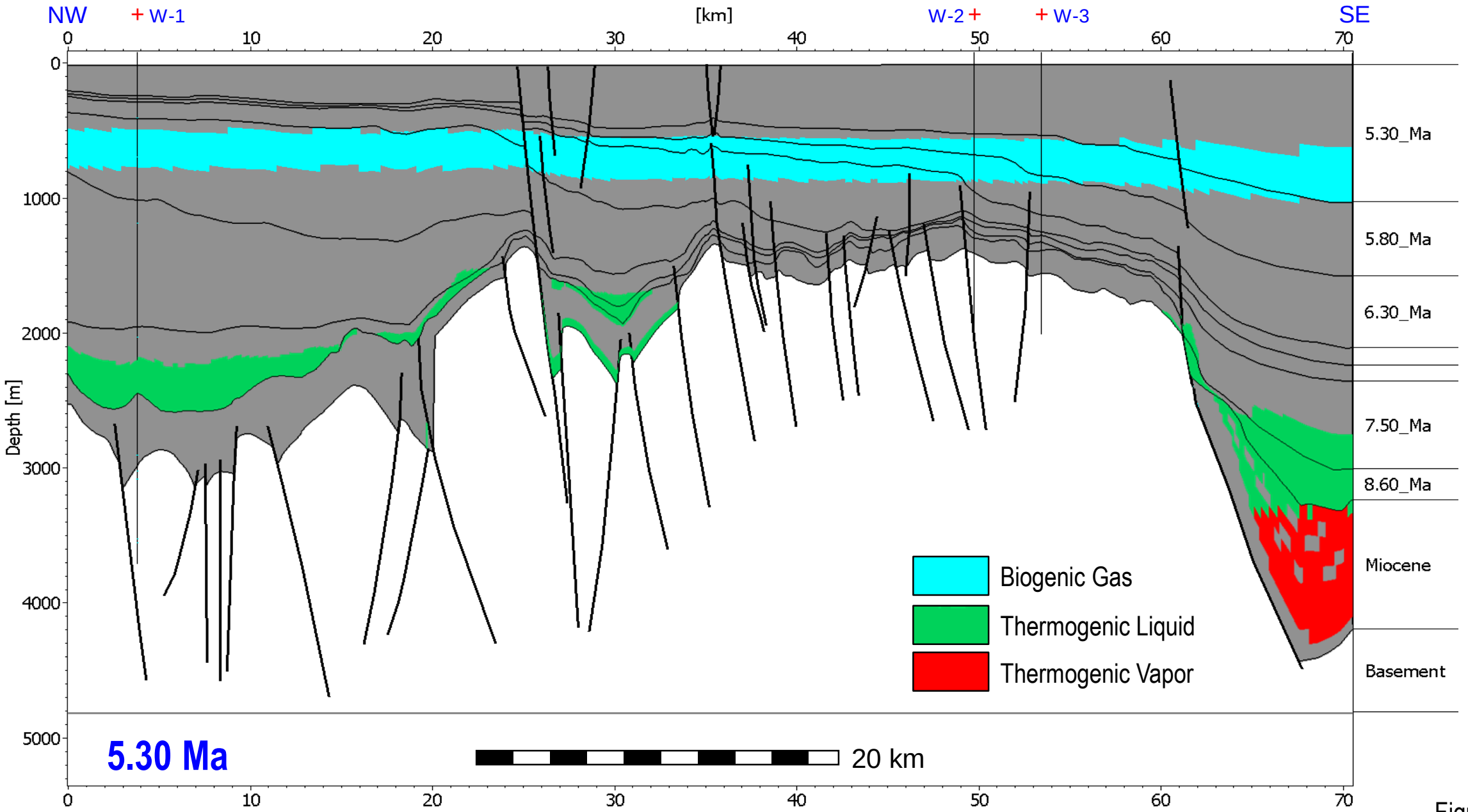

Figure 45

Controlling Factors: Interplay Between Biogenic and Thermogenic Source Rocks

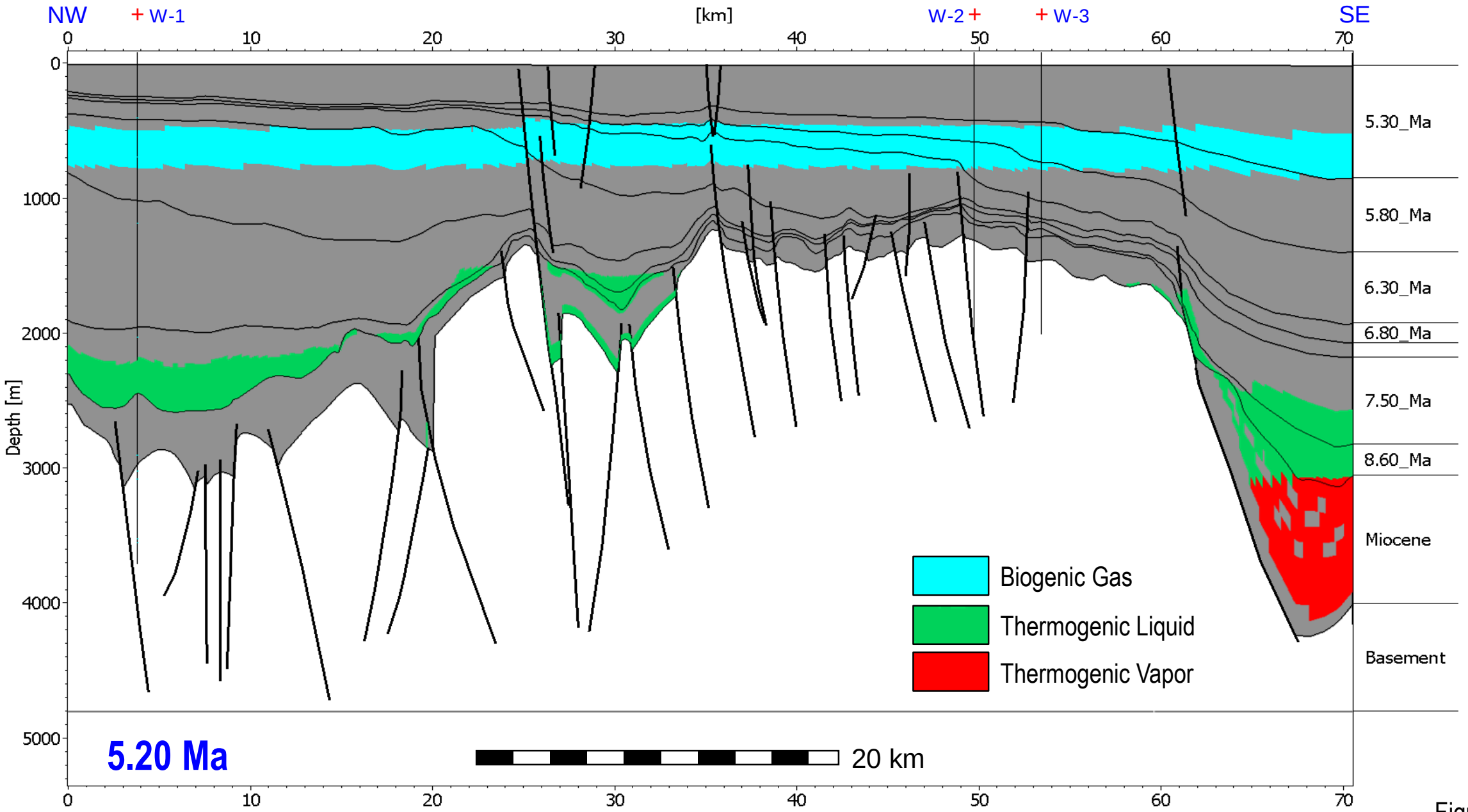

Figure 46

Controlling Factors: Interplay Between Biogenic and Thermogenic Source Rocks

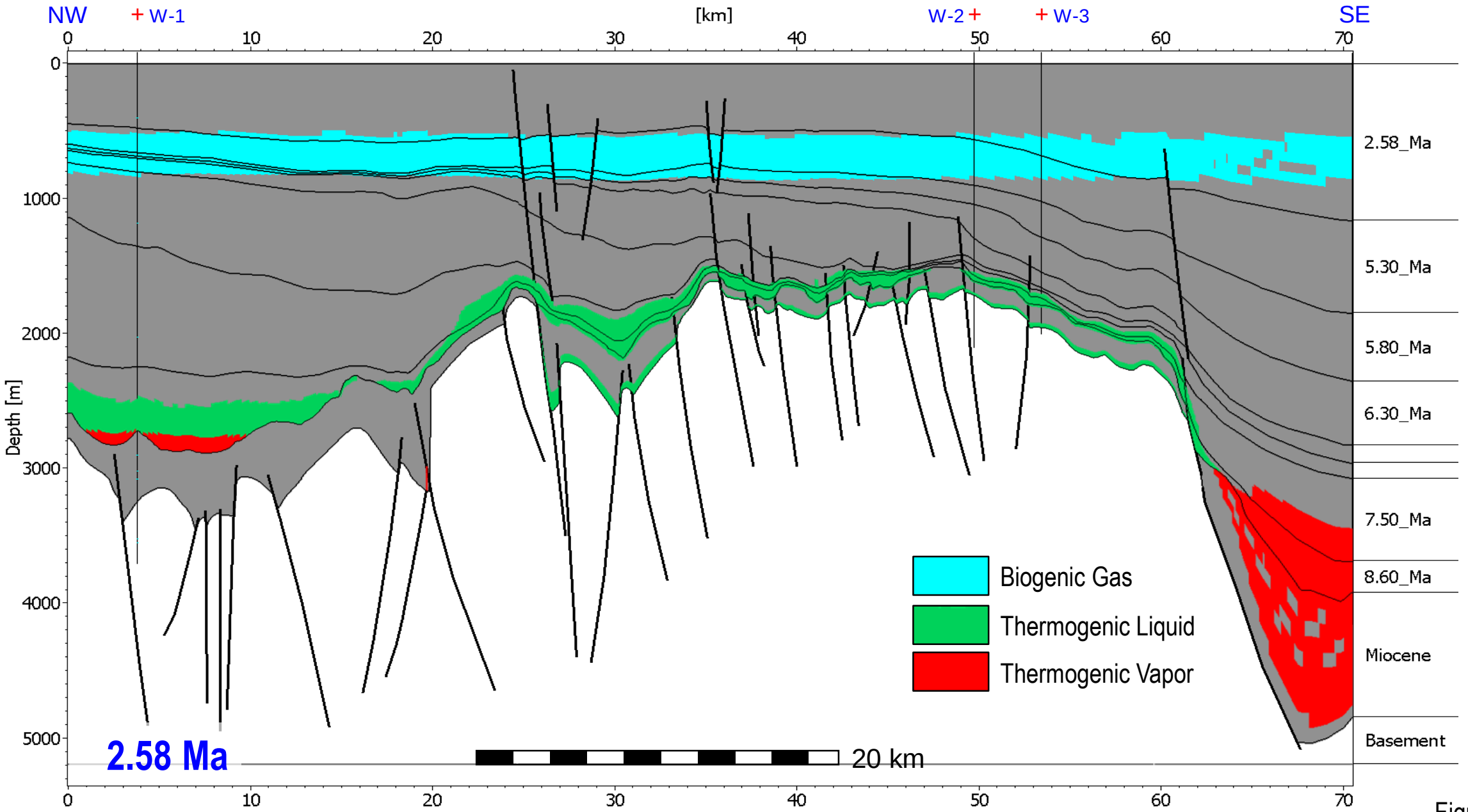

Figure 47

Controlling Factors: Interplay Between Biogenic and Thermogenic Source Rocks

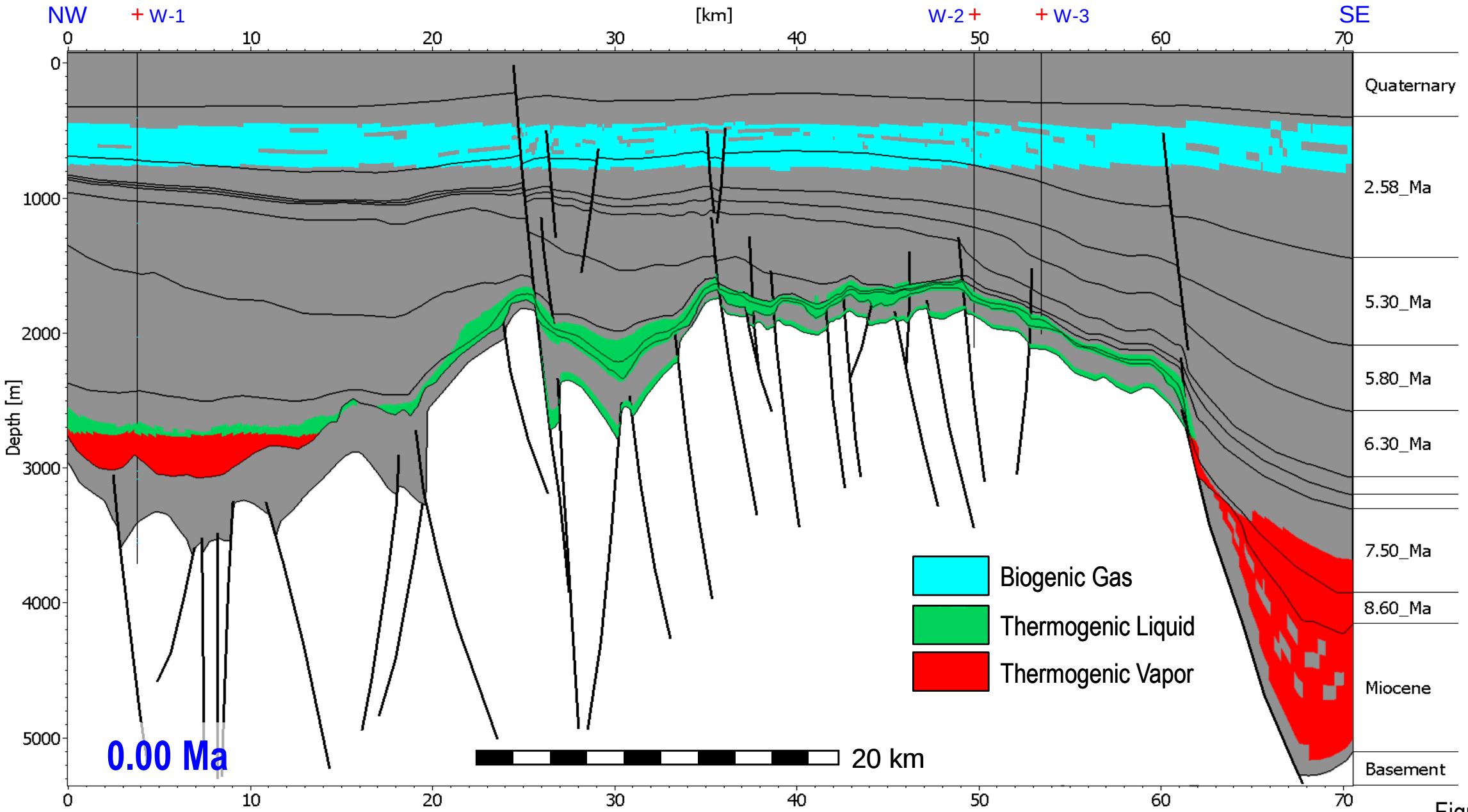

Figure 48

Controlling Factors: Gas Hydrates Could Act as a Barrier for Both Biogenic and Thermogenic Gases

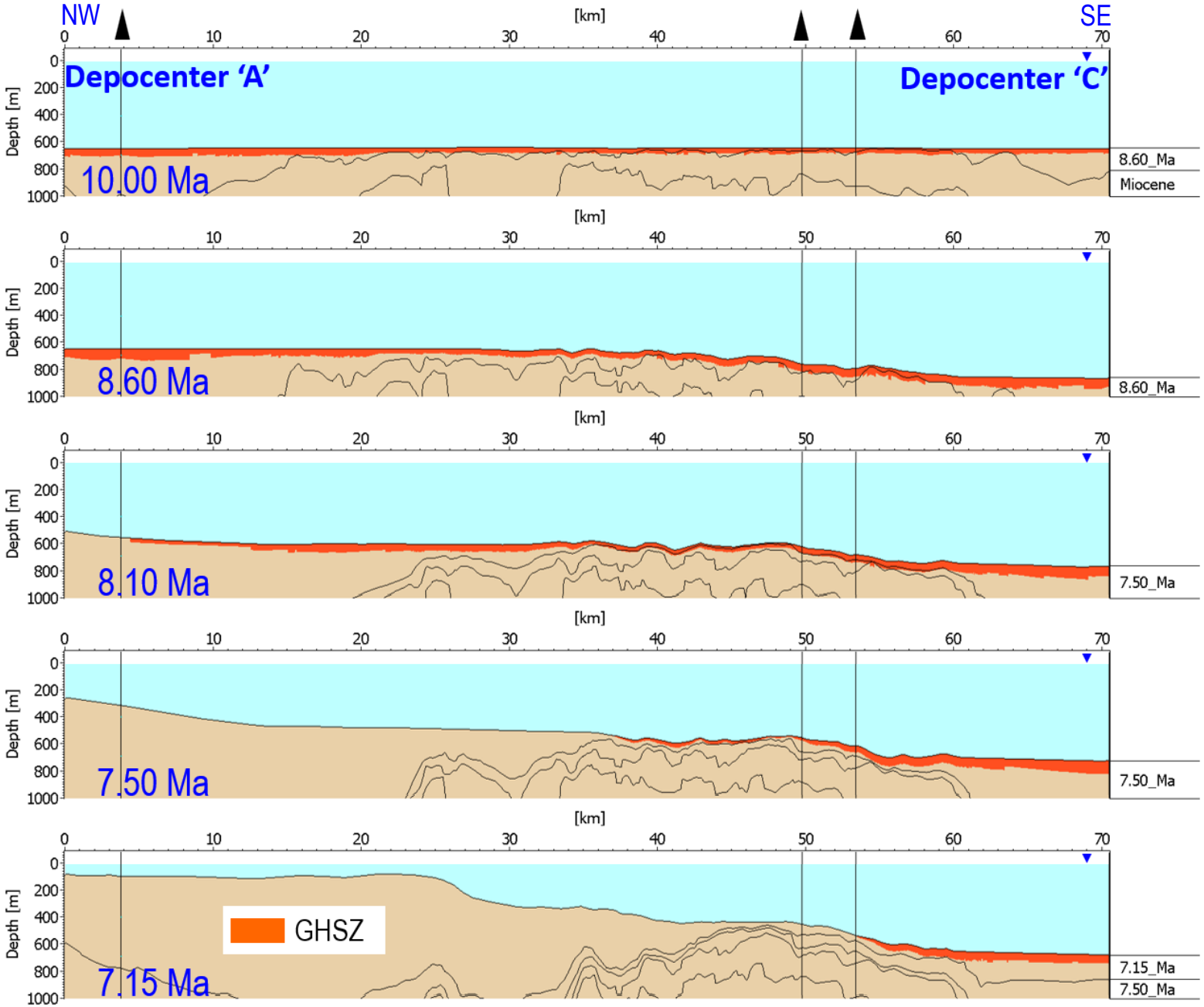

Gas Hydrate Stability Zone (GHSZ)

Paleo Water Depth > 600 m
Temperature ~ 5.0-9.0°C
Pressure ~ 6.0-9.0 MPa

Figure 49

Migration Model: High Resolution Darcy + Invasion Percolation

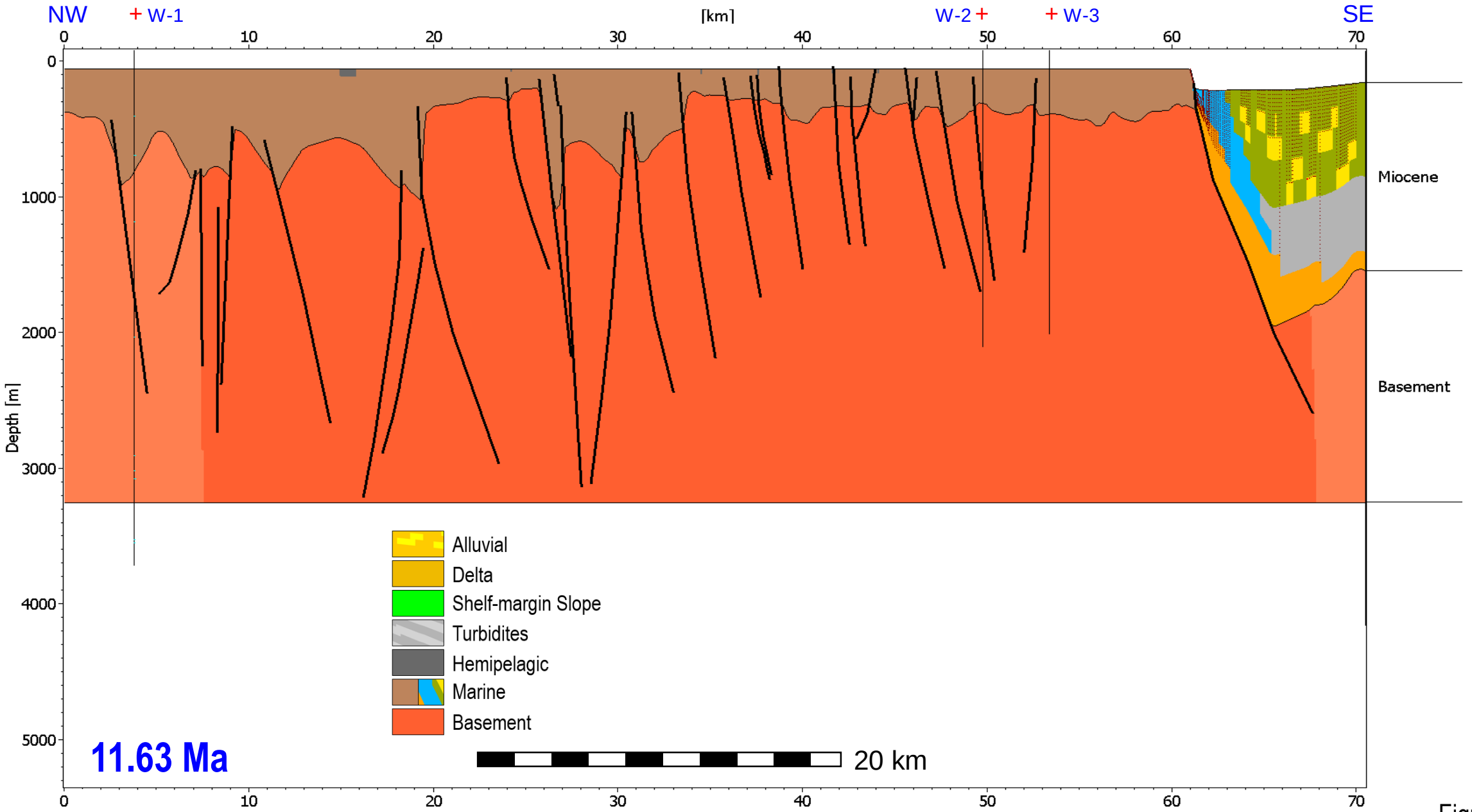

Figure 50

Migration Model: High Resolution Darcy + Invasion Percolation

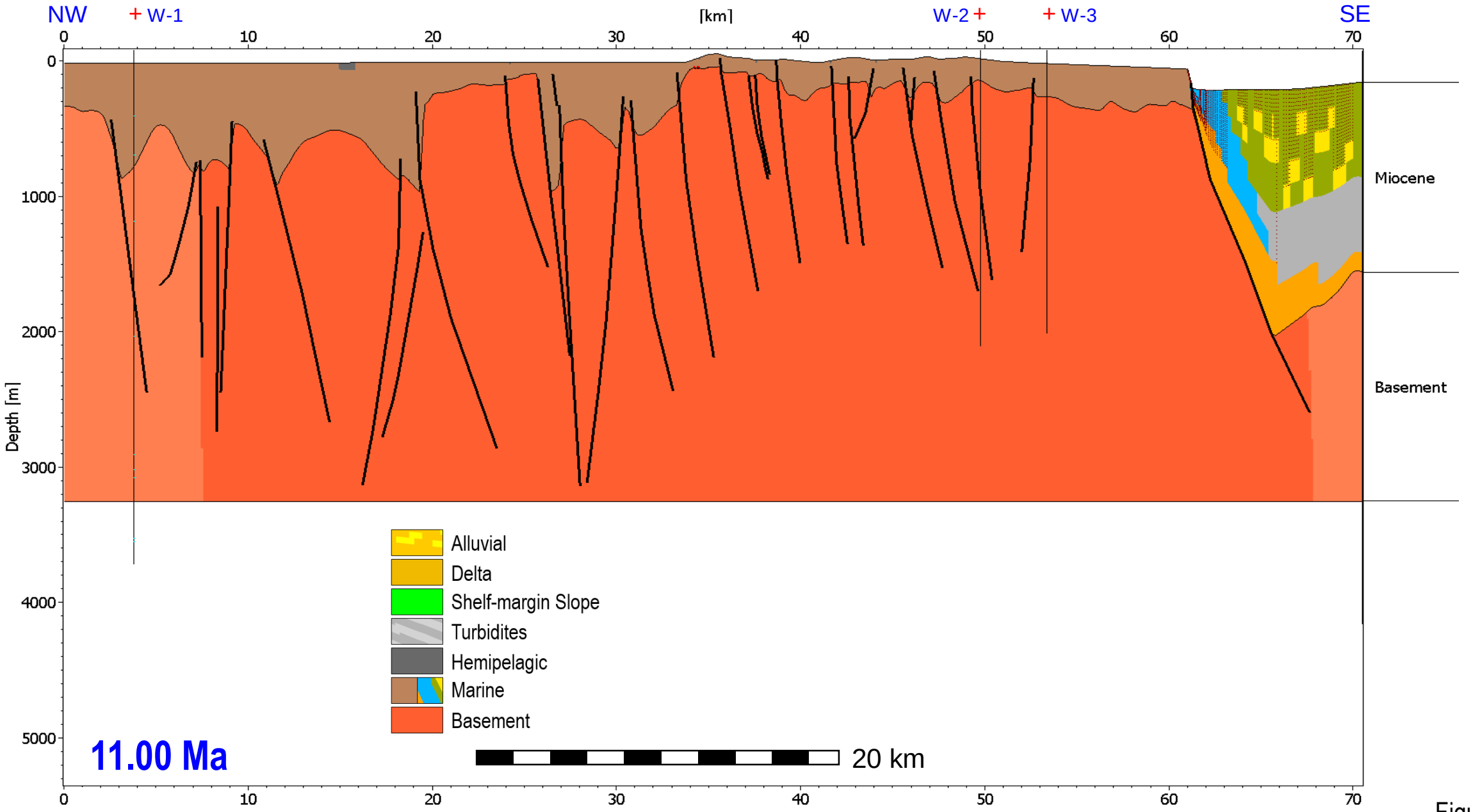

Figure 51

Migration Model: High Resolution Darcy + Invasion Percolation

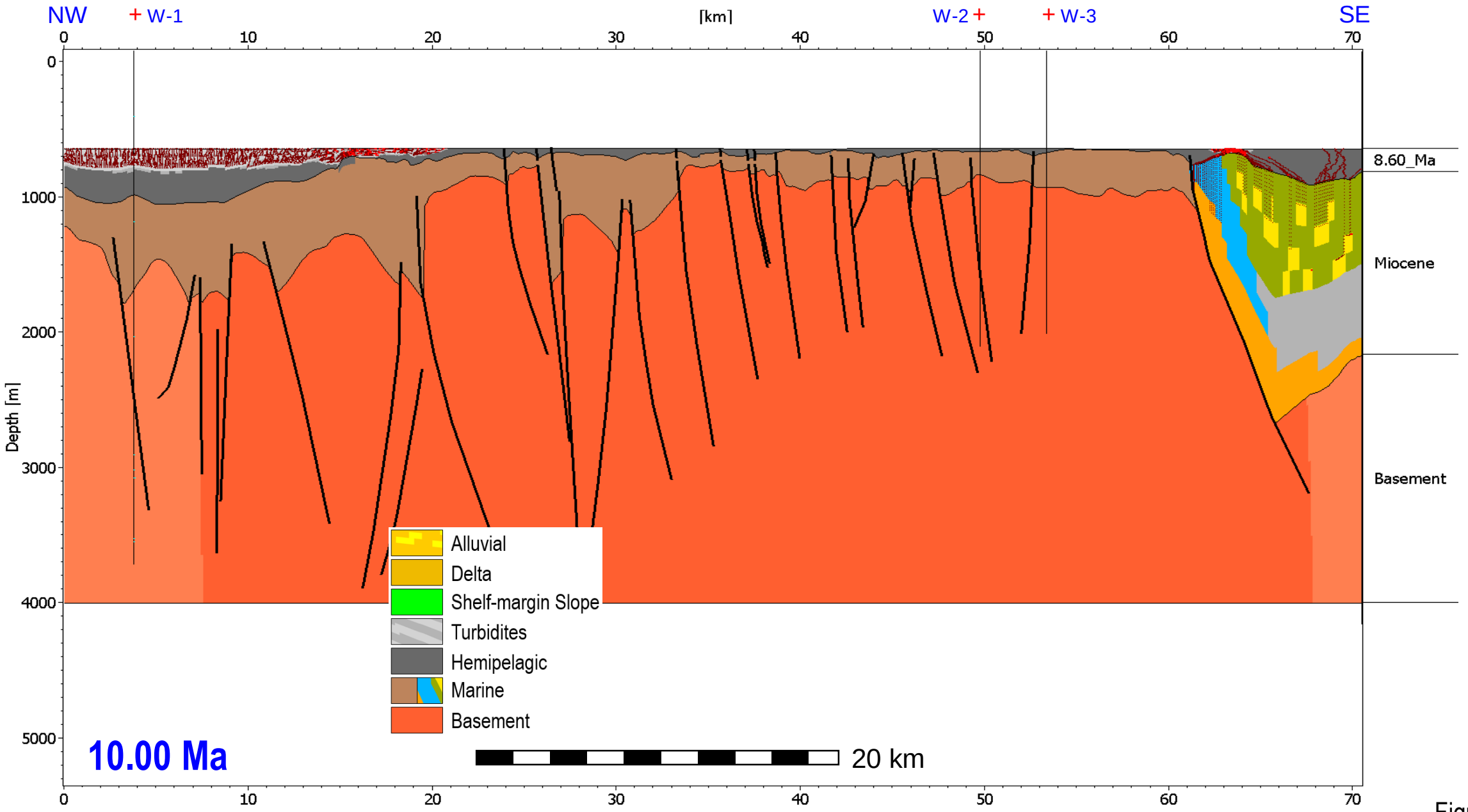

Figure 52

Migration Model: High Resolution Darcy + Invasion Percolation

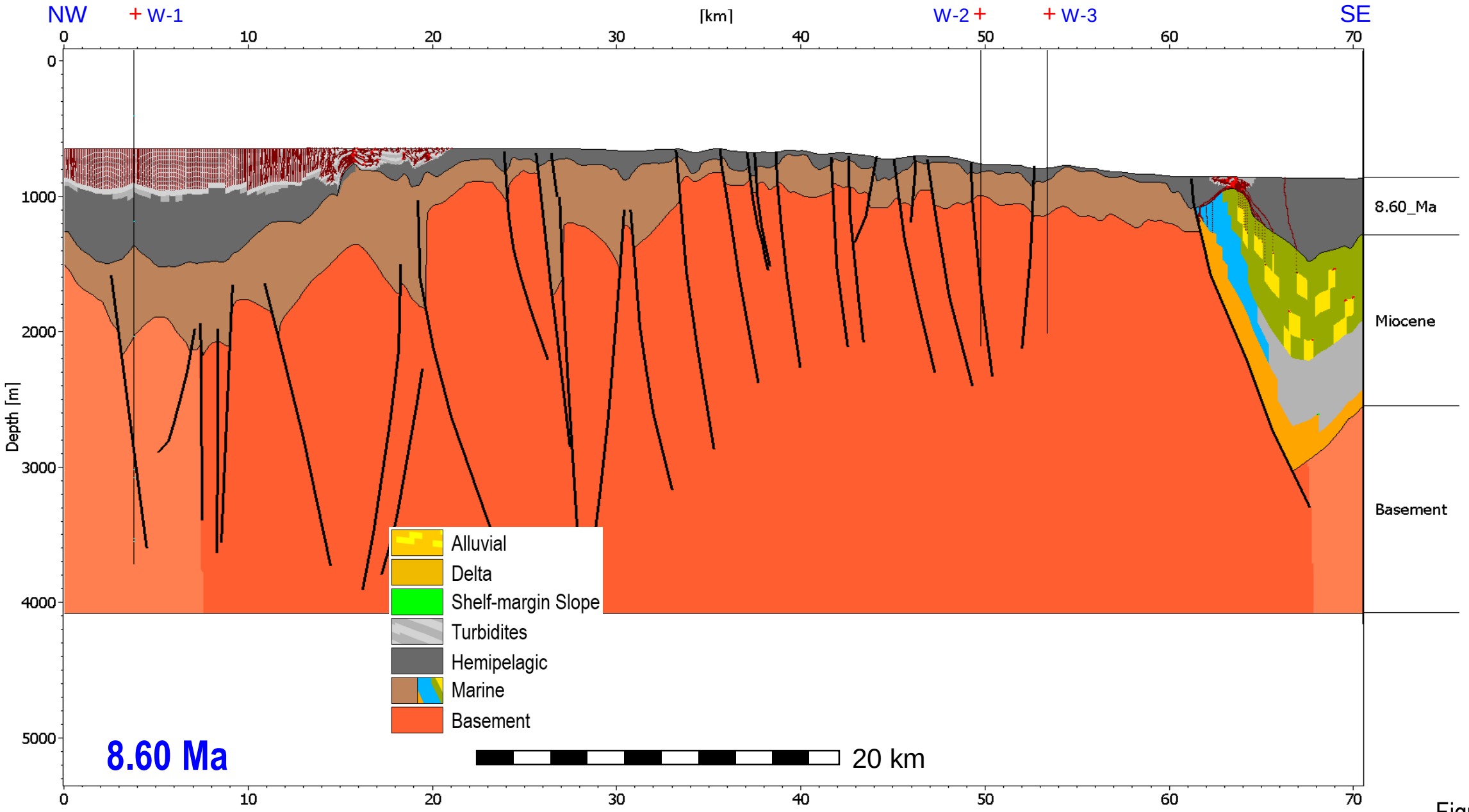

Figure 53

Migration Model: High Resolution Darcy + Invasion Percolation

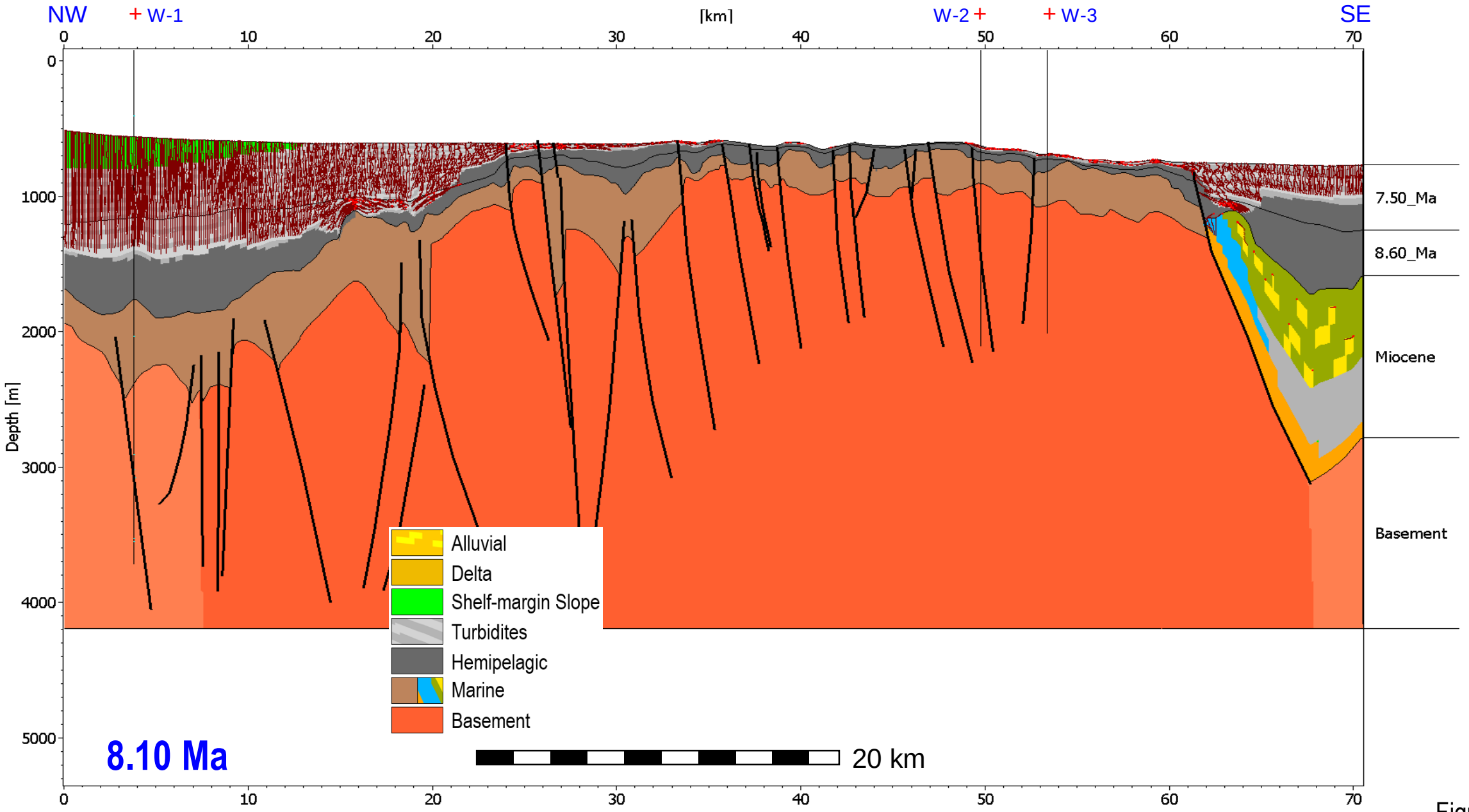

Figure 54

Migration Model: High Resolution Darcy + Invasion Percolation

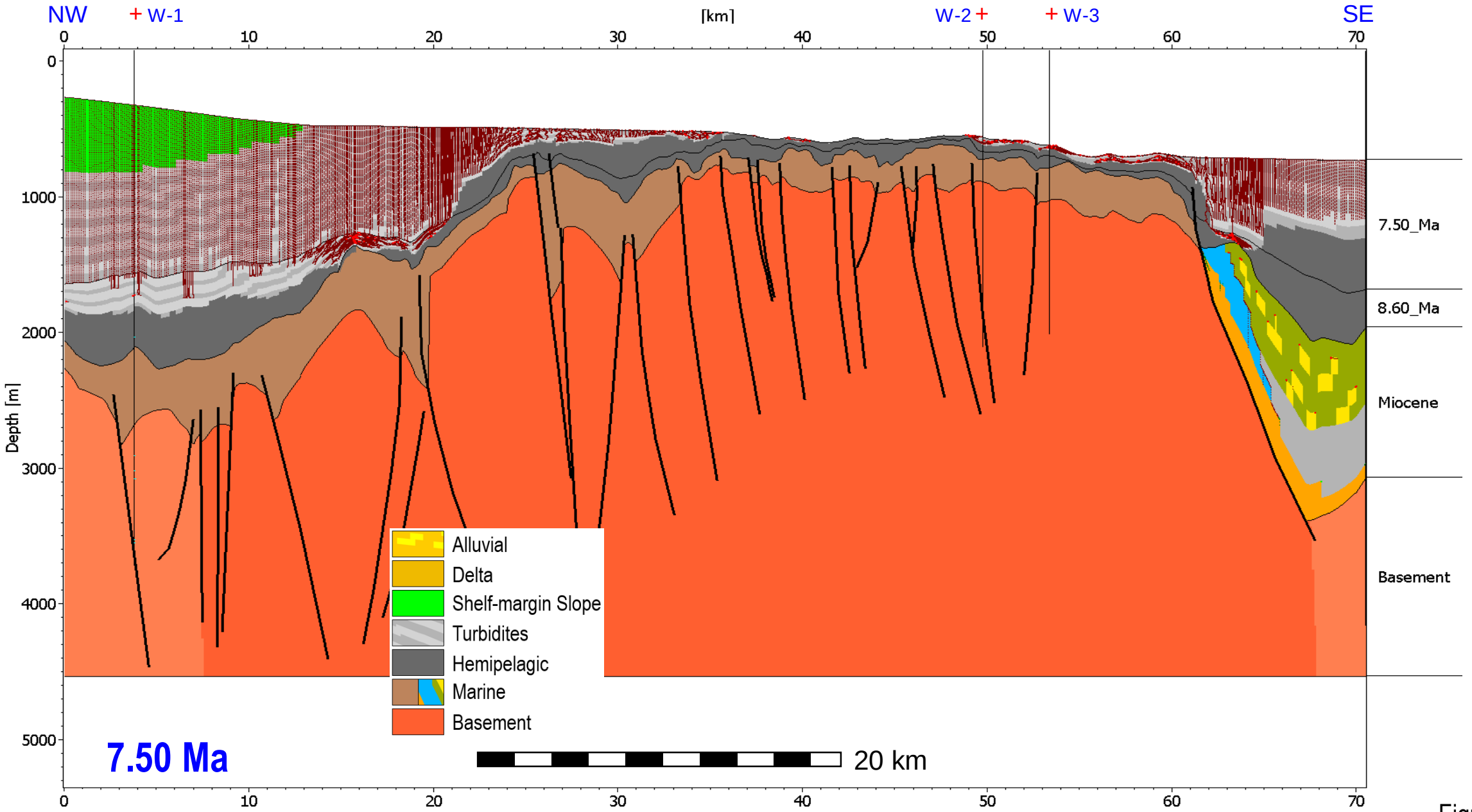

Figure 55

Migration Model: High Resolution Darcy + Invasion Percolation

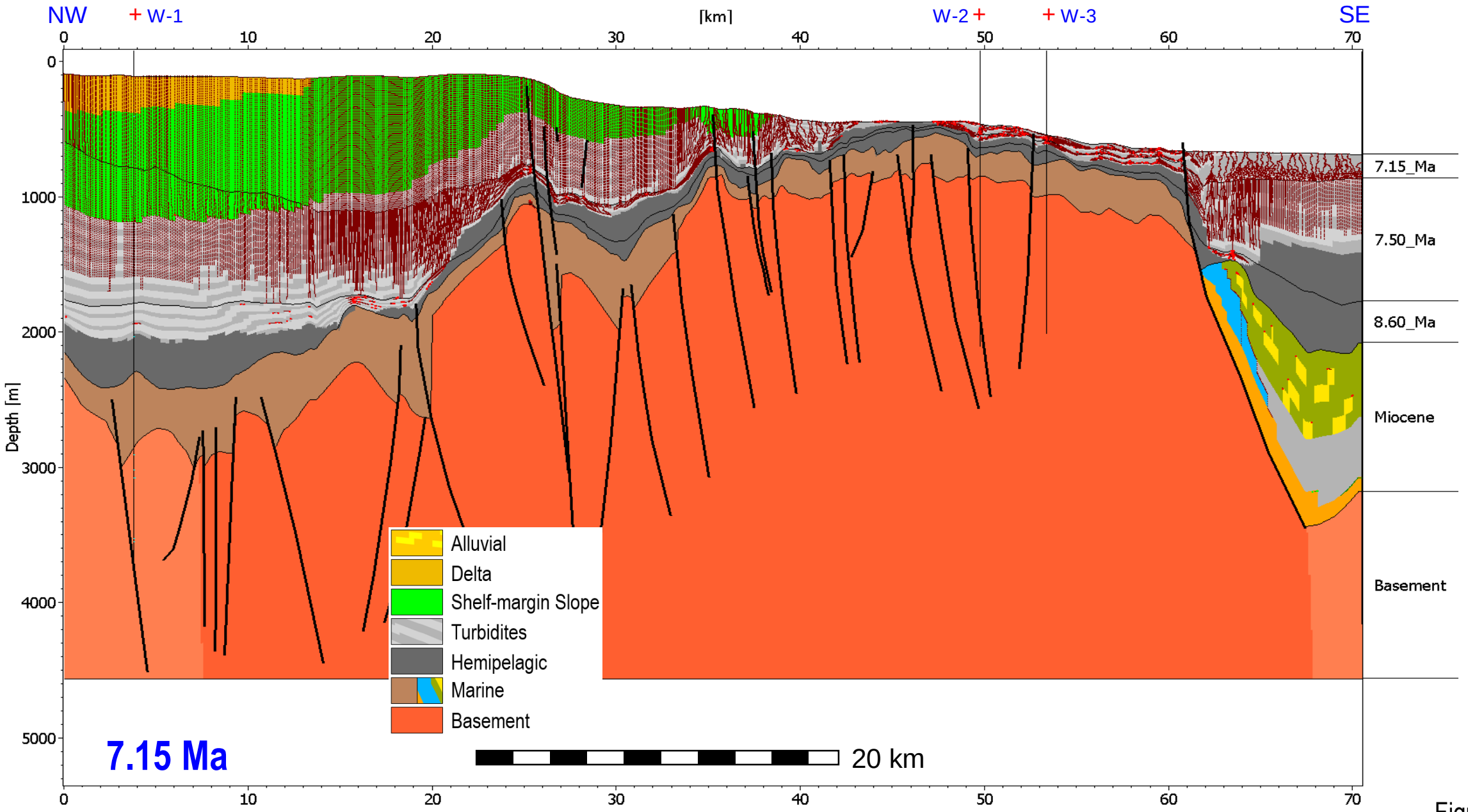

Figure 56

Migration Model: High Resolution Darcy + Invasion Percolation

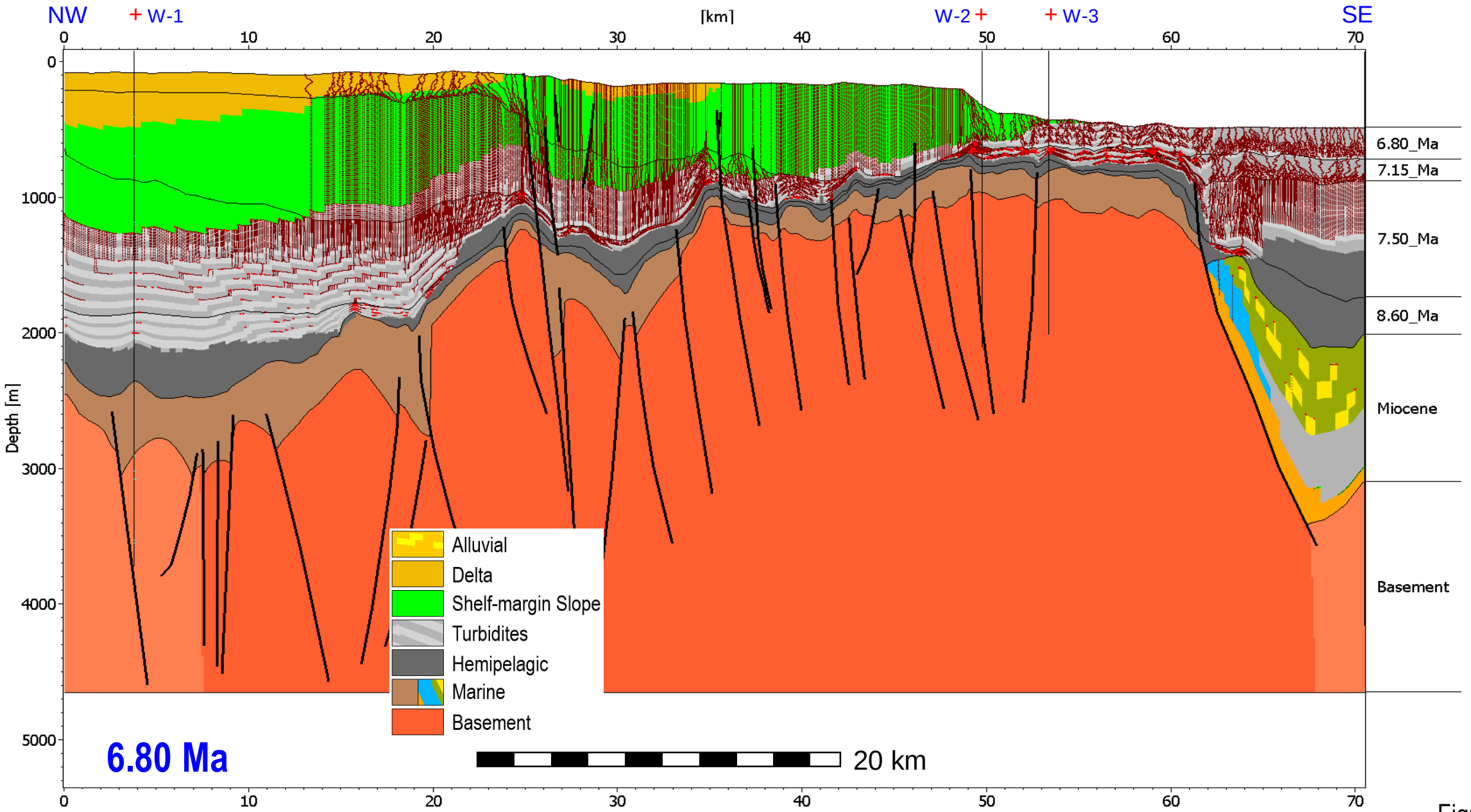

Figure 57

Migration Model: High Resolution Darcy + Invasion Percolation

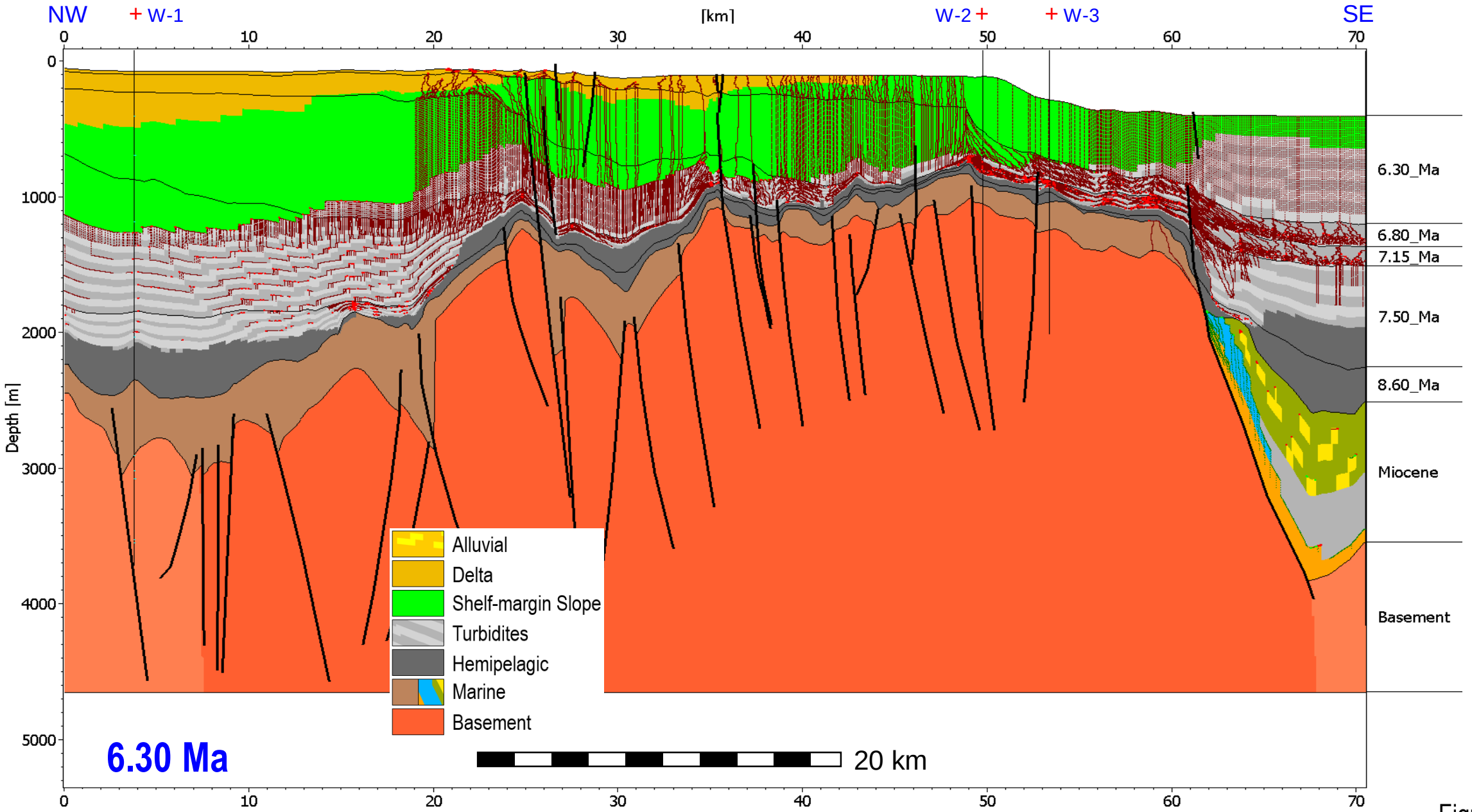

Figure 58

Migration Model: High Resolution Darcy + Invasion Percolation

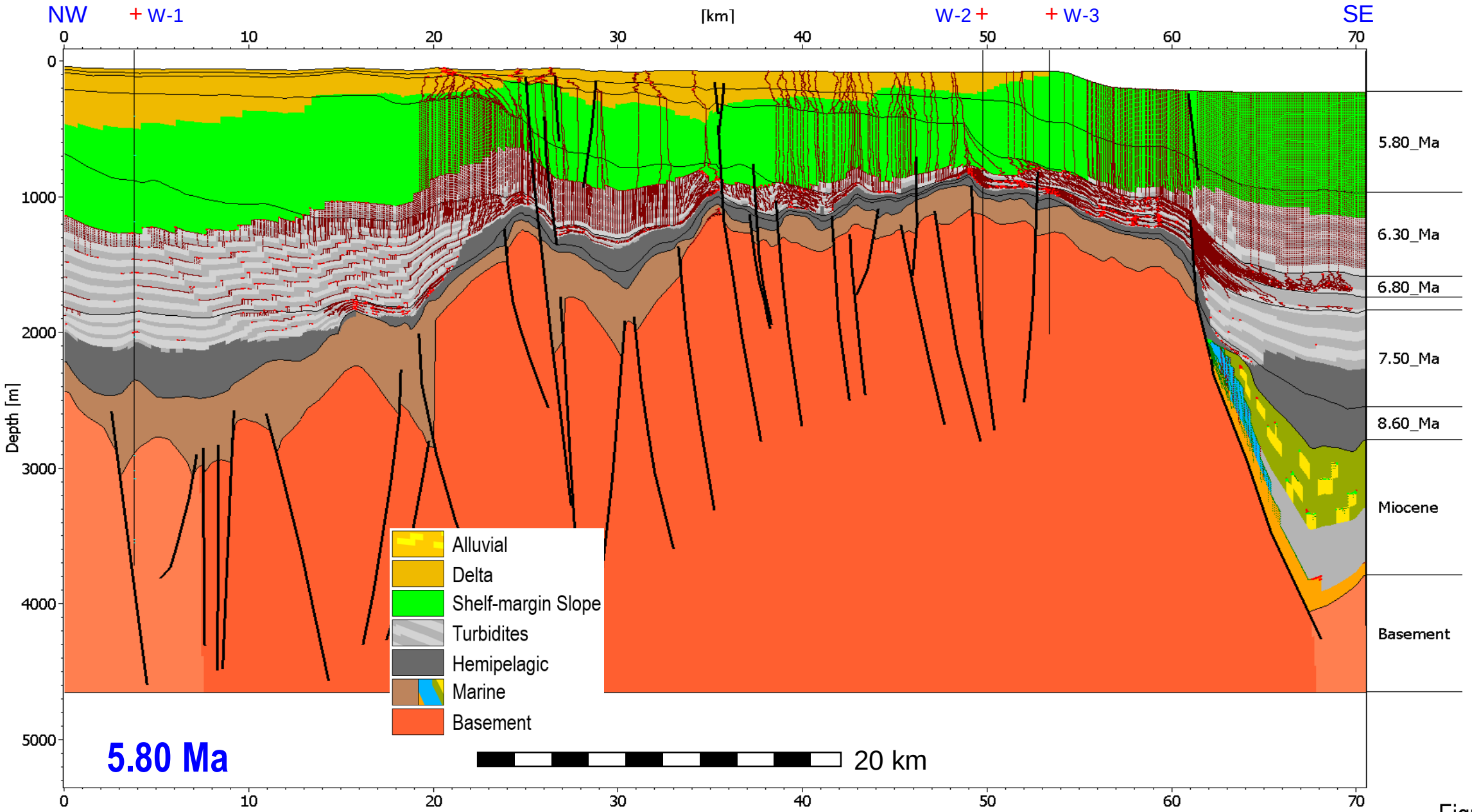

Figure 59

Migration Model: High Resolution Darcy + Invasion Percolation

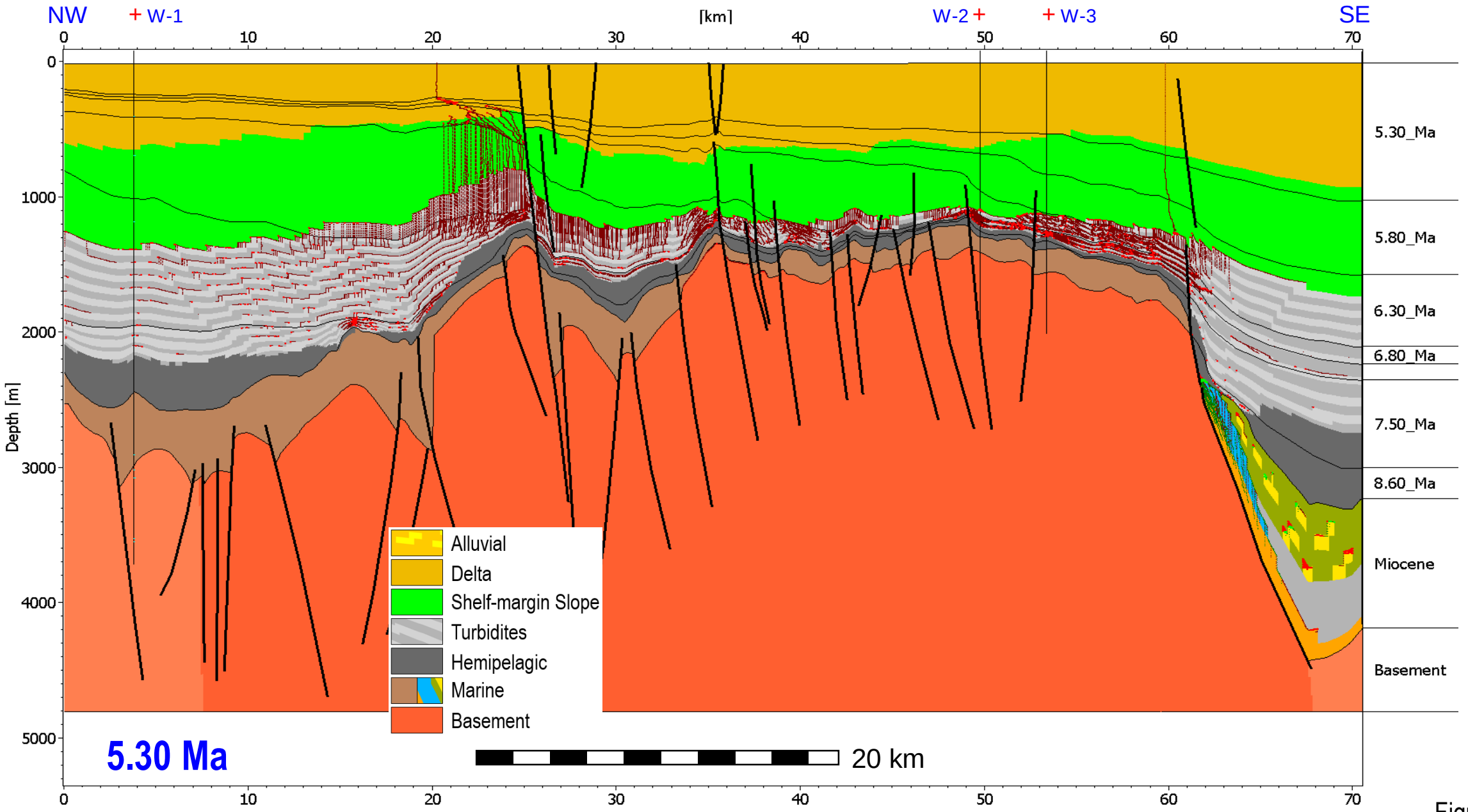

Figure 60

Migration Model: High Resolution Darcy + Invasion Percolation

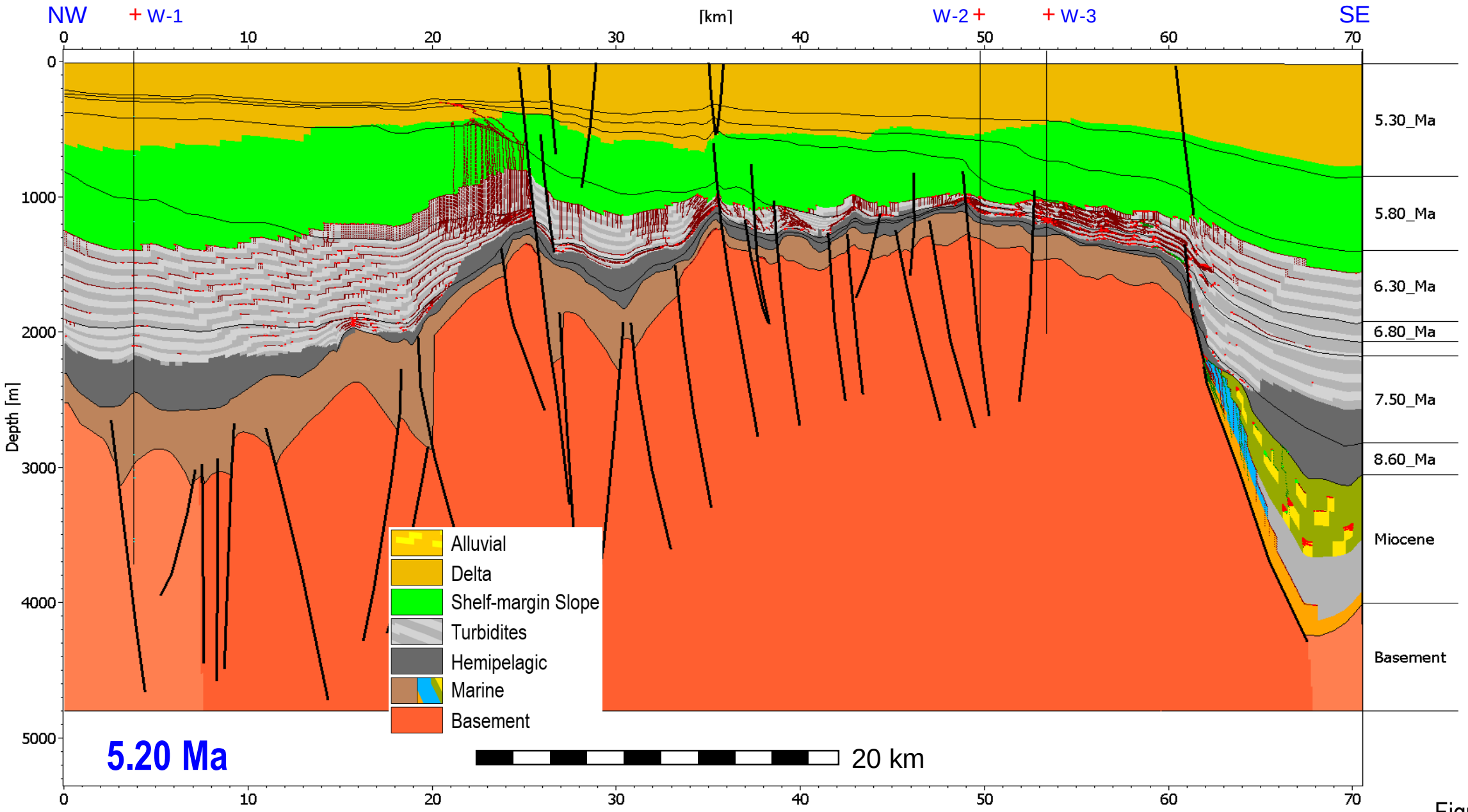

Figure 61

Migration Model: High Resolution Darcy + Invasion Percolation

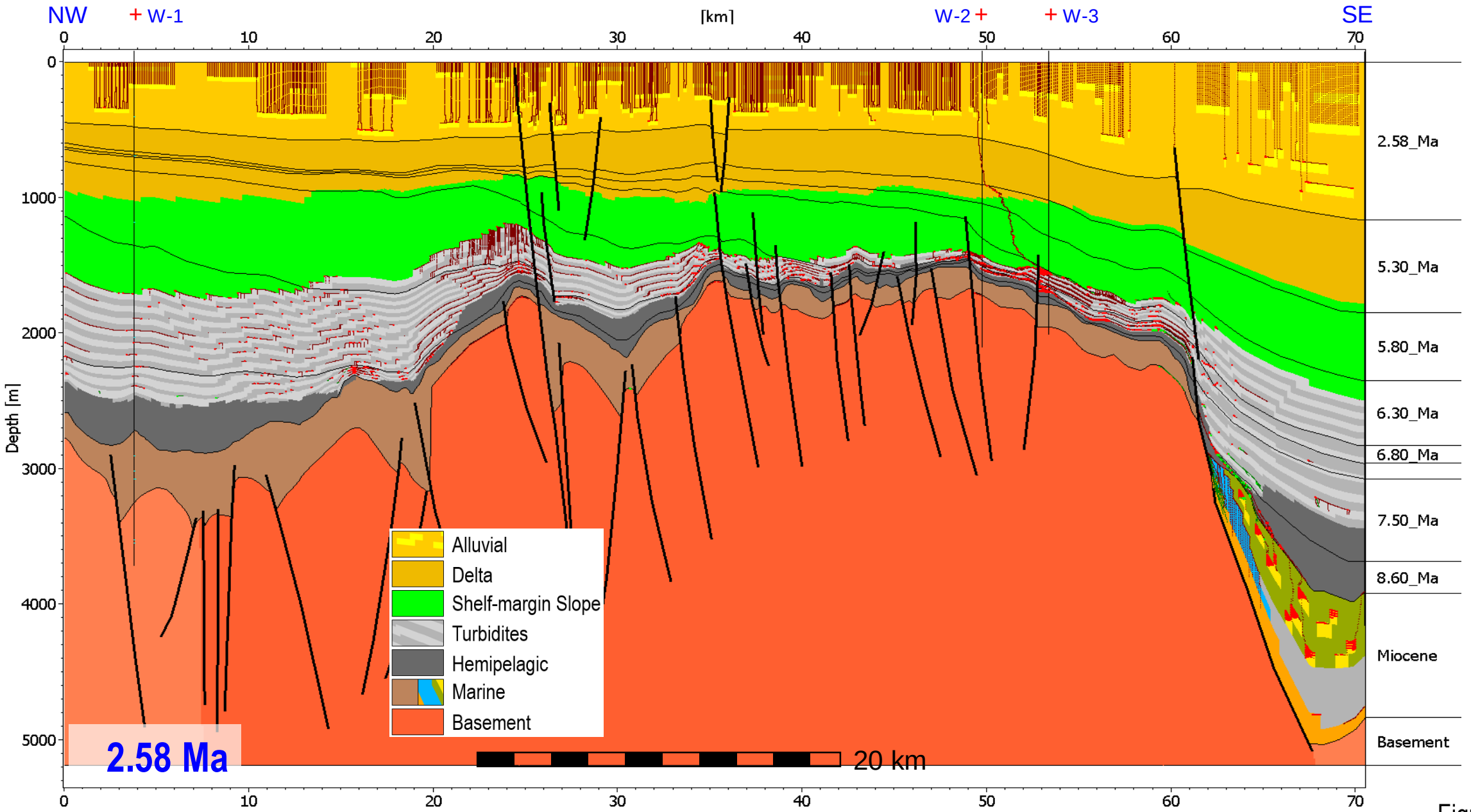

Figure 62

Migration Model: High Resolution Darcy + Invasion Percolation

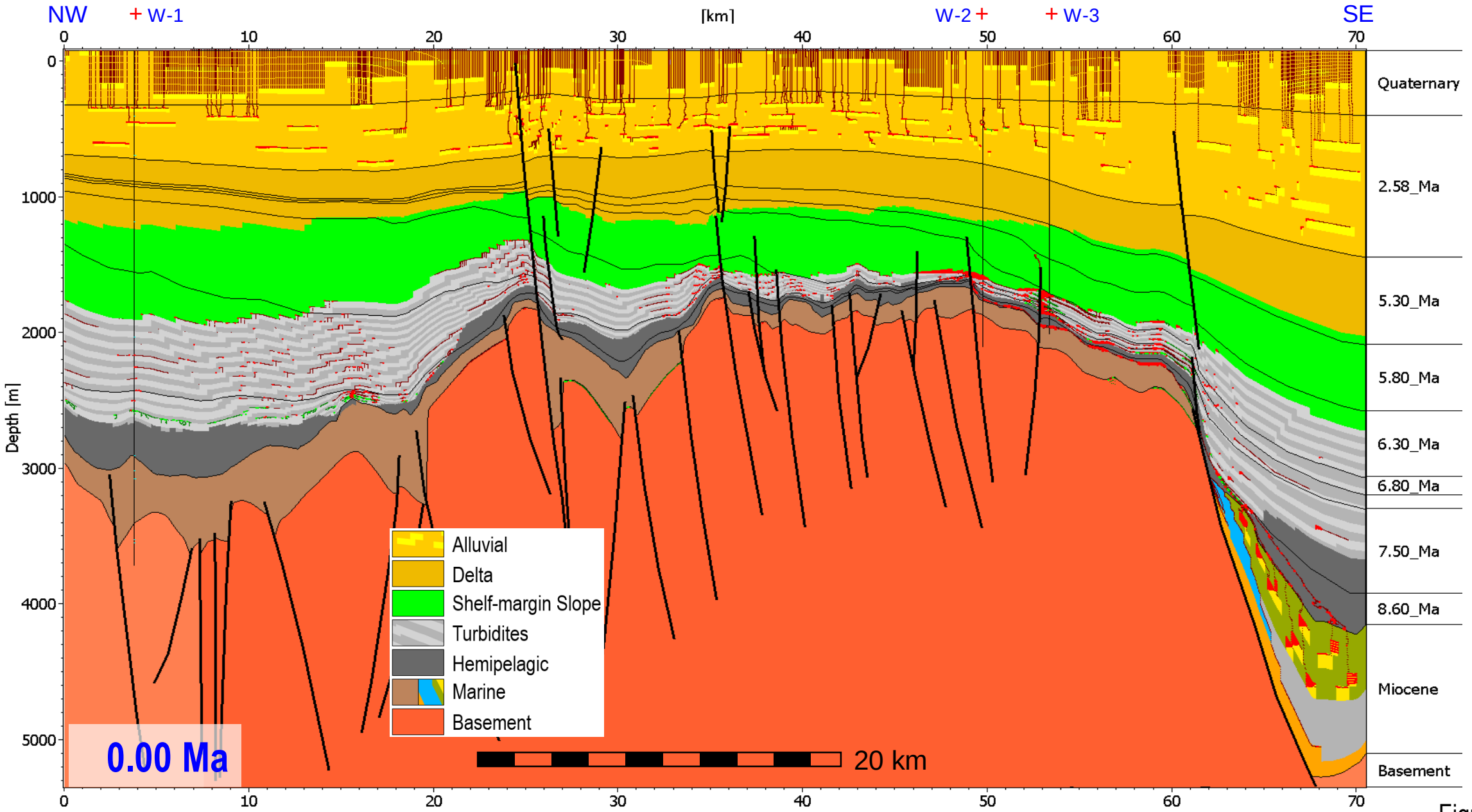

Figure 63

Migration Model: Hydrocarbon Charge through Geologic Time

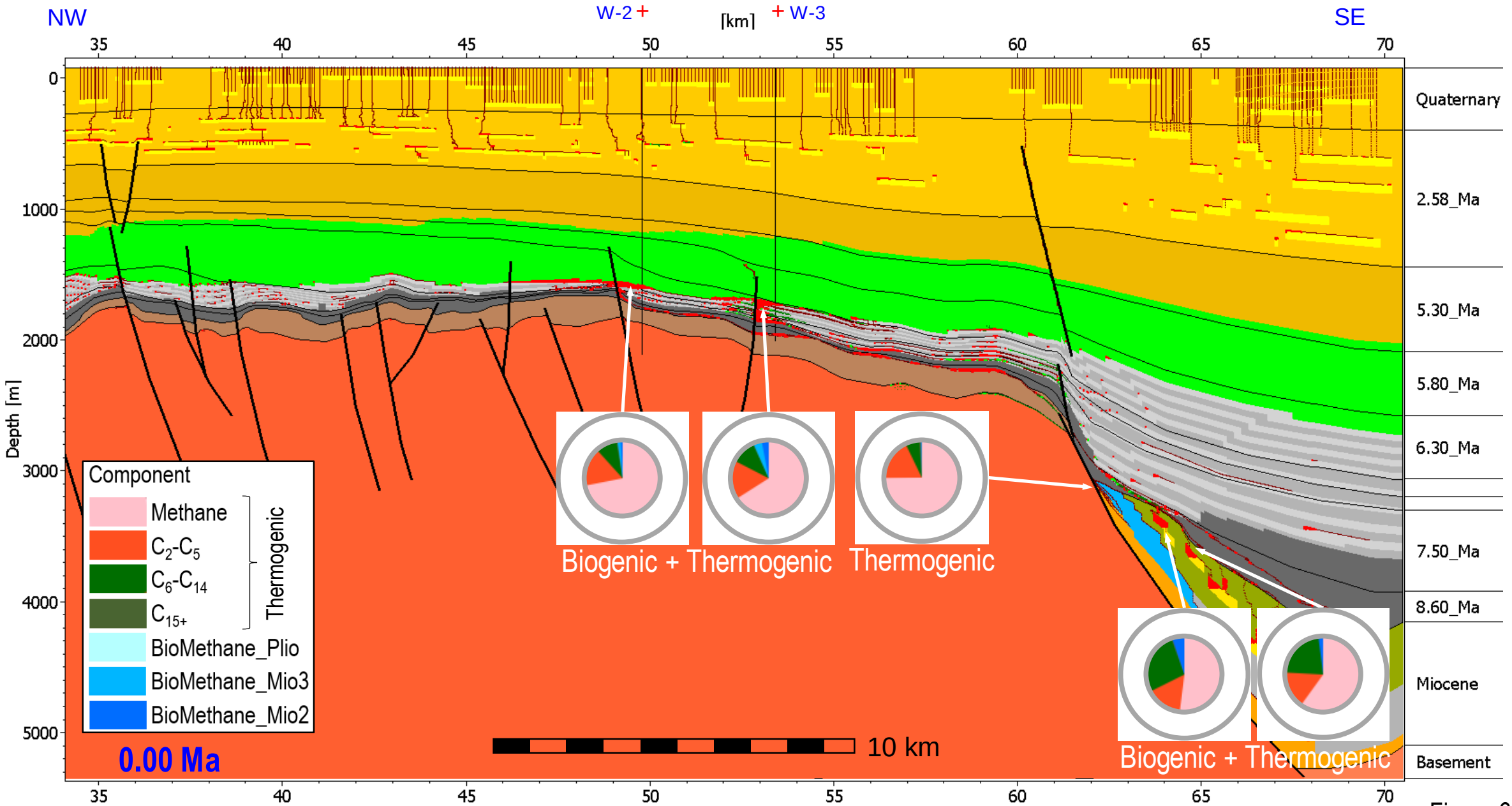

Figure 64

Migration Model: Hydrocarbon Charge through Geologic Time

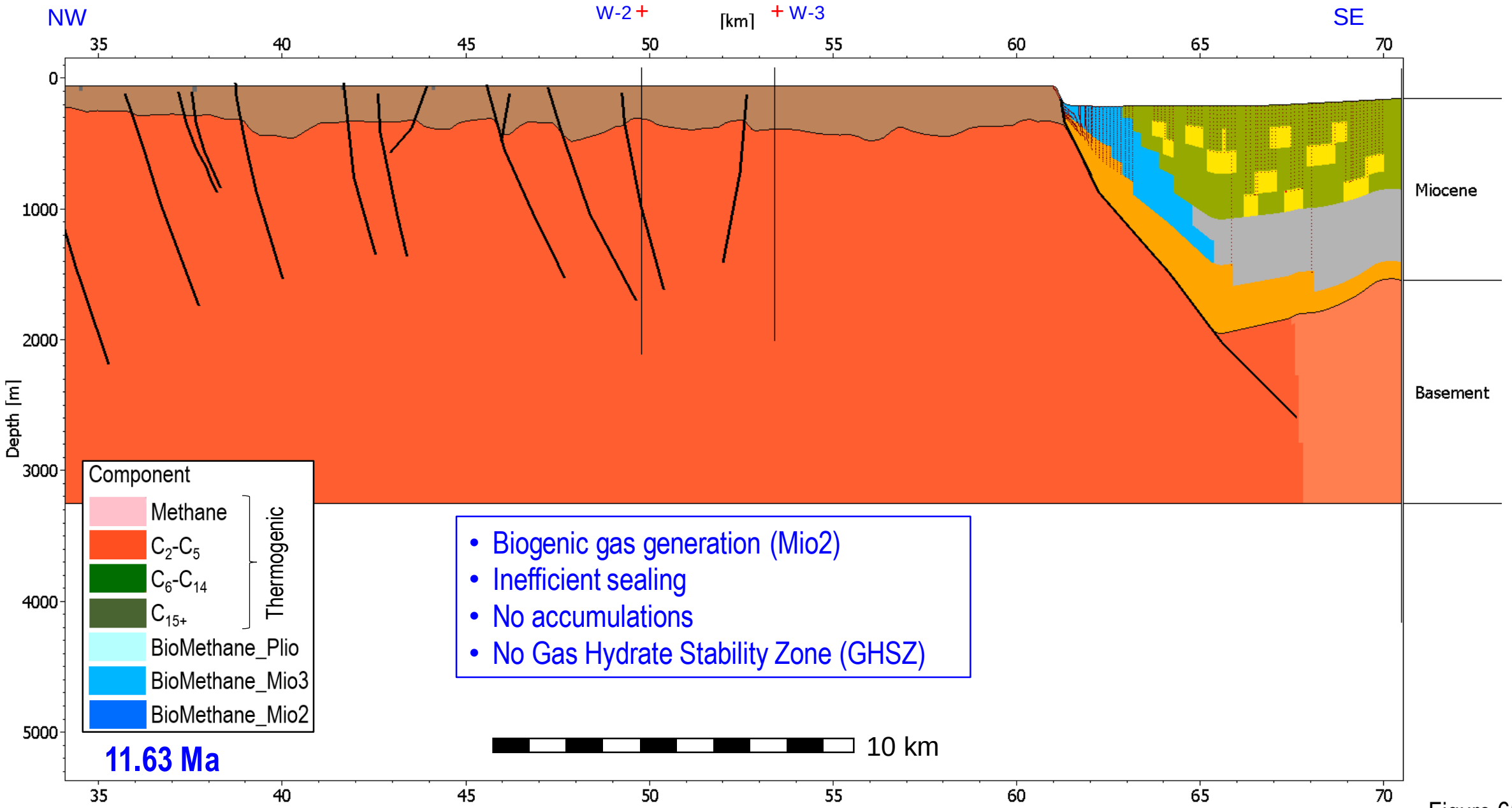

Figure 65

Migration Model: Hydrocarbon Charge through Geologic Time

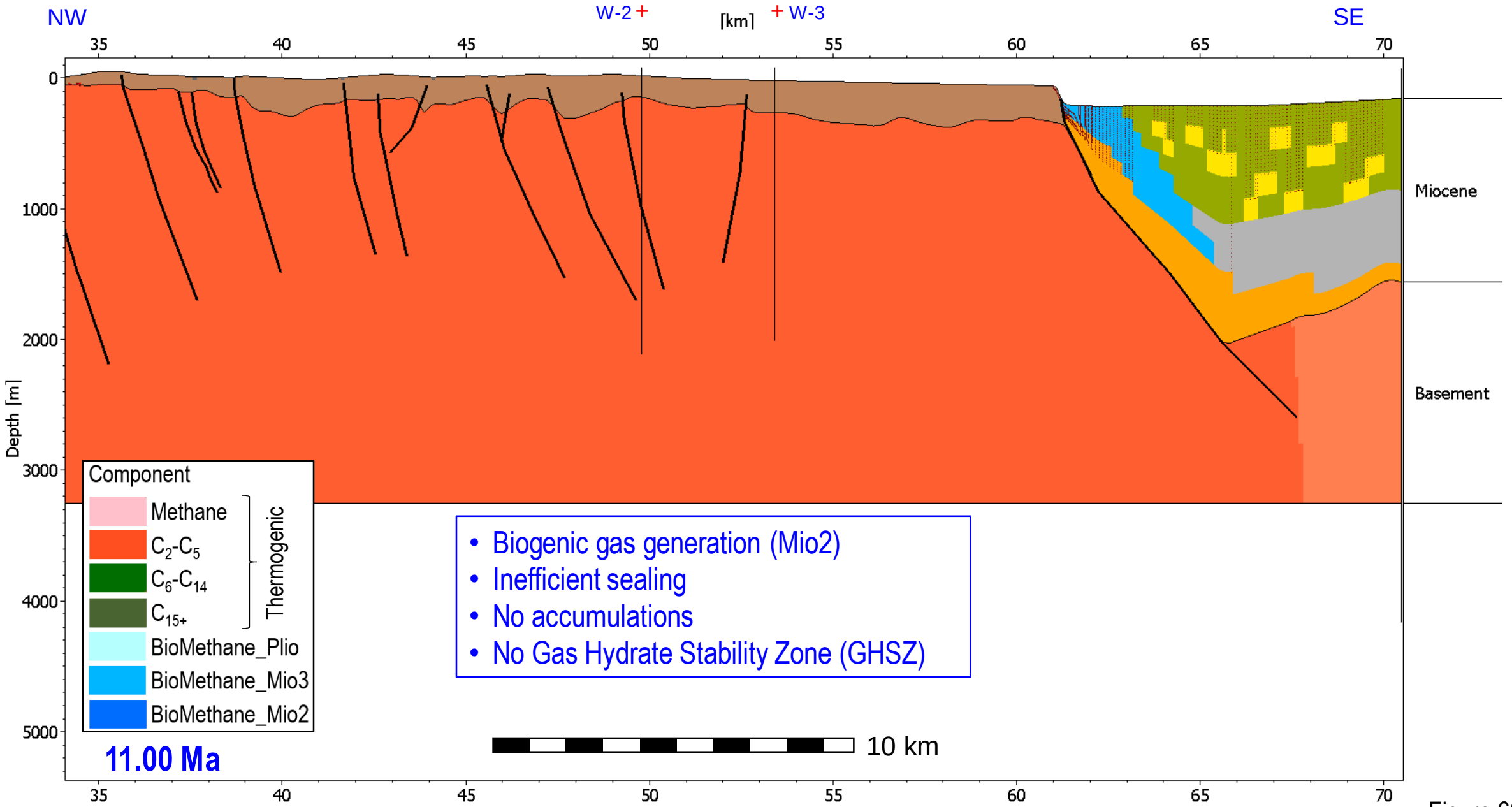

Figure 66

Migration Model: Hydrocarbon Charge through Geologic Time

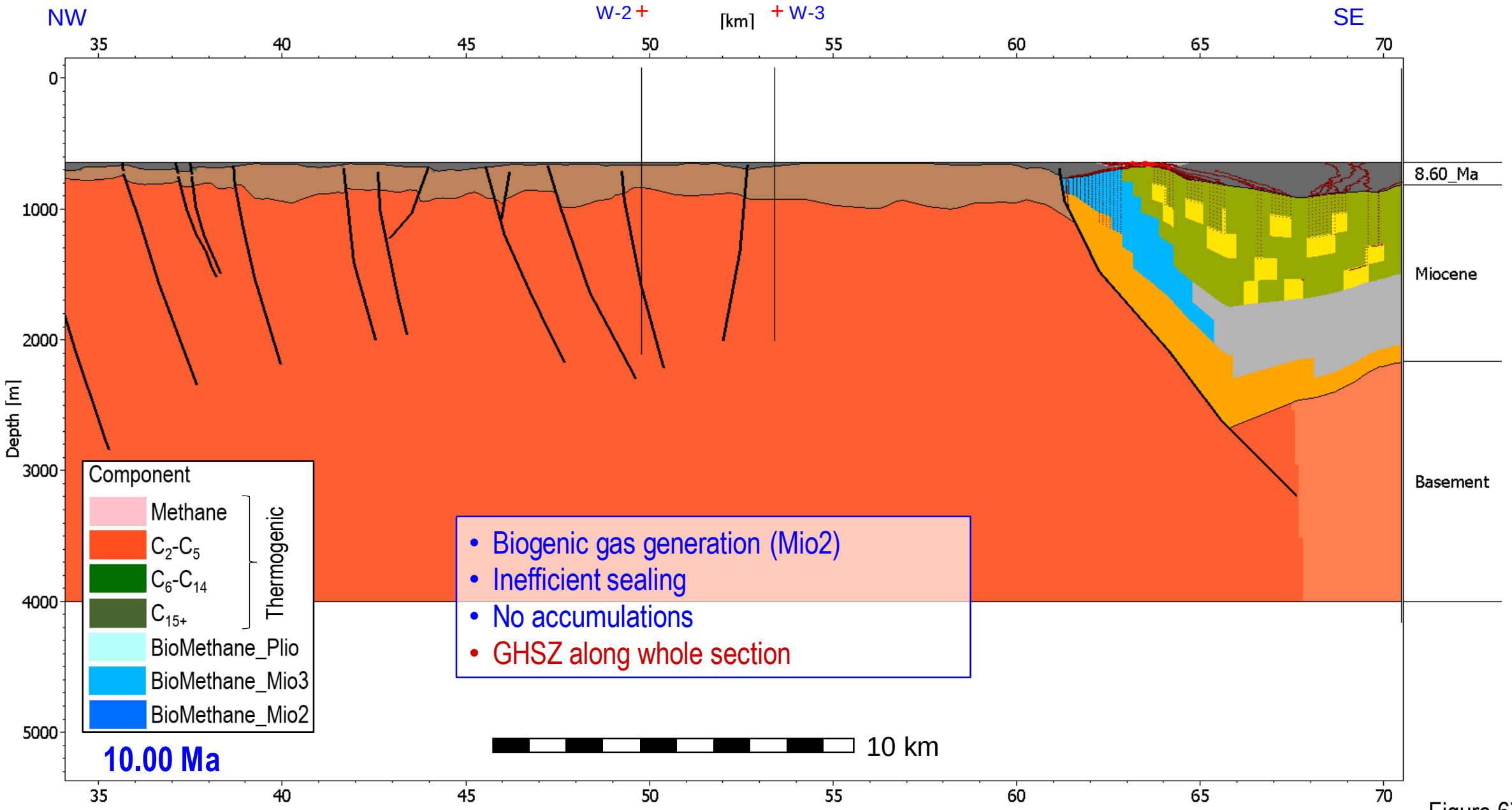

Figure 67

Migration Model: Hydrocarbon Charge through Geologic Time

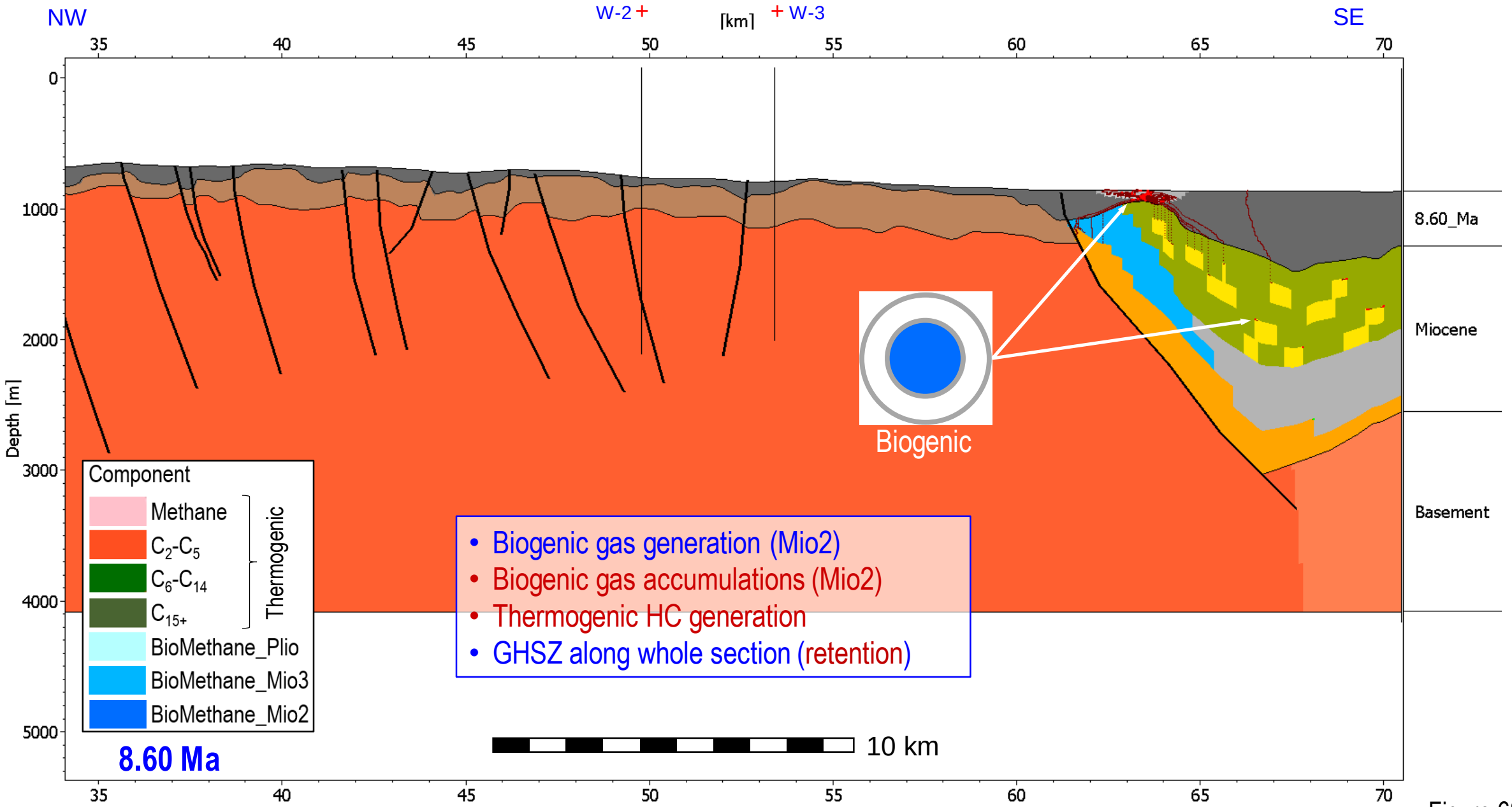

Figure 68

Migration Model: Hydrocarbon Charge through Geologic Time

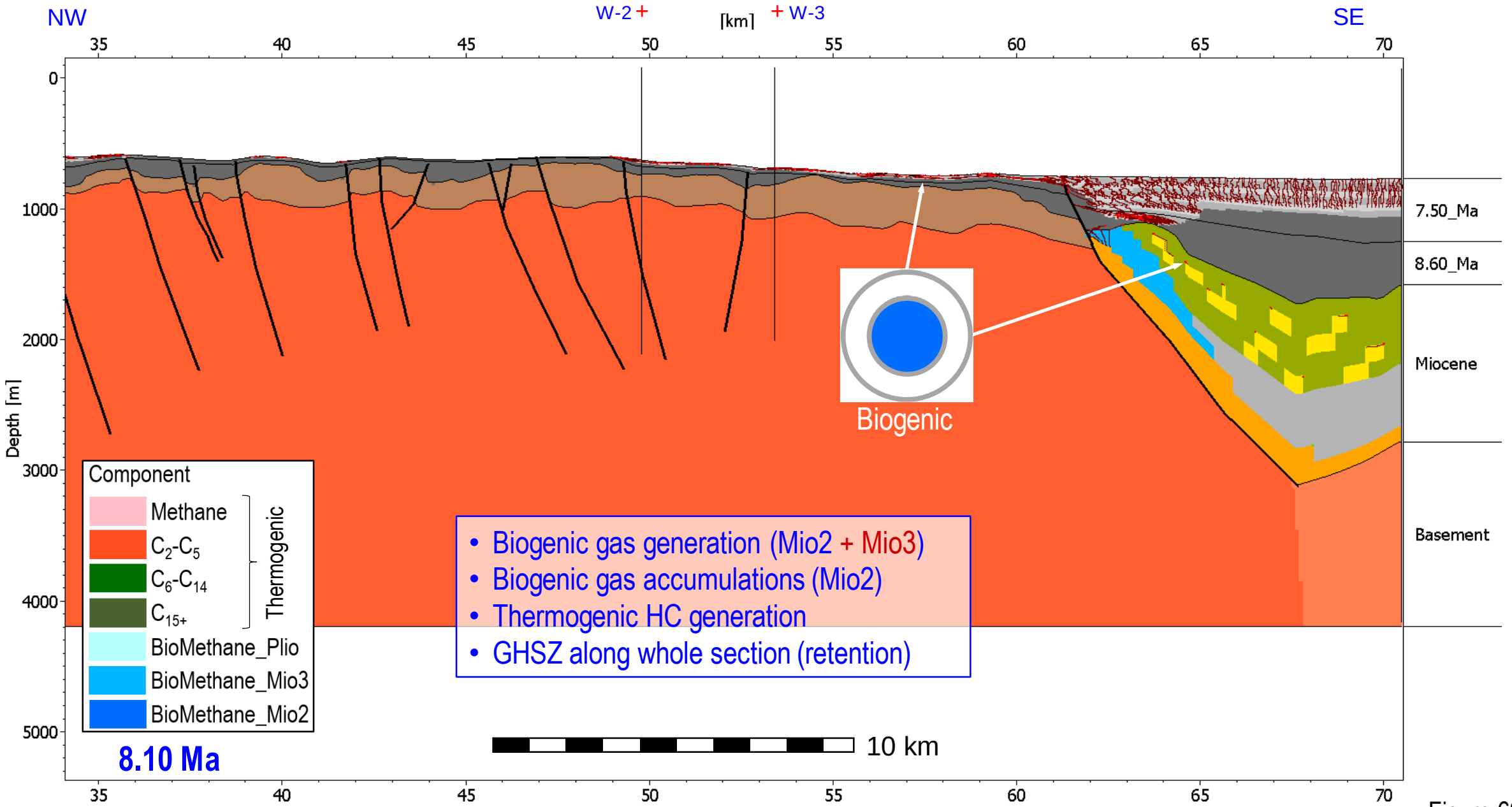

Figure 69

Migration Model: Hydrocarbon Charge through Geologic Time

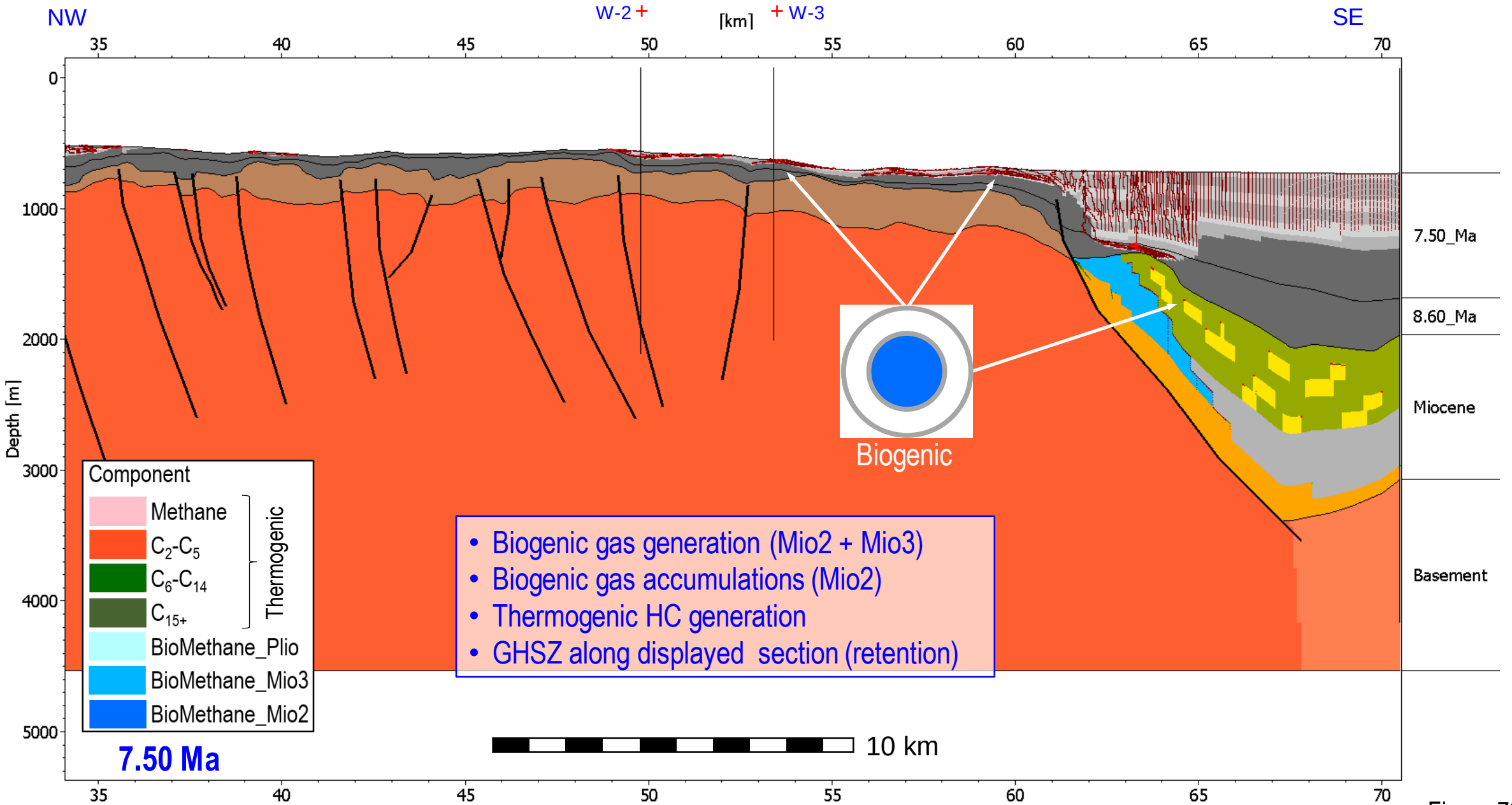

Figure 70

Migration Model: Hydrocarbon Charge through Geologic Time

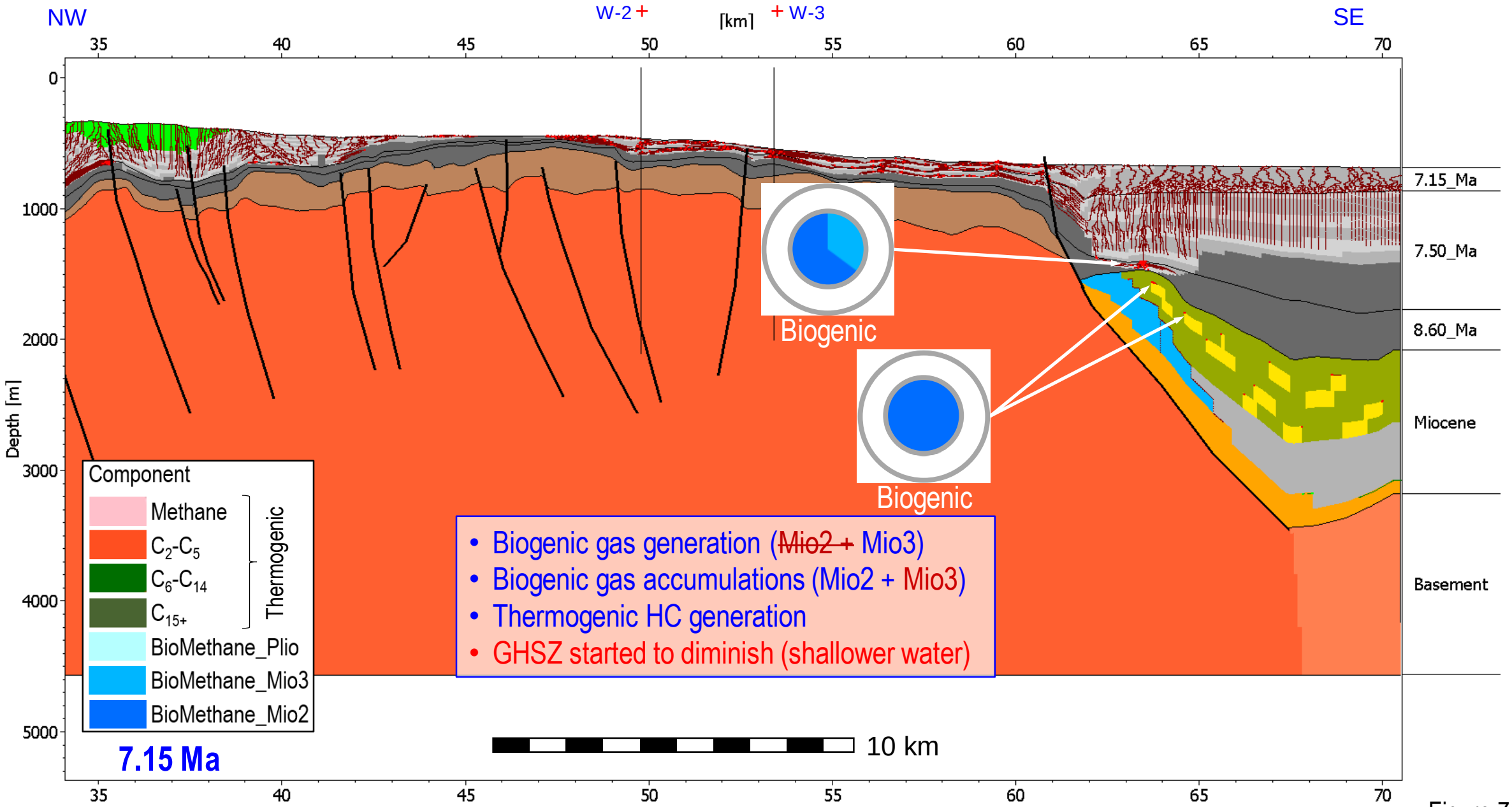

Figure 71

Migration Model: Hydrocarbon Charge through Geologic Time

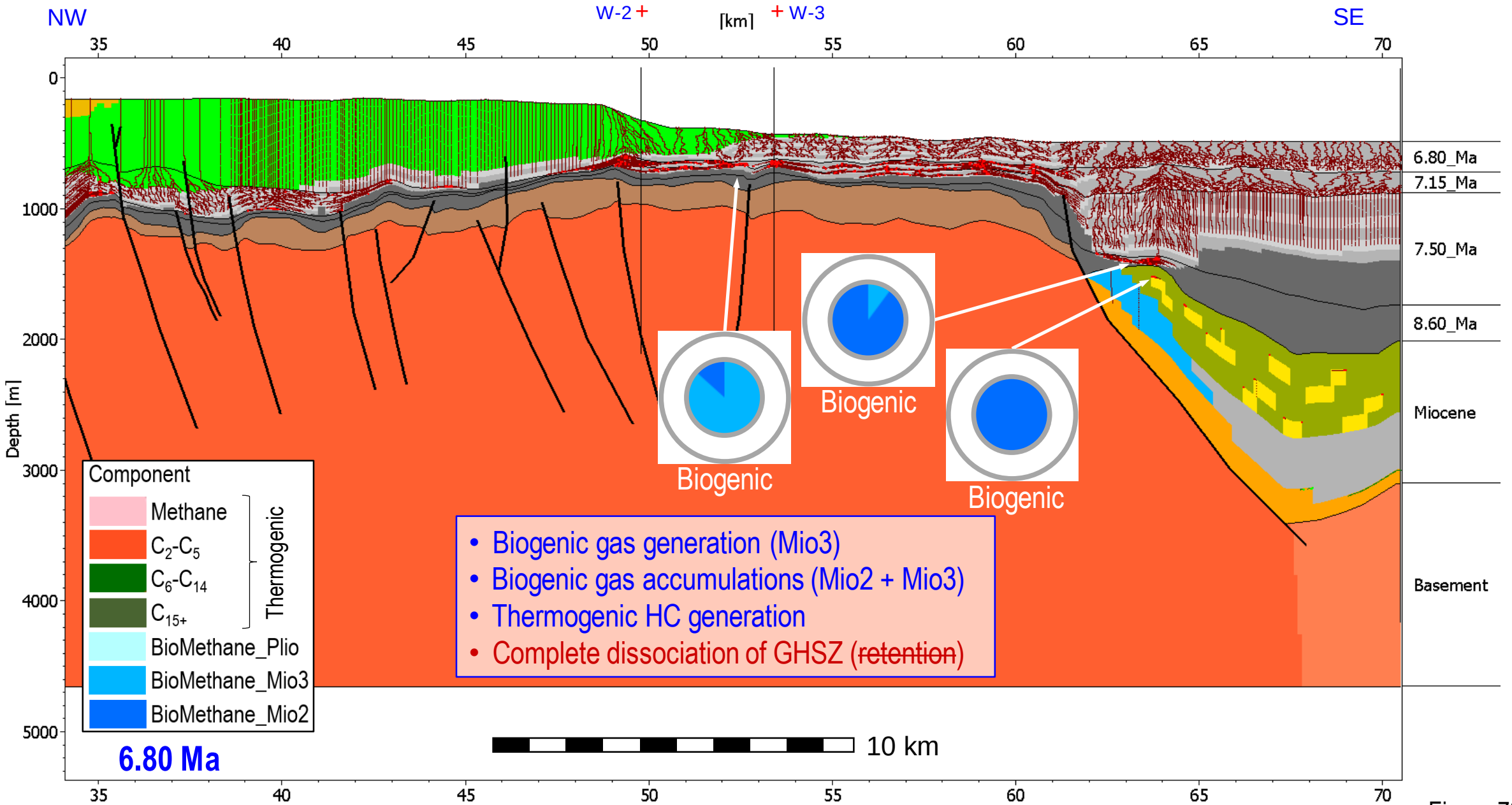

Figure 72

Migration Model: Hydrocarbon Charge through Geologic Time

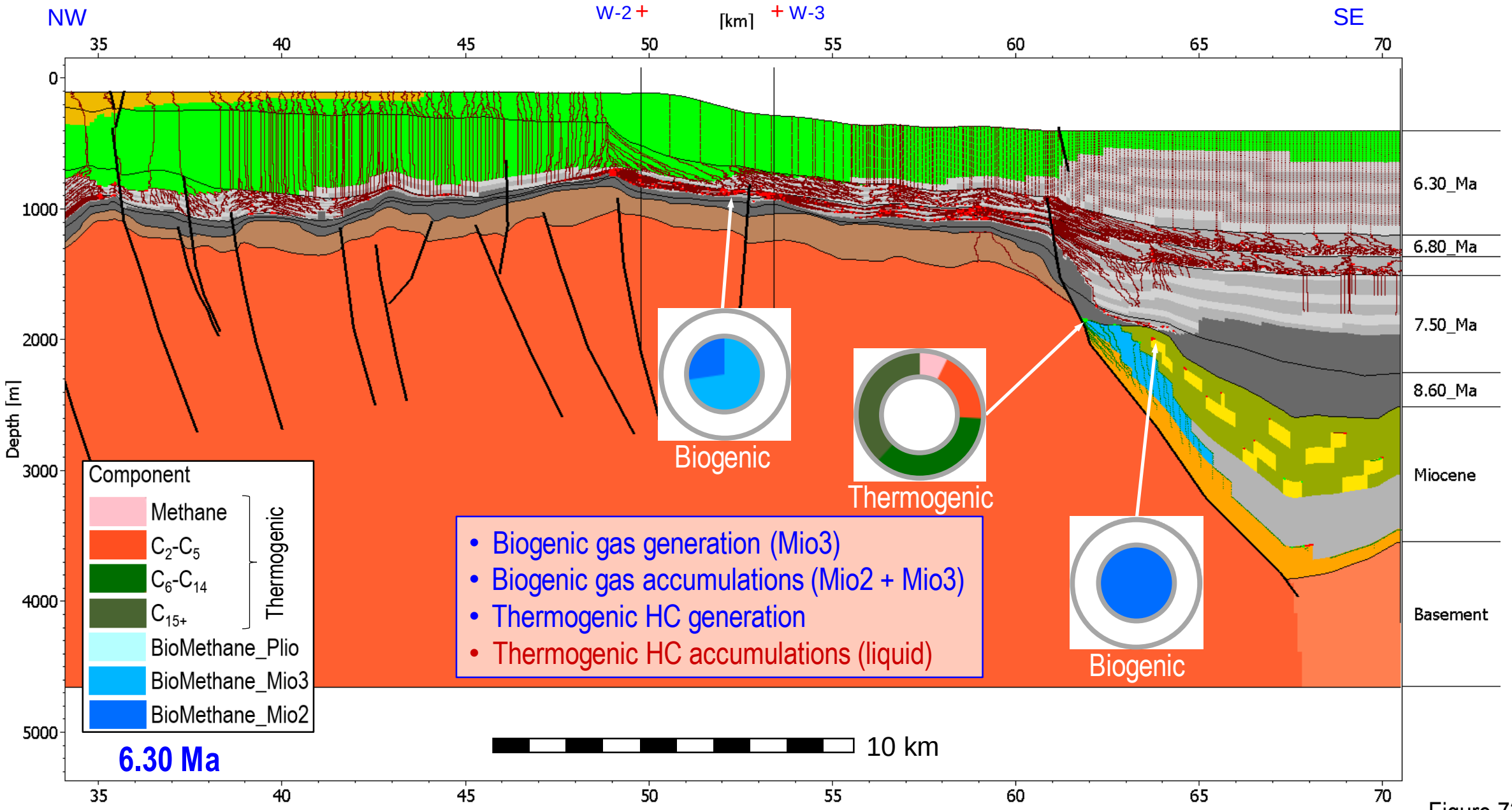

Figure 73

Migration Model: Hydrocarbon Charge through Geologic Time

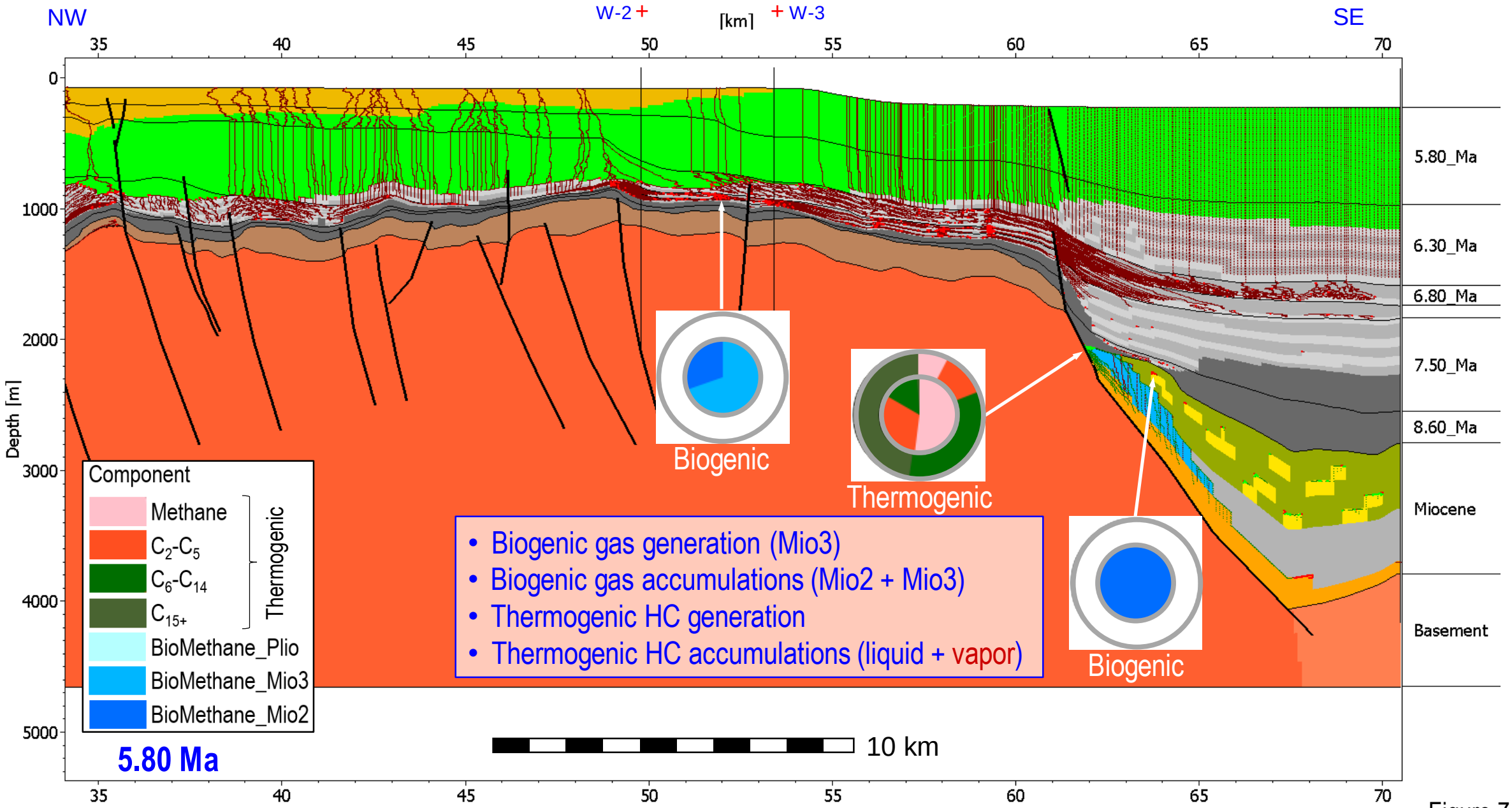

Figure 74

Migration Model: Hydrocarbon Charge through Geologic Time

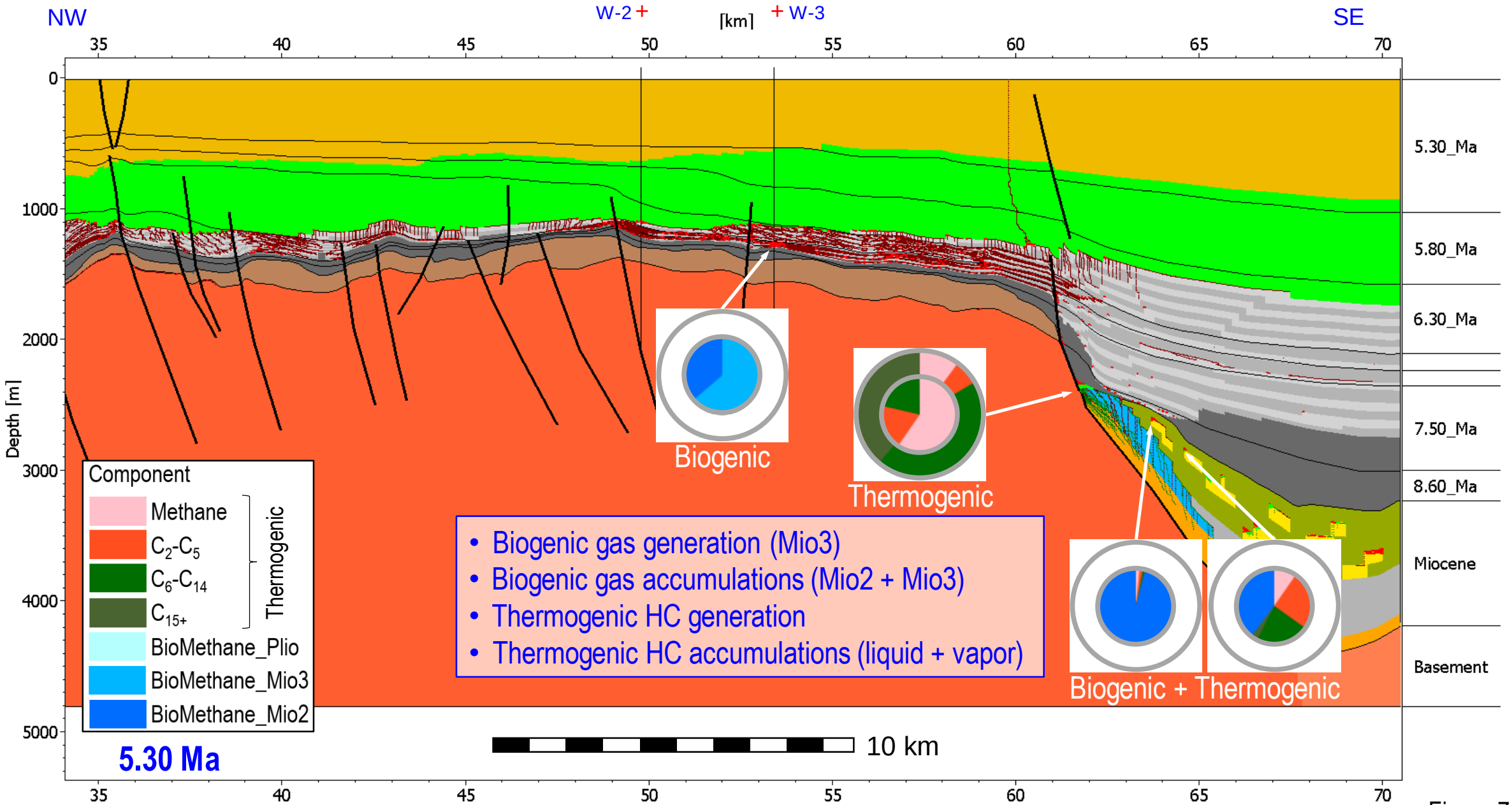

Figure 75

Migration Model: Hydrocarbon Charge through Geologic Time

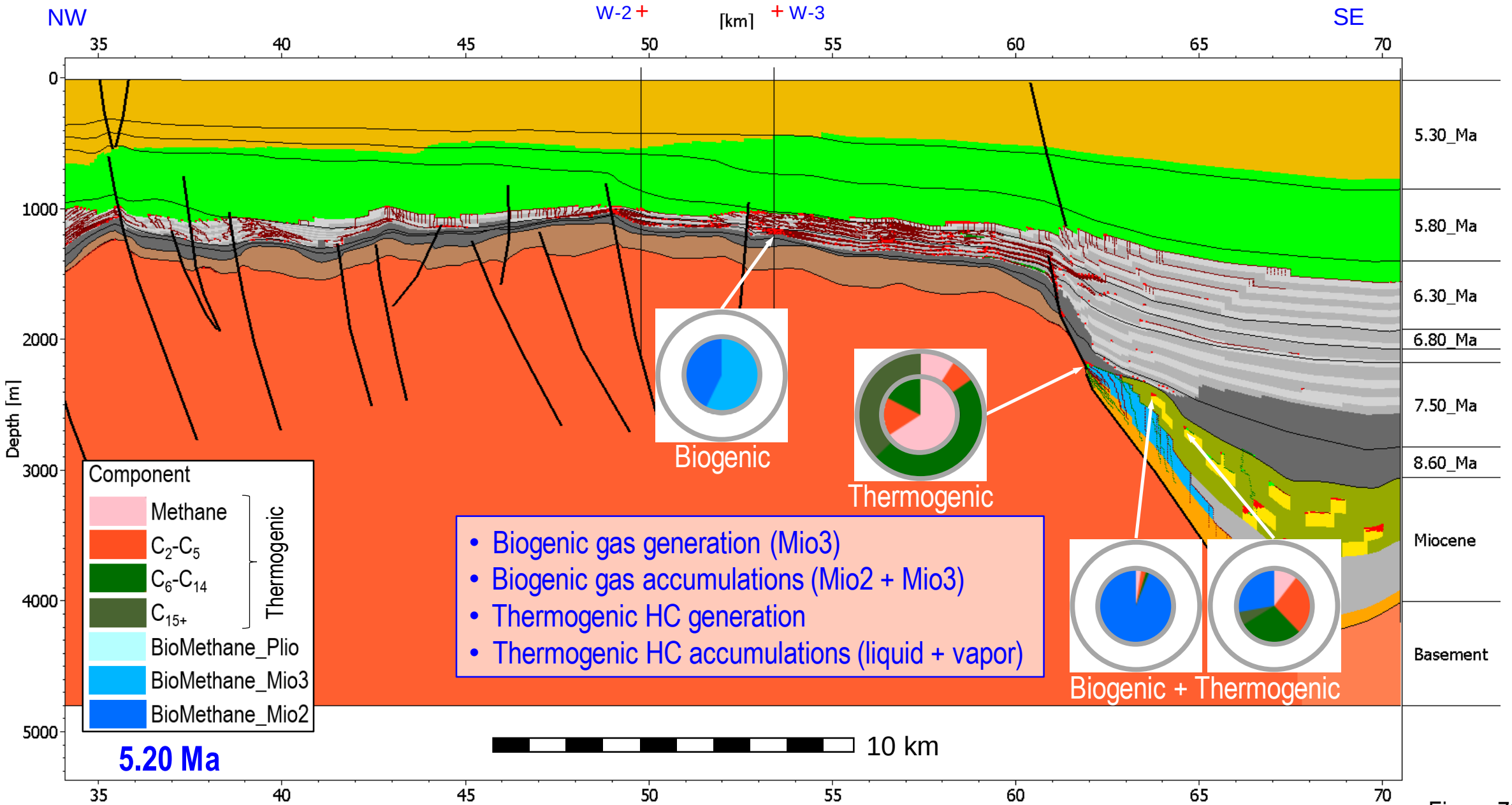

Figure 76

Migration Model: Hydrocarbon Charge through Geologic Time

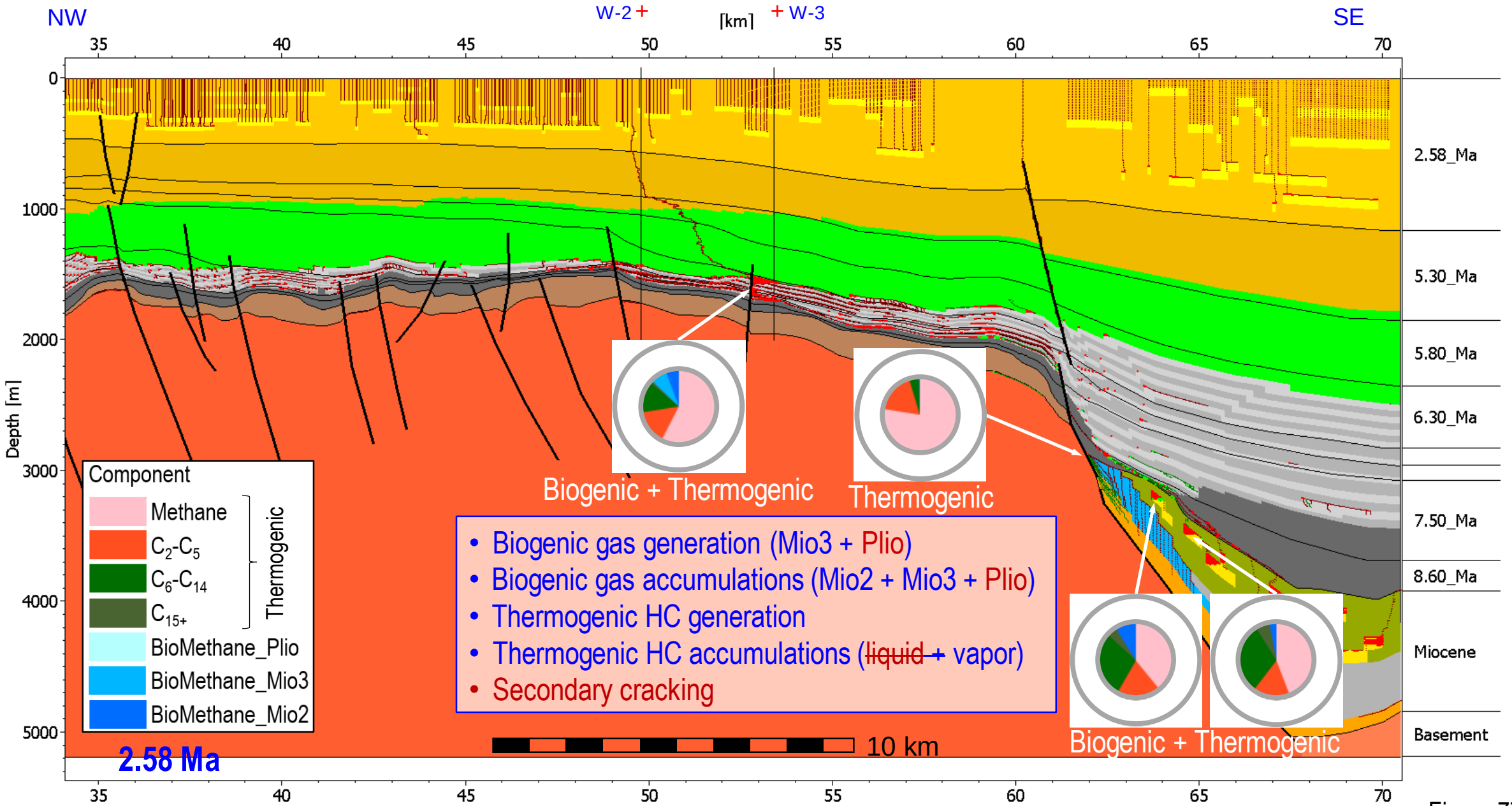

Figure 77

Migration Model: Hydrocarbon Charge through Geologic Time

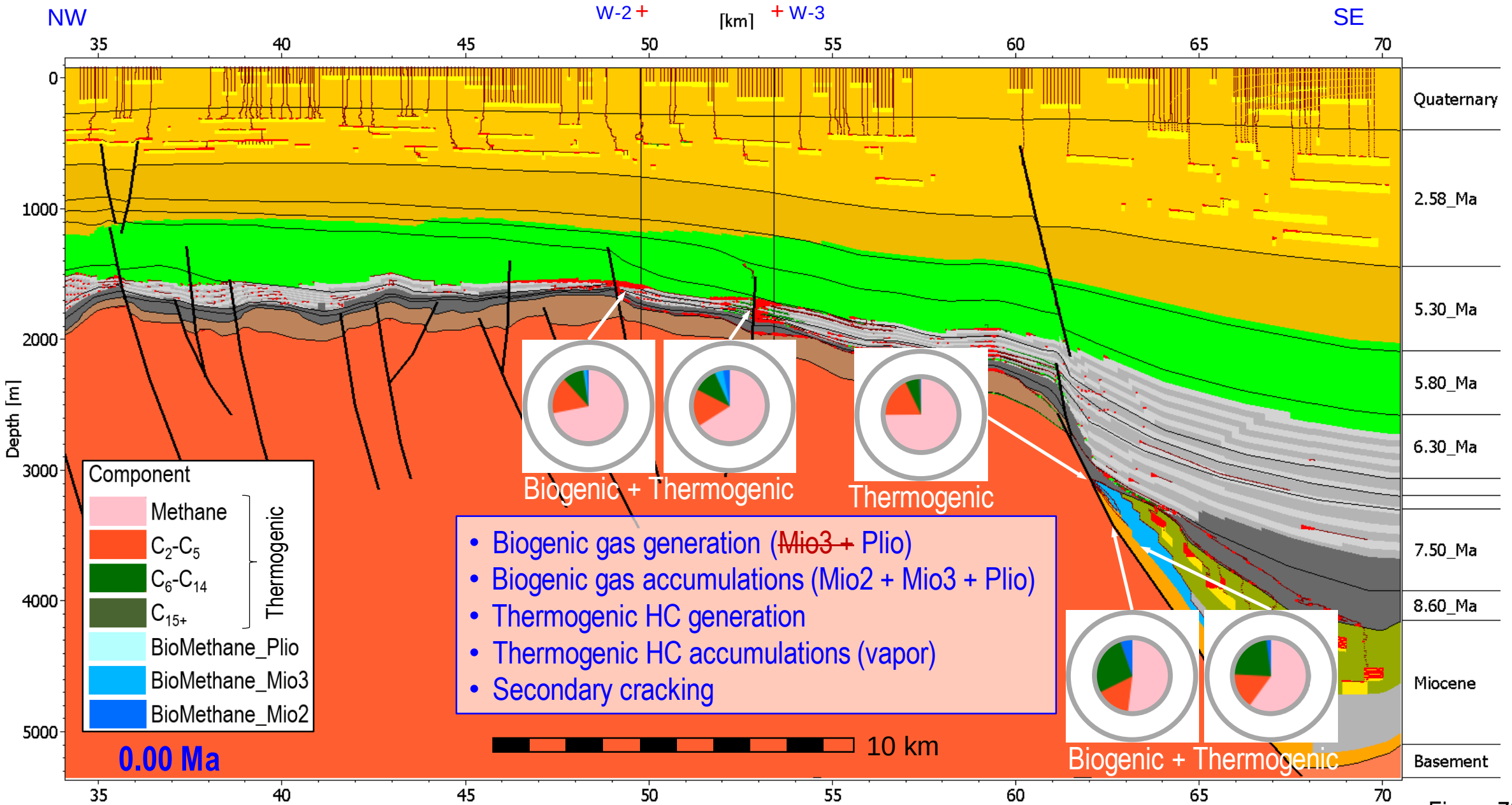

Figure 78

Hydrocarbon Balance: Accumulated Thermogenic and Biogenic Gases in Reservoirs (Present-day)

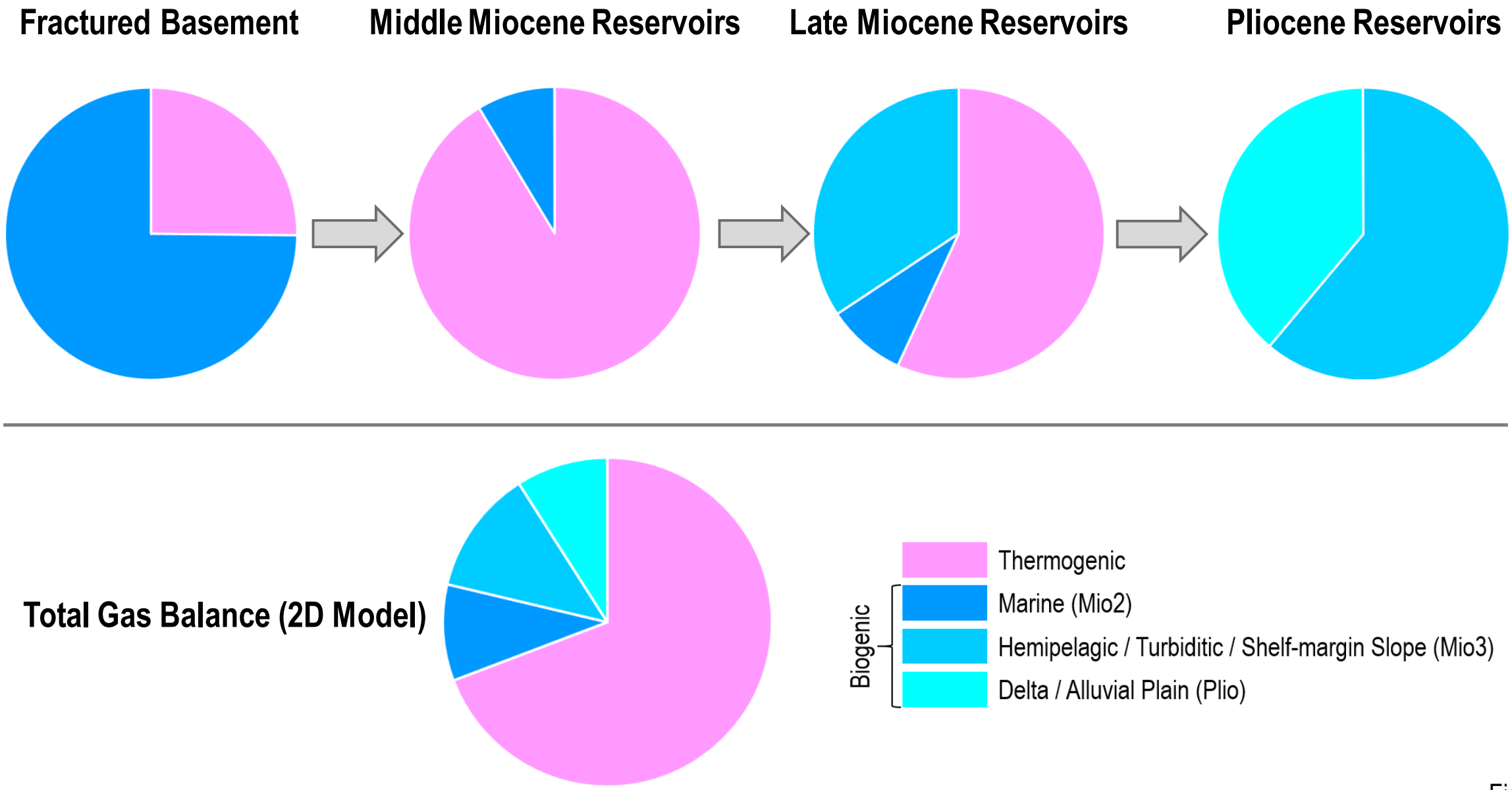

Figure 79

Hydrocarbon Balance: Accumulated Thermogenic and Biogenic Gases in Reservoirs (Present-day)

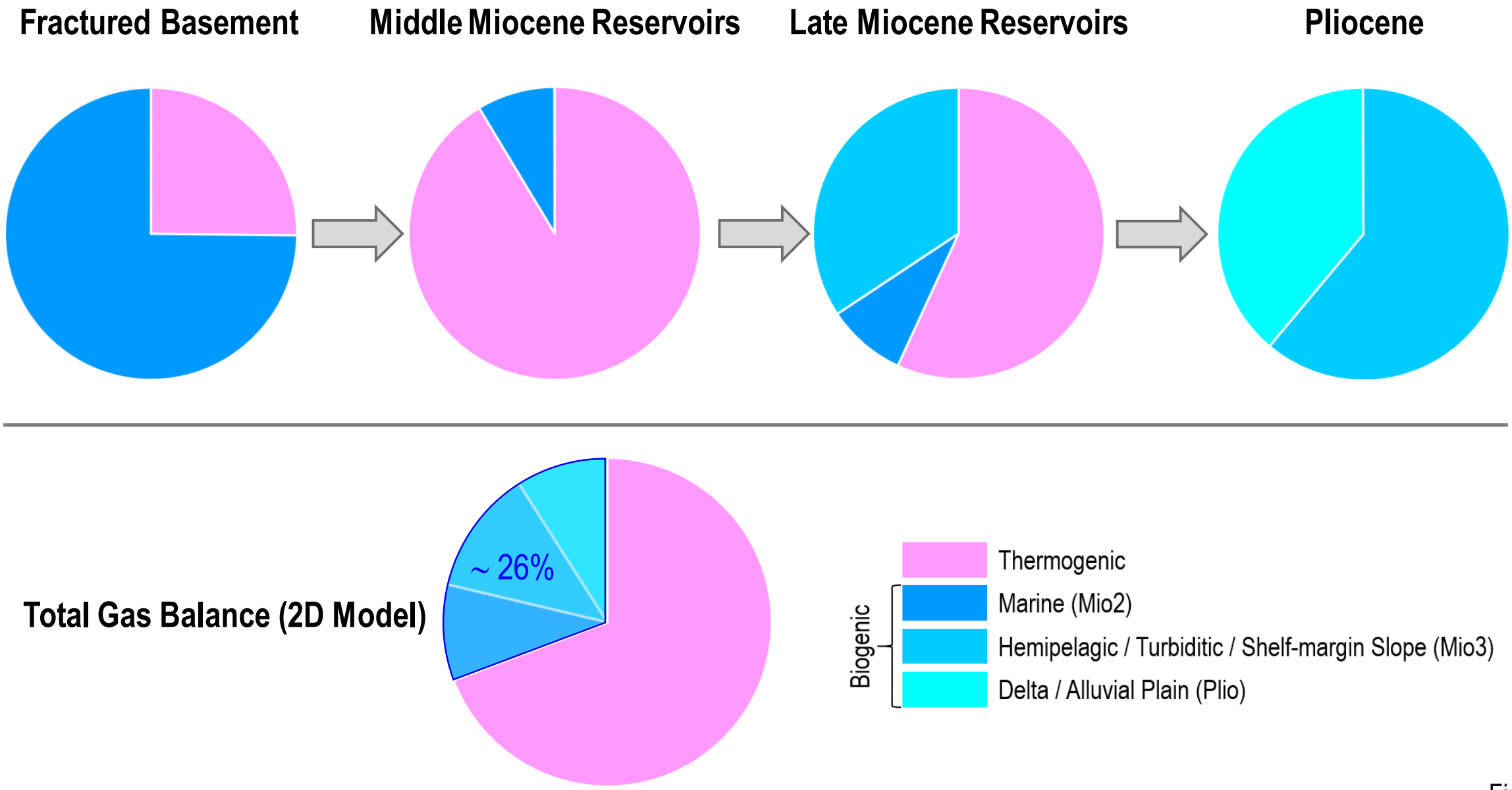

Figure 80

Gas Generation: Thermogenic vs. Biogenic Gases in Reservoirs (2D model)

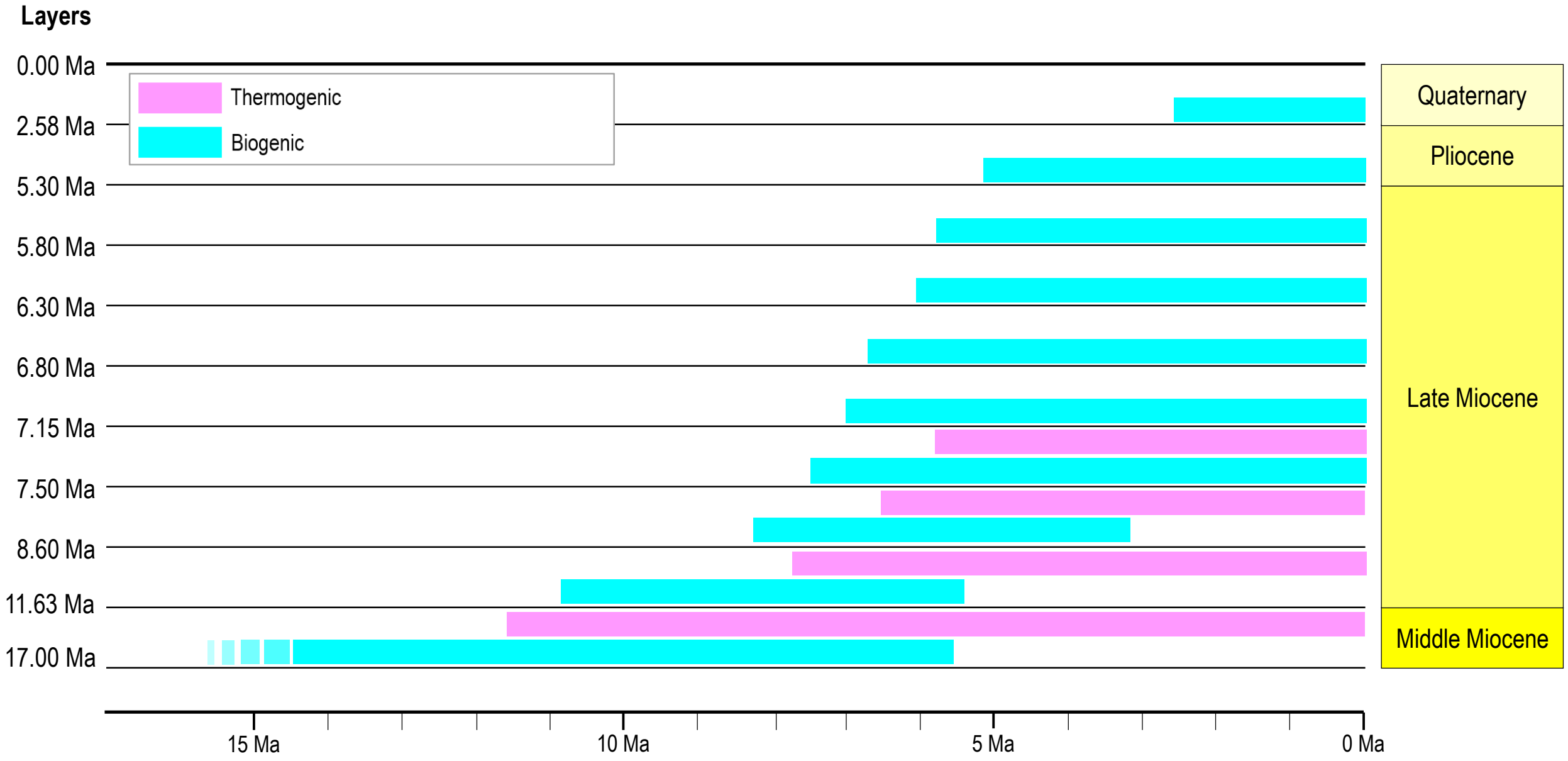

Figure 81

Model Results: Good Agreement with General Observations in Pannonian Basin

Carbon Isotope Ratio ($\delta^{13}C$)

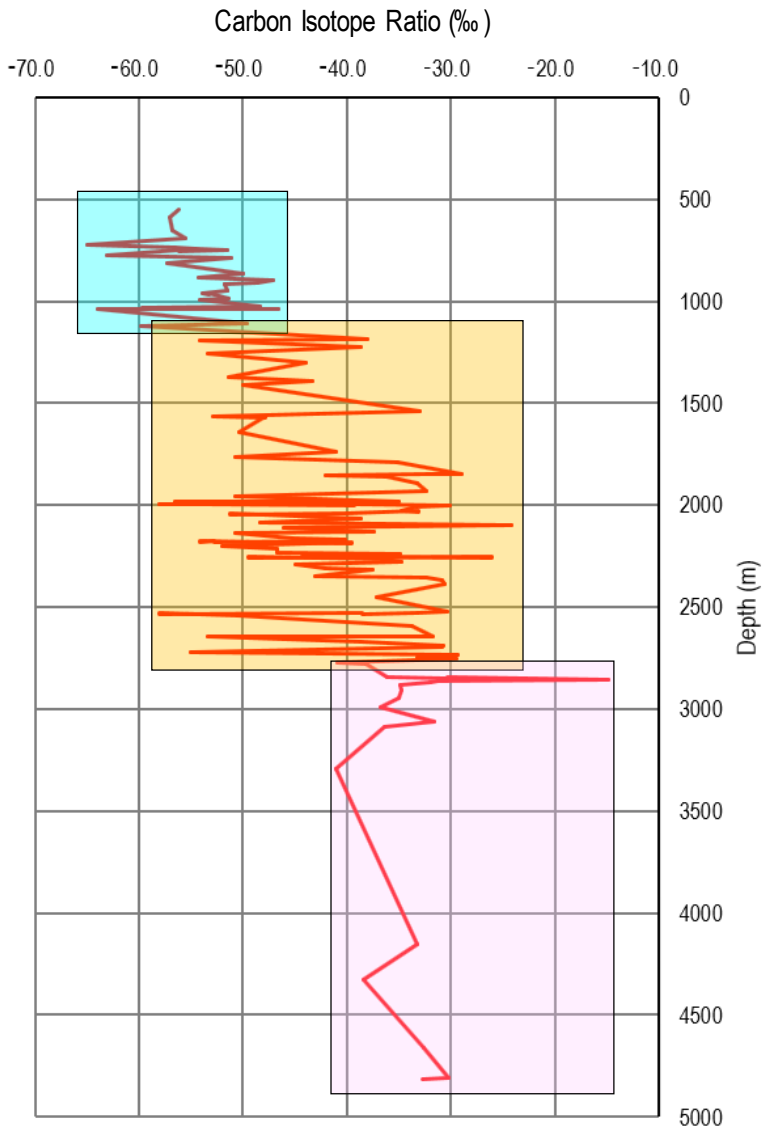

Gas Wetness [$(C_2/C_1+C_2)x100$]

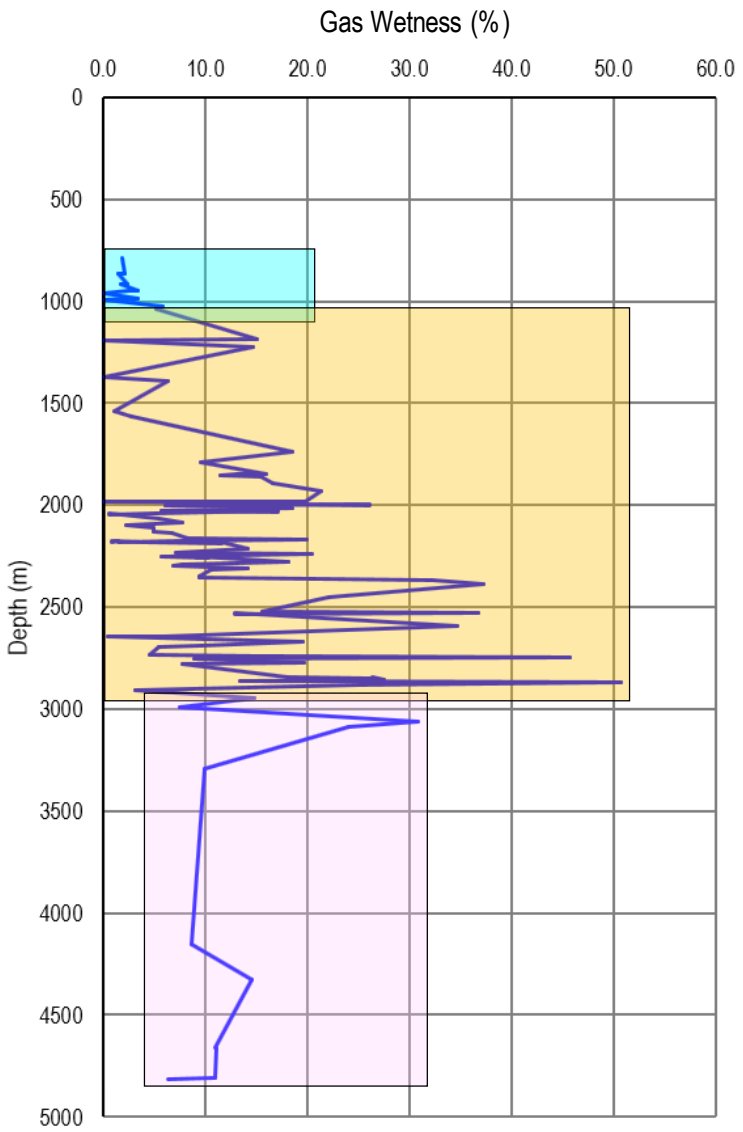

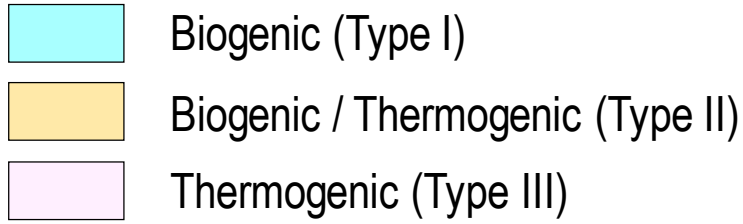

Figure 82

Technical Solution: High Definition Model for Facies Refinement Workflow

Technical Challenges:
- diachronous depositional setting
- mixed thermogenic-biogenic sourcing
- mixed fault-stratigraphic trapping
- calibration with known fields

Technical Solutions:
- hi-res facies modeling (well/seismic calibrated)
- coupled Darcy/IP migration simulator

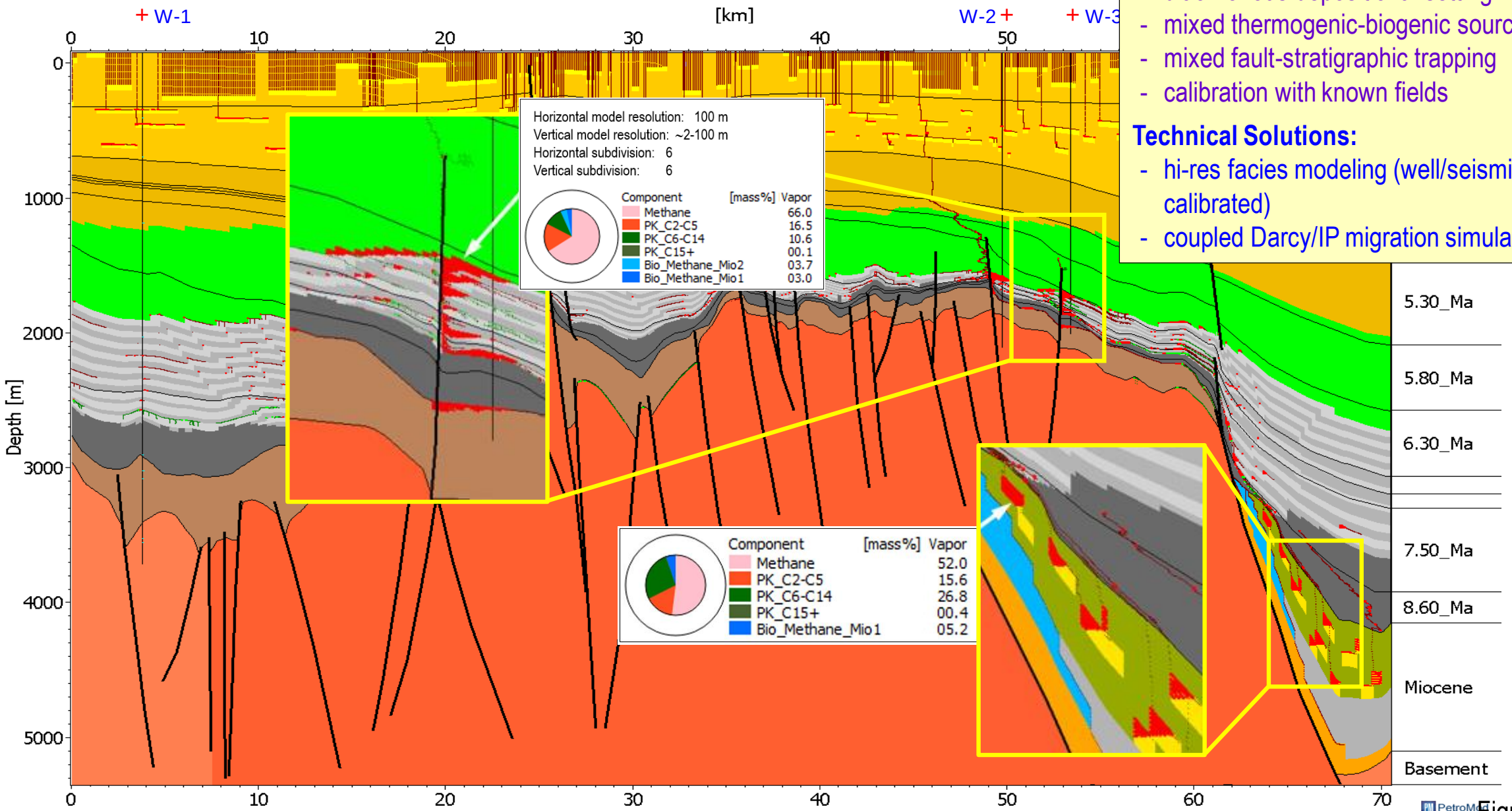

Figure 83

Conclusions

- Two gas generation systems are present in the Pannonian Basin, which:
  - developed in a unique tectono-stratigraphic framework
  - coexisted and interacted in time and space
  - resulted in 3 types of gas accumulations: thermogenic (III), mixed (II), and biogenic (I)
- Good agreement between simulation results and observations: $\delta^{13}C$ trends and gas wetness plots
- Further exploration opportunities exist for mixed (II) and biogenic (I) gas accumulations related to stratigraphic/combined traps

Figure 84